Pre-white dwarf pulsation—variations on a theme

by

Michael Sean O'Brien

A dissertation submitted to the graduate faculty

in partial fulfillment of the requirements for the degree of

DOCTOR OF PHILOSOPHY

Major: Astrophysics

Major Professor: Steven D. Kawaler

Iowa State University

Ames, Iowa

1998

Graduate College
Iowa State University

This is to certify that the Doctoral dissertation of

Michael Sean O'Brien

has met the dissertation requirements of Iowa State University

Committee Member

Committee Member

Committee Member

Committee Member

Committee Member

Major Professor

For the Major Program

For the Graduate College

To Amy, my wife.

TABLE OF CONTENTS

LIST OF TABLES

LIST OF FIGURES

ACKNOWLEDGEMENTS

"I am tormented with an everlasting itch for things remote."

—Herman Melville, *Moby Dick (1851)*

My favorite stories leave me wondering right up to the last page how things will turn out, but afterwards the ending seems inevitable. The path I took to the completion of this thesis was an awful lot like some of those stories. Many different people contributed to the current shape of my life, and though I can't imagine it turning out any other way, I know that I would not have arrived here without the unyielding support of every one of them.

I learned astronomy from two masters of the trade, Steve Kawaler and Chris Clemens. They could not be more different in their approaches to science (and to life), but both base their lessons on a fundamental respect for and honesty about the craft of science. Each excels in different ways at showing me the extent of my ignorance and the lack of polish in my work. Sometimes the high standards they required of me left me a bit shocked and chagrined, until I realized they held even higher standards for themselves. They both like to say that what they do is *only* astronomy, but I've never seen two people more in love with their work than Steve and Chris. Finally, I learned from them that science rests ultimately upon method. I don't mean they taught me the Scientific Method, Steps 1–6, but that the way we approach problems, and the way we comminicate what we find, ultimately determines our success as scientists. I have a long way to go before I master the methods of science, but I owe the direction I'm taking toward this goal to Steve and Chris.

I could not have maintained my studies as a graduate student in astronomy without the support of my wife, Amy. She had the unenviable task of waiting while both our fates were decided by qualifier exam committees and thesis committees and hiring committees, all based

on work she had no control over except in support of me. Her career has at least the same promise as mine, yet she has been unswerving in her willingness to alter her ambitions so I could finish school. And frankly, she is more fun than anyone else I know. How could I have come through without that?

The list of people who deserve co-authorship on this thesis based on their contributions to my continued hope and sanity gets long at this point, and it extends far back in time. The first two people I remember encouraging me in science are my father and my mother's father (Grandpa O'Deegan). My dad taught me to play chess when I was six. I learned from him the joy of solving problems, and when I was twelve or thirteen he gave me a telescope. Soon after, I announced to the family (to the chagrin of many) that I was going to be an astronomer. Grandpa started sending me books on astronomy that I eagerly read; I still have all those books. Lots of kids play games with their dad and look through telescopes without becoming scientists, but for me, those little things—chess and astronomy books and a telescope—really changed my life.

It's amazing what goes into a thesis. There's Steve Carr's poetry, and Rick Overton listening to my worries and self-doubt for fifteen years, and my brothers Chris and Tim smiling while letting me ramble about sunsets and the colors of rainbows, and fun with Chuck Winrich, Mike Sindberg, and Mike and Marina Reed. The whole Texas WET group, Don and Ed and Scot and Atsuko and Todd and Judi, never failed to treat me like family, and they are always ready with choice stories about my graduate advisors. Lee Anne Willson, Phil Appleton, Curt Struck, Russ Lavery, Mark Bransford, Ben Dehner, Vassilis Charmandaris, and the rest of the Iowa State astronomy faculty and graduate students taught and supported me during six years of graduate school. My undergraduate advisor, Dr. Reimann, and the rest of the gang back at Boise State, helped me when I wasn't sure where I might be headed in life. Leslie Kawaler joined Steve in helping me when I was *really* down, once upon a time. My family, and my wife Amy's family, never failed in their support even while they must have wondered if I would *ever* finish school. The best way I can think of to thank everybody is to finish school and get a job. Here goes.

ABSTRACT

One of the least understood aspects of white dwarf evolution is the process by which they are formed. The initial stages of white dwarf evolution are characterized by high luminosity, high effective temperature, and increasingly high surface gravity, making it difficult to constrain their properties through traditional spectroscopic observations. We are aided, however, by the fact that many pre-white dwarfs (PWDs) are multiperiodic g-mode pulsators. These stars fall into two classes, the variable planetary nebula nuclei (PNNV) and the "naked" GW Vir stars. Pulsations in PWDs provide a unique opportunity to probe their interiors, which are otherwise inaccesible to direct observation. Until now, however, the nature of the pulsation mechanism, the precise boundaries of the instability strip, and the mass distribution of the PWDs were complete mysteries. These problems must be addressed before we can apply knowledge of pulsating PWDs to improve understanding of white dwarf formation.

This thesis lays the groundwork for future theoretical investigations of these stars. We use Whole Earth Telescope observations to determine the mass and luminosity of the majority of the GW Vir pulsators. With these observations, we identify the common properties and trends PWDs exhibit as a class.

We find that pulsators of low mass have higher luminosity, suggesting the range of instability is highly mass-dependent. The observed trend of decreasing periods with decreasing luminosity matches a decrease in the maximum theoretical g-mode period accross the instability strip. We show that the red edge can be caused by the lengthening of the driving timescale beyond the maximum sustainable period. This result is general for ionization-based driving mechanisms, and it explains the mass-dependence of the red edge. The exact observed form of the mass-dependence provides a vital starting point for future theoretical investigations of the driving

mechanism. We also show that the blue edge probably remains undetected because of selection effects arising out of rapid evolution. Finally, we show that the observed rate of period change in cool GW Vir pulsators will constrain neutrino emission in their cores, and we identify appropriate targets for future observation.

CHAPTER 1 INTRODUCING THE PULSATING PRE-WHITE DWARF STARS

"So many worlds, so much to do,
So little done, such things to be . . . "
—Alfred Lord Tennyson, *In Memoriam A. H. H. (1833)*

1.1 Introduction

The development of all scientific fields, from astronomy to zoology, generally proceeds through recognizable stages. New phenomena are first cataloged and organized into groups sharing common characteristics. As databases grow, underlying interrelationships are discovered within and among different groups. Finally, enough information accumulates to fuel searches for and tests of general rules that unify the objects of study into a coherent whole. When this leap—from cataloging to scientific unification—takes place, new frontiers of study inevitably open themselves to inquiry. Applications are found to areas previously thought unrelated to the phenomena recently unified. New fields arise, and the process repeats.

This is the story of one small step toward unification in a field less than twenty years old. The group under study is a class of stars called the pulsating pre-white dwarfs.[1] These stars show periodic brightness variations up to a few percent of their total brightness (in white light) on timescales from minutes up to almost an hour. Until recently, little was known about all but one—PG 1159-035, the class prototype. With this work, we examine other members in detail, and provide a picture of their group properties. This inevitably leads to new questions, and we will answer some of them.

[1] Hereafter, we use the acronym PWD for "pre-white dwarf."

All single stars born with less than eight to ten times the mass of our Sun will become white dwarf stars.[2] Such stars evolve through multiple series of expansion and contraction before passing through the evolutionary stage represented by the pulsating PWDs. Do all such stars become pulsating PWDs, or do some enter the white dwarf stage quietly? In other words, is pulsation a necessary phase caused by cooling through an "instability strip," as it is for the cooler DA white dwarfs passing through the ZZ Ceti strip (Fontaine et al. 1982; Greenstein 1982)? There are non-pulsating PWDs, some apparently identical spectroscopically to known pulsators (Werner, Heber, & Hunger 1991). However, surface temperature and luminosity—which represent a star's approximate evolutionary status—are difficult to measure for a PWD star. Perhaps more precise measurements will determine that the pulsators have temperatures or luminosities different from those of the non-pulsators.

Another possibility is that pulsators share a common composition, a chemical "signature" for pulsation. This bears on two questions. First, a chemical signature might provide a clue to the cause of their pulsation. Second, if pulsators are found to represent only a subset of the stars destined to become white dwarfs, then knowledge gained about the pulsators might have more limited application to questions of white dwarf formation in general.

What then, are the true parameters which determine which PWD stars pulsate? This is the first question we will attempt to answer, through the study of several individual PWDs spread over a large range of luminosity and effective temperature. With this clue in hand, we hope to find the common threads which bind the pulsators into a group. We will also encounter several new questions posed by the unusual nature of these stars. We shall see that all of the questions are related to two fundamental processes: the driving of pulsation in the stellar interior, and the response of the star to this driving.

One of the primary goals of this investigation, therefore, is to address the cause of the pulsational driving using the clues provided by the observed properties of the group. We will evaluate our answers based on how well they account for the observed facts. Additional observations and theoretical calculations will be needed to test our hypothesis, and we will

[2] Very low mass stars will, however, take many times the current age of the universe to do so.

suggest how some of these might be carried out.

New knowledge often finds application in unforeseen areas. From our pulsation studies, we will precisely measure the mass and luminosity of individual PWD stars—with some unexpected implications. These measurements allow us to make precise claims about a star's evolutionary status. In the case of at least one PWD star, results from our pulsation studies indicate its evolution is dominated by neutrino emission. What is more, since it pulsates, we can in theory determine its rate of evolution from changes in its pulsation period. Such a measurement would represent the first test of standard lepton theory in dense plasma.

1.2 Overview of Stellar Evolution

Stars contain within them a record of their prior evolution. Historically, we have read this record by measuring their luminosity, L, their effective temperature, $T_{\rm eff}$, and their surface composition. More recently, we have learned to delve into the interior properties of pulsating stars using the tools of asteroseismology (to be discussed more fully in the Chapter 2). We have then interpreted these observations using stellar models. Our understanding is always incomplete, and in many cases our models predict behavior never observed in real stars. On the other hand, the stars sometimes behave in ways we are unable to reproduce in our models. However, despite many remaining problems, a general picture has emerged.[3]

Figure 1.1 shows the H-R diagram for stars in the solar neighborhood (from Iben 1991). The most striking feature in this plot of log L versus log $T_{\rm eff}$ is the diagonal strip of stars running from upper left to lower right, known as the Main Sequence (MS). These are stars which, like our Sun, burn hydrogen (H) quiescently in their cores. Stars in the H-R diagram outside the MS derive their luminosity in other ways. These were all once MS stars, but having used their core H supply, they left to pursue other means of support against gravity. The character of these support mechanisms, combined with the methods by which energy is transported to the stellar surface, determines where in this diagram stars of a given mass reside.

Each stage of evolution is characterized by a different means of staving off gravitational

[3]For a more comprehensive general discussion of stellar evolution, see for example Iben (1991) and Hansen & Kawaler (1994).

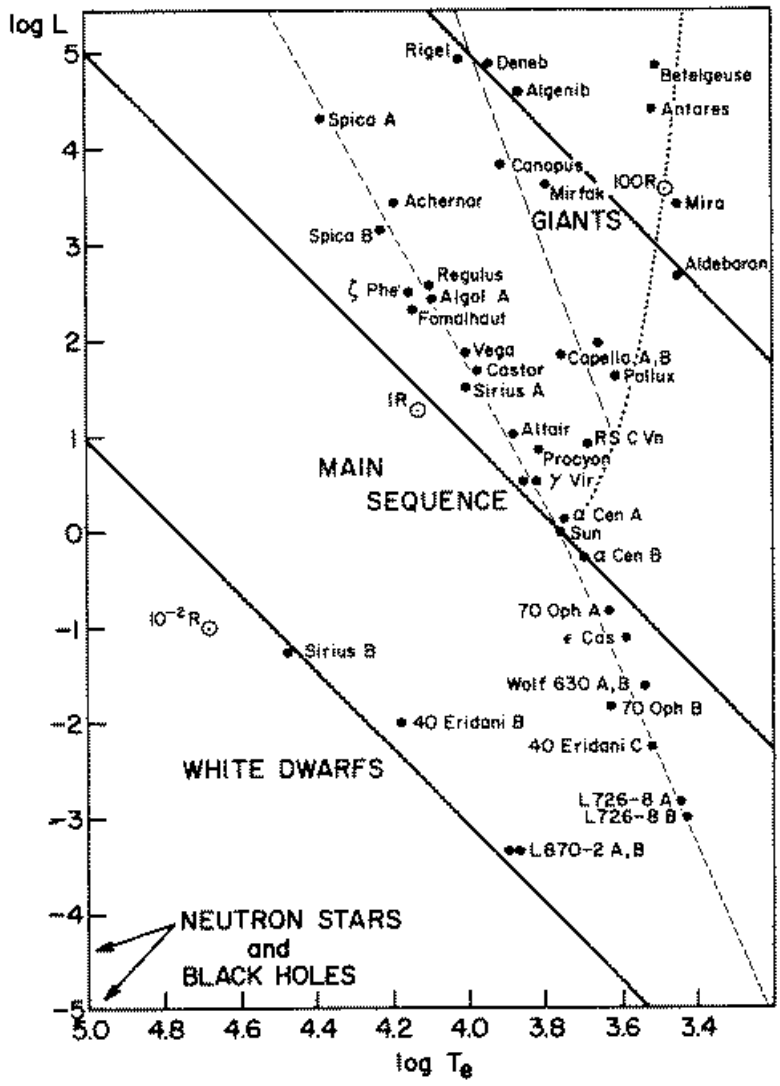

Figure 1.1 Hertzsprung-Russell diagram showing nearby and bright stars. Reproduced from Iben (1991).

collapse. One of the broader goals in the study of stellar evolution has been to identify and characterize these support mechanisms. Another is understanding of energy transport within the stellar interior. Both kinds of understanding are needed to unify the myriad kinds of stars we observe into a single continuous chain of stellar evolution, of which the PWDs make up one small but vital link.

1.2.1 Evolution To the Asymptotic Giant Branch

When a main sequence star exhausts its H fuel, it can no longer maintain a pressure gradient that is sufficient to precisely withstand gravity. Its core begins to contract relatively rapidly so as to raise raise the interior temperature, as gravitational potential energy is converted to heat. The star leaves the MS at nearly constant luminosity toward lower and lower $T_{\rm eff}$. This decrease in temperature halts with the onset of convection in the envelope, which can much more efficiently transport heat from the core to the surface. From this point on the star evolves to higher luminosity at almost constant $T_{\rm eff}$ along the "red giant branch" (RGB) of the H-R diagram. The star is now cooler (at the surface), more luminous, and far larger than when it left the MS. At this point, different things happen depending on the mass of the star.

In stars above about 8 $M_{\odot}$, central temperatures eventually become high enough to burn helium (He) into carbon (C) and oxygen (O), halting contraction in the core. Soon enough, core He is exhausted, and the C/O core contracts until hot enough to burn into even heavier elements. The process continues, leading to a Type II supernova explosion. The evolution of high mass stars is an intriguing field of study, but such stars don't make white dwarfs. From here on we will therefore restrict our attention to the other 90% or so of stars which do.

What happens to stars with mass below 8 $M_{\odot}$ when their core temperatures become high enough to ignite He depends on which of two different means of support against gravity they employ at the time. Stars above about 2.2–2.3 $M_{\odot}$ are supported by ideal gas pressure at He ignition (Iben & Renzini 1983). Core contraction halts in response to the new energy source, and the star enters another relatively stable phase of core nuclear burning similar to the H burning MS. When all available He has been converted to C and O, the core contracts once again, the envelope expands, and the star once again climbs toward the red giant branch. This stage is called the asymptotic giant branch (AGB). While core temperatures never rise high enough to ignite the C/O core, core compaction and therefore stellar radius and luminosity all become much greater than during the previous red giant branch phase.

Stars with mass below about 2.2–2.3 $M_{\odot}$ ignite He at the tip of the giant branch in a core supported not by normal gas pressure but by electron degeneracy pressure. Here the

rapidly increasing energy output of He reactions cannot (at least initially) drive an expansion of the core, because the pressure provided by degenerate material depends only weakly on temperature. This could be disastrous for low mass red giant stars. The core remains compact as the energy generation rate increases. In response, the temperature rises rapidly, increasing the nuclear reaction rates, which further increase the temperature. A thermonuclear runaway must occur.

Yet real stars apparently don't destroy themselves at this stage. We know this because we observe low mass stars which must have passed through the giant phase, undergone this "helium flash," and now remain very much intact. It is thought that stars probably transport excess energy away from the ignition site via convection. Neutrino energy losses should cool the center, inducing a temperature inversion in the core. Thus He ignition in low mass stars takes place off-center, closer to the convective envelope. This is one of several cases where our theories of lepton interactions are crucial to stellar astronomy. Degenerate material, which is highly conductive, does not support convection. The prescriptions employed in most stellar model codes to describe convective energy transport and mixing, however, are *ad hoc* at best, and the exact reason stars survive this stage of evolution is not well understood. It would be helpful to directly confront our theories with observations of stars undergoing the He flash. Such observations might even provide tests of different theories of neutrino physics. However, the helium flash is virtually an instantaneous event in the life of a star, and we have yet to knowingly observe one "in the act."

Following core He ignition, the temperature eventually rises high enough that normal gas pressure becomes important, and the pressure increases, driving core expansion and then resulting in thermal regulation once more. Helium burning continues more or less as it does in the higher mass stars discussed above, with a shell of H burning providing additional energy at the core-envelope interface. At this point the post-helium flash star resides on the so-called Horizontal Branch (HB) of the H-R diagram. Observations of horizontal branch stars lend us clues about many different aspects of stellar evolution.[4]

[4]We are aided in their study by the happy circumstance that some HB stars pulsate. There are two types of pulsating stars in this region of the H-R diagram: the RR Lyrae variables on the HB proper, and the recently

Stars do not in general evolve along the HB during core He burning. They evolve down from the giant branch, and the particular spot they will occupy along the HB depends on the mass of the H envelope left above the He core. The smaller the envelope, the higher the surface temperature and the farther to the left the star resides on the HB. Stars at the far end of the HB have virtually no H left at all.

Due to the poorer energy yield of He burning, and the higher luminosity, stars spend much less time on this He "main sequence" than on the MS. For instance, a typical 1 $M_\odot$ star spends 10^{10} years (about 90% of its total fusion burning existence) on the MS but only about 10^8 years on the HB. When core He is exhausted, HB stars leave for the AGB.

AGB evolution is complex. The broad picture is of a shrinking core, composed of some combination of C and O, surrounded by a shell of nearly pure He and then an extended, H-rich envelope. In general, temperatures are high enough for nuclear burning to take place at the base of both the H and He layers. Once fully established on the AGB, most of the luminosity comes from the H burning shell, which continues to build up the He layer beneath. The He burning shell in turn continues to enlarge the C/O core. As the core grows, the total luminosity increases well beyond that achieved on the RGB.

Eventually, the base of the He layer becomes slightly degenerate, causing a sort of mini-helium flash known as a "thermal pulse." The resulting expansion and cooling of the outer layers temporarily snuffs out H burning, while briefly increasing the total luminosity of the star. Subsequently, L decreases again with the return to more stable He burning. Soon, core contraction resumes, and H burning recovers until the onset of the next thermal pulse. Understanding the process of thermal pulsing is critical not only to explain the observed properties of AGB stars but also to reproduce the behavior of post-AGB white dwarfs as well (Iben 1984, 1991).

Another important feature of AGB evolution is mass loss. AGB stars are observed to lose mass at incredible rates, up to and perhaps beyond $\sim 10^{-5}\ M_\odot \mathrm{yr}^{-1}$ (Loup et al. 1993). Some mass is probably lost during thermal pulsing. However, Bowen and Willson (1991) succeeded in

discovered EC 14026 variables which occupy a high temperature "tail" of the distribution known as the Extended Horizontal Branch (EHB).

reproducing observed mass loss rates with models of pulsationally driven mass loss, calibrated using known properties of pulsating AGB stars called Mira variables.

AGB evolution continues to be the target of intense observational and theoretical scrutiny. Other outstanding problems concern the synthesis of neutron-rich elements during He shell flashes, which can be dredged to the surface by convection, and then lost to the interstellar medium via mass loss. The final ratio of C to O in the core is also in great doubt, due primarily to the uncertainty with which the $^{12}C(\alpha,\gamma)^{16}O$ reaction rate is known. As with most AGB processes, observational constraints on these processes are hard to come by. Part of the problem is the calibration of the required physical parameters. They generally outnumber the available observational parameters many to one, leaving us to guess which theoretical quantities to hold fixed and which to vary. For a comprehensive review of AGB evolution, see Iben & Renzini (1983).

Whatever the exact mechanism, or combination of mechanisms, responsible for mass-loss in AGB stars, they eventually succeed in ejecting the bulk of their envelopes into space. Once 10^{-2} M_* of H is all that remains, they evolve rapidly (in about 10^4 yr) to higher and higher temperatures at almost constant luminosity, revealing what was previously the innermost core of the AGB star. The naked core is bright enough to ionize the expanding shell of its former envelope, creating a beautiful planetary nebula. At the nucleus of the short lived nebula is a newly formed PWD with nearly the same luminosity it had on the AGB but only a millionth its former volume. With the last fires of nuclear burning dying out near its surface, the newly formed PWD star is ready to begin the final stage in its long evolution.

1.2.2 Beyond the AGB

The initial appearance and makeup of a PWD star depends on the phase of the thermal pulse cycle at which it left the AGB. If the star leaves during the phase of stable H burning between shell flashes, then this burning will continue through the planetary nebula nucleus stage (Schönberner 1981, 1986). When what is left of the H envelope becomes too thin and too cool, the H reactions will finally shut off, and the star will begin to cool and become a H

atmosphere (DA) white dwarf.

If the star leaves the AGB *during* a thermal pulse, while the H shell is extinguished, then it can lose its entire H-rich envelope, exposing the He layer below. Such a star is probably a precursor to a DB (He dominated) white dwarf.

If on the other hand the star leaves the AGB close enough to the shell flash phase, then a final flash might occur during or even after the planetary nebula phase, causing a brief return to the AGB before a final burst of mass loss rids it of its entire H envelope and even some of the He as well. This is a likely method of producing PG 1159 stars, which show strongly enhanced C and O at their surfaces (Iben 1984, Werner & Rauch 1994).

A small digression is in order concerning white dwarf and PWD spectral types. Because of their evolutionary histories, these stars are severely stratified in composition with heavier elements beneath and lighter ones above. Their high surface gravities enhance this effect through gravitational settling and diffusion. This means most have very simple spectra showing only lines of one or two elements. DA white dwarfs only show lines of H in their spectra. Non-DA white dwarfs include the DB (HeI lines), DO (HeII lines), DQ (C lines), DZ (other metals), and even the DC stars (no lines). Other important classifications exist such as the PG 1159 PWD stars, which show lines of HeII, CIV, and OVI. Unlike the main sequence spectral classification system, the DA–DB/DO white dwarf spectral classes are not related in any simple way to temperature (though DOs are hotter than the DBs).

If AGB mass-loss was constant, the expected ratio of DA to non-DA white dwarfs resulting from AGB evolution would correspond roughly to the ratio of the times spent during each phase of the thermal pulse cycle. Unfortunately, mass loss probably changes rapidly near the tip of the AGB (again, see Bowen and Willson 1991). The problem gets worse when one adds to the mix the uncertainty of white dwarf formation directly from the extended horizontal branch. Observationally, some 80% of all white dwarfs are DAs. Most of the rest are DB white dwarfs. A fundamental problem is that the exact ratio of DA to non-DA white dwarfs changes with effective temperature. We will return to this issue shortly.

1.2.3 White Dwarf Evolution

As the last remnants of nuclear burning in post-AGB stars die out, the stars enter their final stage of cooling and contraction. By now their surface temperatures are among the highest of any stars known (the hottest have $T_{\rm eff} \gtrsim 170,000$ K). Their luminosity is also high, in excess of 1000 $L_\odot$, but without hope of further nuclear burning, they have nowhere to go but down.

Figure 1.2 shows a log g-log $T_{\rm eff}$ diagram for a sample of stars near the so-called "knee" of the post-AGB evolutionary track. Lines represent the paths stellar models follow after leaving the AGB. Though their surface gravities are already high (about log $g = 7$ at maximum $T_{\rm eff}$)

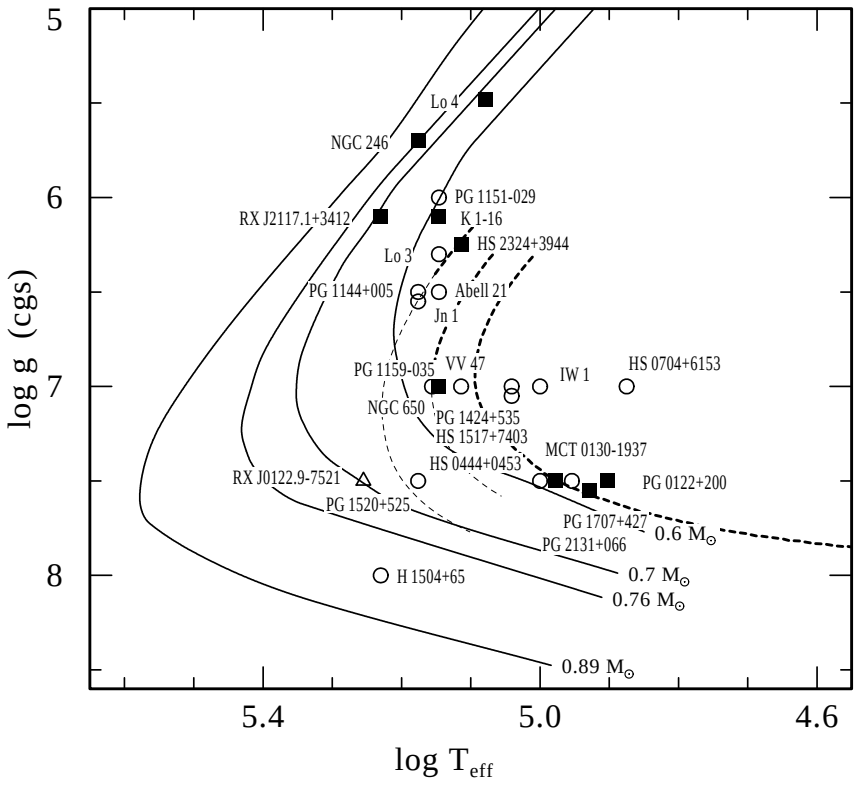

Figure 1.2 Log g–log $T_{\rm eff}$ diagram with the observed locations of PWD stars (Dreizler et al. 1998). Error bars are not shown because of their huge extent: typically ± 0.5 in log g and $\pm 10,000 - 20,000$ K in $T_{\rm eff}$. Evolutionary tracks are from Wood & Faulkner (1986, solid lines) and Gautschy (1997, dashed lines).

PWDs continue to shrink until degeneracy halts their contraction at about $\log g = 8$. Initially, evolution during this phase is rapid: within about 500,000 years, $T_{\rm eff}$ is cut in half, and L plummets to less than 1 $L_\odot$. The inner regions of the newly formed white dwarf star are now completely degenerate, surrounded by a thin, non-degenerate envelope.

Observed white dwarf masses cluster closely around a mean value of 0.56–0.58 $M_\odot$ (Bergeron, Saffer & Liebert 1992, Weidemann & Koester 1984). The primary reasons for such a tight mass distribution despite a wide range of progenitor mass involve the basic features of AGB evolution: high L and high $\dot{M}$. The luminosity of an AGB star is very sensitive to the core mass (Paczynski 1970). Mass loss accelerates when the the core mass, $M_{\rm c}$, reaches approximately 0.6 $M_\odot$, with the higher mass AGB stars losing mass more slowly at a given luminosity than AGB stars of lower mass. The theoretical high-mass limit of AGB cores—and therefore of white dwarf stars as well—is 1.4 $M_\odot$. This represents the greatest amount of mass it is possible to support via electron degeneracy (Chandrasekhar 1939). On the low-mass side, stars with $M_{\rm c} \lesssim 0.53\ M_\odot$ will never reach the AGB in the first place (Dorman, Rood, & O'Connell 1993).

Until about twenty years ago, the placement of stars in the transition region between the PNN track and the upper end of the white dwarf cooling sequence was problematic. This was due not only to the rapidity with which stars must make this transition (making observational examples hard to come by) but also to the difficulty of specifying $\log g$ and $T_{\rm eff}$ for such objects. Determining these quantities from spectra requires that we construct a reasonable model of the star's atmosphere. This is very difficult for compact stars with $T_{\rm eff}$ in excess of 50,000 K. The assumption of local thermal equilibrium (LTE), so useful in modeling the spectra of cooler stars, breaks down severely at such high temperatures and gravities.

PWD evolution can be driven by energy losses due to neutrino interactions in the core. Unlike solar neutrinos, these are not the by-product of nuclear fusion, but instead result from electron scattering processes in the hot, dense regions of the PWD core. And unlike photon energy, which must diffuse relatively slowly through the entire star before emerging into space, neutrinos created near the center of the PWD escape directly. This neutrino luminosity cools

the center of the star, maintaining a temperature inversion similar to that within stars at the tip of the red giant branch. The importance of neutrino reactions to PWD evolution was first recognized in the 1960s (see for instance Savedoff, Van Horn, & Vila 1969) before such stars were confirmed to exist. Calculations of the relevant reaction rates were performed initially by Beaudet, Petrosian, and Salpeter (1967) based on the theory of weak interactions proposed by Feynman & Gell-Mann (1958). Later, Dicus (1972) and Dicus et al. (1976) recalculated these rates in the unified electroweak theory of Weinberg and Salam (Weinberg 1967, Salam 1968). All of these calculations are theoretical, however. We have no direct experimental or observational confirmation of neutrino production rates under conditions appropriate to PWD interiors.

Fortunately, the known sample of stars which occupy this phase of the evolutionary picture has grown over the last two decades. The most important discovery was that of a new spectral class called the PG 1159 stars. Over two dozen are known, ranging in $T_{\rm eff}$ from over 170,000 K down to 80,000 K. About half are central stars of planetary nebula. The most evolved PG 1159 stars merge with the log g and $T_{\rm eff}$ of the hottest normal white dwarfs. This class thus forms a complete evolutionary sequence from PNN to the white dwarf cooling track (Werner 1995, Dreizler & Huber 1998).

PG 1159 stars probably don't represent the precursors of the majority of white dwarfs, however. First, all but one of the PG 1159 PWDs show no evidence of H in their spectra, and it is unlikely they can therefore evolve into DA white dwarfs. It is more likely that they evolve into DO and DB white dwarfs.

About half of the PG 1159 stars are pulsating variable stars, spread over the entire range of log g and $T_{\rm eff}$ occupied by members of the spectral class. This represents the widest instability "strip" (temperature-wise) in the H-R diagram. Central star variables are usually denoted as PNNV stars (planetary nebula nucleus variables). Variable PG 1159 stars with no nebula make up the GW Virginis (or simply GW Vir) stars. PG 1159 serves as the prototype for both a spectroscopic class and a class of variable stars. Farther down the white dwarf sequence, we find two additional instability strips. At surface temperatures between about 20,000 and

25,000 K (Koester et al. 1985; Liebert et al. 1986; Theji, Vennes, & Shipman 1991), we find the DBV (variable DB) stars. Even cooler are the ZZ Ceti (variable DA) stars, with $T_{\rm eff}$ between 11,000 and 13,000 K (Greenstein 1984; Weidemann & Koester 1984; Bergeron, Wesemael, & Fontaine 1992). Variability in all three strips results from g-mode pulsation (for the ZZ Cetis, see Chanmugam 1972, Warner & Robinson 1972; for the DBVs, see Winget et al. 1982; for the PG 1159 variables, see Starrfield et al. 1983). The pulsation periods provide a rich mine for probing the structure of white dwarf and PWD stars.

Pulsations can help to answer the question of whether the PG 1159 stars and the DB white dwarfs share a common evolutionary life line. For instance, Winget et al. (1994, see also Bradley & Winget 1994) used an analysis of the pulsation periods of the DBV star GD 358 to measure the thickness of its He layer. Using the techniques discussed in Chapter 3, they obtain a He layer thickness of $10^{-6}\ M_{\odot}$. The same technique applied to the observed periods of PG 1159 yield a He layer mass of $10^{-3}\ M_{\odot}$. This presents a problem if the two are assumed to be related. However, Dehner (1996) and Dehner & Kawaler (1995) showed that diffusion at the base of the He layer can cause a shift in the apparent location of that base, consistent with both measurements, during evolution from the 140,000 K of PG 1159 to the 23,000 K of GD358.

Another problem is linking the PG 1159 stars to the DBV white dwarfs is that no DB stars are observed in the approximate temperature range 30,000–45,000 K (Greenstein 1986, Sion 1984). This DB "gap" lies in the evolutionary path from PG 1159 to GD 358. Fontaine & Wesemael (1987) propose that all DB stars retain a small amount of hydrogen which diffuses to their surface until, at around 45,000 K, no He is spectroscopically visible. At 30,000 K, convection mixes the H back into the subsurface layers, and the DBs reappear. However, Dehner (1986) showed that the amount of hydrogen required by this scheme should diffuse to the surface so quickly that it would already be easily visible at the PG 1159 stage. Dehner (1986) points out that a small amount a mass loss could "mask" this amount of hydrogen in PG 1159 stars, but detailed calculations of this process have not been made. Since mass loss occurs in PNN stars, this seems a likely solution to the problem.

The thickness of the surface layers in both DA and DB type white dwarfs and PWDs is important for another reason. Once their cores are completely degenerate, white dwarfs cool at almost constant radius, both L and $T_{\rm eff}$ becoming smaller. Due to the high conductivity of degenerate matter, and the fading of neutrino emission, the core quickly becomes isothermal. The overlying He layer (and H layer in DAs) then acts as a thermal blanket, controlling the rate at which energy leaks away to space and therefore the rate of evolution of the star. Since the He layer comprises the bulk of the envelope even in DA stars, its overall mass is an important factor which determines the speed at which a white dwarf travels down the white dwarf cooling track (Wood 1992, Winget & Van Horn 1987).

The time scale for white dwarf cooling can provide a robust determination of the age of the galactic disk (Winget et al. 1987). Since white dwarfs cool more slowly as their temperatures decrease, we observe more low-temperature white dwarfs than high-temperature ones. However, below about 4,000 K ($L \sim 10^{-4.4}\ L_{\odot}$), we suddenly find far fewer white dwarfs than expected. This is attributed to the finite age of the galaxy: simply, no white dwarfs are old enough to have cooled below $10^{-4.4}\ L_{\odot}$. The exact position of this cutoff, coupled with knowledge of the time it takes a star to get there, gives a lower limit to the age of the galaxy. A fundamental ingredient in this measurement is the He layer mass of white dwarfs and—by extension—PWDs (Wood 1992, Winget & Van Horn 1987).

1.3 The Purpose and Plan of this Work

We would like to use the observed properties of pulsating PWDs to determine their physical structure, clarify their evolutionary relationship to other post-AGB stars, and help calibrate measurement of the age of the galaxy through the white dwarf luminosity function. We would like to know whether the theories of lepton interactions correctly describe the production rates and therefore neutrino cooling of PWD evolution. A measurement of neutrino cooling effects might limit the set of possible models that could help solve the solar neutrino problem.

Without an underlying observational groundwork, we can accomplish none of these exciting and potentially useful goals. We will lay that groundwork, paving the way for future researches

to answer these questions, by providing the first comprehensive study of the pulsation properties of the GW Vir stars. We will identify their underlying pulsation patterns and use these patterns to determine stellar structure. We will find trends within the group of GW Vir pulsators which observationally define *when* during their evolution pulsation ceases, and *why* it does so. We will show how this information contains the seeds of an eventual explanation of the origin of the pulsations themselves. Finally, we will apply our new knowledge of GW Vir structure to show how future pulsation studies can test the underlying neutrino physics which controls the rate of PWD evolution.

This dissertation is divided into seven chapters. The first one has provided a context for the investigation by stating our general goals and outlining the current state of our knowledge of stellar evolution and the relation of our investigation to it. The second chapter reviews asteroseismology, developing the tools used to translate pulsation periods into knowledge of stellar properties. After that we present a summary of our prior knowledge of pulsating white dwarf and PWD stars. Chapter 4 presents observational results for additional PWD stars analyzed in the course of this thesis work. Next, we identify the characteristics of the group and then explain them in terms of a suggested type of driving mechanism. The sixth chapter develops the idea for a test of standard lepton theory based on observations of pulsating PWD stars. In the last chapter we summarize our conclusions, examine implications of this work for future studies of the formation of white dwarf stars and the age of the galaxy, and outline further avenues of investigation.

CHAPTER 2 TOOLS OF THE TRADE

"Although the growth of our knowledge is ever accompanied by a proportional growth of our estimate of the unknown, we seem already entitled to say that we have

Come on that which is, and caught
The deep pulsations of the world
Æonian music, measuring out
The steps of Time."

—Richard A. Proctor, *Other Worlds than Ours (1879)*

2.1 Introduction

Every physicist knows that one of the best ways to learn about the mechanical properties of any physical system is to study its normal modes of oscillation. This is true of metal bars and molecules, and also of stars. Whenever we find a group of stars that pulsate, we have the opportunity to study their structure in greater detail than is normally available to our instruments. Luckily, pulsating stars abound in the H-R diagram, and most stars will undergo several different kinds of pulsation during their lives. In the case where several modes are expressed by a star, we can, in analogy to terrestrial seismology, use bulk vibrations to sample depths inaccesible to direct observation. This application of normal mode analysis is known as asteroseismology

The best-known pulsators include the Cepheid variables, which alter their brightness on a timescale of days to weeks, and the RR Lyrae stars, which vary on a timescale of several hours. Though monoperiodic, the Cepheids are famous for the period-luminosity relationship which governs their light-curves. This relationship allows us to calibrate the distances to

other galaxies in which these bright supergiants are detected. The periods of RR Lyrae stars (which occupy the horizontal branch of stellar evolution) are used to measure their mass and luminosity. They are important for calibrating the distances to stellar clusters within and around our own galaxy.

Still, since these stars pulsate in a single radial mode, the probe afforded by their pulsation is limited. While the "famous" pulsating stars undergo a radial pulsation, *non*-radial oscillation provides a very large number of possible modes. The greater the number of different modes we can detect in a star, the more information we have with which to test our models. The grand champion pulsator in this sense is our own Sun. Due to its proximity, we have detected millions of different frequencies of variation (Harvey et al. 1996). Partly because of this, our knowledge of the solar interior is more extensive than that of any other star (see for instance Bahcall & Pinsonneault 1996). Fortunately, the white dwarf variables are nonradial pulsators as well.

As mentioned previously, there are three different regions of pulsational instability connected with white dwarf evolution. The first, and the subject of this thesis, is the PWD instability strip occupied by the PNNV and GW Vir stars. PG 1159, the prototype of the GW Vir class, is among the richest pulsators known. As we will discuss in the next chapter, over one hundred different periods have been identified in its lightcurve, providing strict tests for stellar models. The remaining white dwarf instability strips are the aforementioned DAV stars (also called ZZ Ceti stars after their class prototype) and the DBV stars.

Stellar pulsations come in two basic flavors, corresponding to two different kinds of restoring force. Pulsations in the Sun and in most other pulsators, including Cepheids and RR Lyrae stars, are p-modes, so called because gas pressure serves as the restoring force (like in sound waves). On the other hand, the PNNV, GW Vir, ZZ Ceti, and DBV stars are all g-mode pulsators. Here buoyancy serves as the restoring force. For a given mean density, p-modes are generally much higher in frequency (shorter in period) than g-modes, since pressure is a much stiffer "spring" than buoyancy.[1] However, because of the steep gravitational gradient in white

[1]The bobbing of a cork in a pool of water is far slower than the oscillations of the sound it makes in doing so.

dwarf and PWD stars, their characteristic g-mode periods are quite short by stellar measures, anywhere from a hundred to several thousand seconds. In such stars, p-modes would have even shorter periods, though: a second or less (Saio, Winget & Robinson 1983). Searches for variability on such short timescales in white dwarfs have been so far unsuccessful (Kawaler et al. 1994).

In Cepheids, motion is strictly radial. Each pulsation cycle causes the star's overall radius to expand and contract by 5-10% (see, e.g., Nikolov & Tsvetko 1972). The ratio of the non-radial to the radial component of motion in white dwarf pulsation is about a thousand to one—to high precision, the radius remains constant throughout the pulsation cycle (Robinson, Kepler, & Nather 1982). The Cepheids and white dwarf variables do have one thing in common, however. For both, the luminosity variations we see are due to changes in surface temperature caused by the mass motions. In white dwarfs, the mean surface temperature changes by about 200 K over a pulsation cycle (Robinson, Kepler, & Nather 1982). The temperature variation in Cepheids is about ten times greater, enough to change the spectral class of the star from week to week (Kukarkin et al. 1969).

The set of periods excited to detectable limits in white dwarf stars is determined by the interplay of several processes. The first is the driving of pulsation by some—as yet unspecified—mechanism (no matter how melodious the bell, it must be struck to be heard). Second is the response of the star to the driving taking place somehere in its innards. A pulsating PWD star is essentially a (spherically symmetric) resonant cavity, capable of sustained vibration at a characteristic set of frequencies. Those frequencies are determined by the structure of the star, its mass and luminosity, as well as the thickness of its surface layers. Finally, the actual periods we see are affected by the mechanism through which internal motions are translated into observable luminosity variations. This is the so-called "transfer function," and clues to its nature are to be found in the observed variations as well.

If we wish to make the most of the observed periods, we must understand all of these mechanisms in as much detail as possible. However, we can learn a great deal by simply comparing the periods of observed light variations to the normal-mode periods of model stars.

We discuss these calculations and what they tell us in the next section. In § 2.3, we discuss the problem of driving pulsation in white dwarf and PWD stars. After that we discuss how stellar evolution can affect pulsation periods, and how we can measure these changes. We summarize all these asteroseismological tools, and how we can and will apply them to pulsating PWDs, in the final section.

2.2 Asymptotic Relations for g-Mode Periods

The normal mode oscillations of white dwarf and PWD stars are most compactly described using the basis set of spherical harmonic functions, Y_m^ℓ, coupled with an appropriate set of radial wave functions R_n. Here n is the number of nodal surfaces in the radial direction, ℓ denotes the number of nodal planes perpendicular to such surfaces, and m is the number of these planes which include the pulsational axis of the star.

2.2.1 Rotational Frequency Splitting

For modes of a given ℓ, there are $2\ell + 1$ available values for m: $-\ell, -(\ell-1), \ldots, (\ell-1), \ell$. Components of different m will have the same period in the absence of azymuthally dependent processes like rotation or a magnetic field. Stellar rotation, for example, increases the frequency of $m < 0$ components and decreases the frequency of $m > 0$ components with respect to $m = 0$. The frequency splitting, $\delta\nu$, for peaks of consecutive m is set by the rotation period Π_{rot} according to

$$\delta\nu_{n\ell} = \Pi_{rot}^{-1} \left(1 - C_{n\ell}\right), \tag{2.1}$$

where $C_{n\ell} \approx (\ell(\ell+1))^{-1}$ for white dwarf stars (Brickhill 1975). We thus have a way to measure the rotation period of pulsating stars, if we can identify—from the number of components in a mode, or by other means—the value of ℓ we observe. This might be an enormously complicated problem if modes of many different ℓ and m were all evident at once in a stellar light curve.

Fortunately, we do not expect to observe modes with ℓ much greater than $\ell = 2$ or 3. This is because as the number of nodal lines on the surface increases, brighter and darker regions on either side tend to cancel each other out when viewed from afar. We observe only the changing

total brightness of a star integrated over its entire visible surface. This will tend to render modes of large ℓ undetectable (Dziembowski 1977).

2.2.2 Period Spacing

The periods of g-modes of given ℓ are expected to increase monotonically as the number of radial nodes n increases. The reason is that the buoyant restoring force is proportional to the total mass displaced, and this mass gets smaller as the number of radial nodes increases. A weaker restoring force implies a longer period (see, e.g., Cox 1980).

One of the simplest methods of calculating the actual oscillation periods available within any resonant cavity is the WKB approximation, familiar to every student of introductory quantum mechanics. The basis for this approximation is the assumption that the radial wavelength is very much shorter than length scales over which the relevant physical variables are changing within the cavity. This will be more nearly true for g-modes of large n. In this "asymptotic limit," the WKB approximation yields the simple relationship

$$\Pi_n \cong \frac{\Pi_0}{[\ell(\ell+1)]^{1/2}}(n+\epsilon) \qquad\qquad n \gg \ell, \tag{2.2}$$

where Π_n is the g-mode period for a given value of n, and Π_0 is a constant that depends on the overall structure of the star (see, e.g., Tassoul 1980, Kawaler 1986).[2]

Equations (2.1) and (2.2) lead us to expect a relatively orderly pattern of modes from observations of pulsating white dwarf and PWD stars. In particular, Equation (2.2) implies that modes of a given ℓ should form a sequence based upon a fundamental period spacing $\Delta\Pi = \Pi_0/\sqrt{\ell(\ell+1)}$. From Equation (2.1), we suspect that each mode in this sequence might exhibit $2\ell+1$ components split equally in frequency, either by rotation or some other mechanism, as long as $\delta\nu < \Delta\Pi/\Pi^2$. This is the overall pattern we seek through the observations described in the next two chapters.

Once we identify the period spacing from a pulsating star's lightcurve, we can compare this spacing to that in models to decipher the star's structure. Kawaler (1986) found that the

[2]The additional constant ϵ is assumed to be small, though its exact value depends on the boundary conditions. Since the actual boundary conditions depend on the period, ϵ probably does, too.

parameter Π_0 in static PWD models is dependent primarily on the overall stellar mass and luminosity, with a weak dependence on composition. Kawaler & Bradley (1994) present the approximate relation

$$\Pi_0 \cong 15.5 \left(\frac{M}{M_\odot}\right)^{-1.3} \left(\frac{L}{100 L_\odot}\right)^{-0.035} \left(\frac{q_y}{10^{-3}}\right)^{-0.00012} \tag{2.3}$$

where q_y is the fraction by mass of He at the surface.[3]

2.2.3 Mode Trapping

A final complication concerning the expected pattern of modes can be caused by composition discontinuities within the star. Recall that post-AGB stars are stratified, with a C/O core overlaid by a relatively pure He layer and perhaps also a thin layer of H at the surface. The WKB assumptions are violated near the transition zone from one layer to another, as the mean molecular weight changes much more quickly than even the highest n wave function. However, the effect of these discontinuities is fairly simple, as first described analytically by Carl Hansen (1987 private communication) and explored by Kawaler & Weiss (1990) and Brassard et al. (1991).

When one of the nodes in a radial wave function coincides with the transition between layers, its amplitude below the transition region is greatly diminished—the mode becomes "trapped" in the outer layers of the star. This will significantly alter the period compared to that if trapping didn't take place. Subsequent modes will have nodes which fall outside the discontinuity. Their periods will be closer to the asymptotic values from Equation (2.2). Eventually, consecutive radial modes will have nodes which again approach the discontinuity, trapping will again become significant, and the pattern will repeat. This cycle of variation away from and then back to an average period spacing is known as the *trapping cycle* (Bradley 1994). The *trapping period*, which is the number of modes of consecutive n between each return to average spacing, depends on the depth of the transition zone causing the trapping. The greater the depth of the discontinuity, the smaller the trapping cycle.

[3]Note that the sign of the exponent in the L term is in error in Kawaler & Bradley (1994).

We are now equipped with some powerful tools for the possible study of white dwarf and PWD stars. We will see in the following chapters that to a large extent their pulsation patterns really do conform to the expectations we have just outlined. Other questions, however, will only be answered from knowledge of the cause of the light variations we measure. In the case of the PWDs, this is chief among the mysteries we would like to solve. The most telling clue will be the extent of the region of instability in the H-R diagram—derived in part from pulsational analysis of the structure of stars which bracket this region. The next section provides some of the background we will need to attack these issues.

2.3 Cause of Pulsation in White Dwarf and Pre-White Dwarf Stars

In a star, energy generally flows down the temperature gradient from the central regions to the surface in a smooth, relatively unimpeded fashion. Of course small, random perturbations to this smooth flow constantly arise. The situation is stable as long as such perturbations quickly damp out, restoring equilibrium. We have already discussed two mechanisms which tend toward equilibrium: the restoring forces of buoyancy and pressure which define the nature of g- and p-modes. They resist mass motions and local compression or expansion of material away from equilibrium conditions.

Thermodynamic quantities such as the derivatives of temperature and opacity affect the question of local equilibrium. In general, if material in a star is compressed, its temperature goes up while its opacity decreases. The higher temperature causes more radiation to flow out to the surrounding material, while lower opacity decreases the efficiency with which radiation is absorbed. From the first law of thermodynamics, an increasing temperature accompanied by net heat loss implies that work is being done on the parcel by its surroundings. Similar arguments show that work is done on the parcel during expansion, also. Thus any initial perturbation will be quickly damped out—each parcel demands work to do otherwise. The requirement that a region lose heat when compressed and gain heat when expanded is the fundamental criterion for stability. When the opposite is true, and work is done by mass elements on their surroundings during compression and expansion, microscopic perturbations

can grow to become the observed variations in pulsating stars.

2.3.1 The κ-γ Mechanism

Under certain circumstances, the sign of the opacity derivative changes compared to that described above. If the opacity, κ, increases upon compression, then heat flowing through a mass element is trapped there more efficiently. Within regions where this is true, work is done on the surrounding material. Thus these regions can help destabilize the star, if this driving is not overcome elsewhere in the star. However, other regions, where work is required to compress and expand material, tend to damp such pulsation out. Global instability arises only when the work performed by the driving regions outweighs the work done on the damping regions over a pulsation cycle. In this case, the flow of thermal energy can do mechanical work, and this work is converted into the pulsations we observe.

This method of driving pulsation is called the κ mechanism. A region within a star will drive pulsation via this mechanism if its opacity derivatives satisfy the condition (see for instance Cox 1980)

$$\frac{d}{dr}\left(\kappa_T + \frac{\kappa_\rho}{\Gamma_3 - 1}\right) > 0 \tag{2.4}$$

where

$$\kappa_T \equiv \left(\frac{\partial ln\kappa}{\partial lnT}\right)_\rho, \qquad \kappa_\rho \equiv \left(\frac{\partial ln\kappa}{\partial ln\rho}\right)_T, \quad \text{and} \quad \Gamma_3 - 1 \equiv \left(\frac{\partial lnT}{\partial ln\rho}\right)_S.$$

Here S represents the specific entropy, κ is the opacity in cm^2/g, and the variables r, ρ, and T all have their usual meaning.

Equation (2.4) is satisfied most commonly when some species within a star is partially ionized. In particular, κ_T usually increases in the hotter (inner) portion of a partial ionization zone and decreases in the cooler (outer) portion. Thus the inner part of an ionization zone may drive while the outer part damps pulsation. The adiabatic exponent, $\Gamma_3 - 1$, is always positive but usually reaches a minimum when material is partially ionized. This enhancement of the κ mechanism is called the γ mechanism. Physically, the γ mechanism represents the conversion of some of the work of compression into further ionization of the species in question. This tends to compress the parcel more, aiding the instability. Release of this ionization energy during

expansion likewise increases the purturbation. Since they usually occur together, instabilities caused by both the opacity and ionization effects are known as the κ-γ mechanism.

The pulsations of Cepheid and RR Lyrae variables, for instance, are driven via the κ-γ mechanism operating within a region where HeI and HeII have similar abundances. This same partial ionization zone is apparently the source of instability for the DBV white dwarfs. The variations observed in ZZ Ceti white dwarfs have long been attributed to partial ionization of H. However, Goldreich & Wu (1998) have recently shown the ZZ Ceti pulsations can be driven through a different mechanism in efficient surface convection.[4] Great efforts have been expended by theorists attempting to explain GW Vir and PNNV pulsations in terms of some combination of C and O partial ionization (Starrfield et al. 1983; Stanghellini, Cox, & Starrfield 1989). A primary difficulty arises from the damping effects of He in the driving zone, which can "poison" the driving. More recently, Saio (1996) and Gautschy (1997) attempted to explain driving in terms of an "opacity bump" in the models, without partial ionization—in other words, using the κ mechanism alone. A fundamental problem has been the lack of information on the exact extent of the instability strip and the structure of the pulsating stars themselves. Our goal in the next three chapters will be to define as precisely as possible the observational attributes which any proposed driving source must reproduce. Whether or not the mechanism we identify is correct, we hope to lay the groundwork for future studies which will eventually provide a definitive answer to this question.

2.3.2 Correlations between Driving and Observed Periods

When pulsation does take place in a star, we wish to know what relationship the driving has to the periods we observe. In general, no star will respond to driving at just any arbitrary period; the range of observed variations is restricted by the driving mechanism. Cox (1980) showed that the approximate pulsation period is determined by the thermal timescale of the

[4]Such convection zones often accompany regions of partial ionization associated with the κ-γ mechanism. However, the driving proposed by Goldreich & Wu is not directly related to ionization. It is possible this theory might eventually be expanded to account for DBV pulsation as well. It is unlikely to find application in PWDs, though, since models of PG 1159 stars generally do not support convection.

driving zone:

$$\Pi \sim \tau_{\rm th} = \frac{c_{\rm v} T m_{\rm dz}}{L}. \tag{2.5}$$

Here $\tau_{\rm th}$ is the thermal timescale, $c_{\rm v}$ is heat capacity, and $m_{\rm dz}$ is the mass above the driving zone. This equation gives the approximate time it takes the star to radiate away—via its normal luminosty, L—the energy contained in the layers above the region in question. Though Cox derived this relationship for radial modes, Winget (1981) showed that it applies equally well to nonradial g-mode pulsation.

The basic idea behind Equation (2.5) is that energy must be modulated at approximately the same rate at which it can be dammed up and released by the driving zone. Consider the question of whether a given zone can drive pulsation near a certain period. If the driving zone is too shallow, then the thermal timescale is shorter than the pulsation period. Any excess heat is radiated away before the compression increases significantly. Thus, it can't do work to create mechanical oscillation on the timescale in question. If the driving zone is too deep ($\tau_{\rm th} > \Pi$), then excess heat built up during contraction is not radiated away quickly enough during expansion; it then works against the next contraction cycle. Of course, this relationship is only approximate, and other factors might intervene to limit pulsation to periods far from from those implied by Equation (2.5). One such factor is the range of pulsations a star can sustain in the form of standing waves. Hansen, Winget, & Kawaler (1985) showed that there is a maximum period for white dwarf and PWD stars above which oscillations will propagate only as running waves that quickly damp out. They attempt to calculate this maximum g-mode period, $\Pi_{\rm max}$, to explain the observed trend of ZZ Ceti periods with $T_{\rm eff}$. However, some of the quantities required for an exact calculation are observationally unconstrained. We will therefore concern ourselves for now only with the dependence of $\Pi_{\rm max}$ on various global stellar quantities. We can recast their equations (6) through (8) as the proportionality

$$\Pi_{\rm max}^2 \propto \frac{R^2}{[\ell(\ell+1)]T_{\rm eff}} \tag{2.6}$$

where R is the stellar radius and ℓ is the pulsation index introduced earlier. For a complete derivation of this equation, see the appendix.

For cool white dwarfs of a given mass, the radius is roughly constant with time, and $\Pi_{\rm max}$ is expected to increase as stars evolve to lower $T_{\rm eff}$ and the driving zone sinks deeper. Cooler ZZ Ceti and DBV stars should in general have longer periods (we will see in the next chapter that, for the ZZ Cetis at least, this is indeed the case).

However, in PWDs degeneracy is not yet sufficient to have halted contraction, and the R dependence is probably still a factor in determining how $\Pi_{\rm max}$ varies through the instability strip. We cannot yet say which dominates: the shrinking radius which tends to decrease $\Pi_{\rm max}$, or the falling $T_{\rm eff}$ which has the opposite effect. We cannot even predict in advance whether $\Pi_{\rm max}$ is a factor in determining the pulsation periods at all. In Chapter 5, we answer these questions in view of the observed properties of both the PNNV and GW Vir stars.

2.4 Rates of Period Change

As white dwarfs and PWDs evolve, the periods of each of their pulsation modes will change in response to changing stellar structure. Due to the relatively rapid evolution especially of PWDs, these period changes are measureable. For the GW Vir and PNNV stars, measurement of dΠ/dt can help constrain the progenitor models. We can also learn the importance of different physical processes to PWD evolution. In Chapter 6 we will discuss the possible calibration of one such process—neutrino emission—via measurement of period changes in cool GW Vir stars.

Unfortunately, the expected changes are too small to detect from simple comparison of the period from one year to that of the next. To determine dΠ/dt in PWD stars, a better technique is to measure the cumulative phase change in a mode with a slowly changing period. This is accomplished by comparing the observed times of maxima (O) in the light curve to the times of maxima (C) calculated from an assumption of constant period. The resulting plot of $(O-C)$ shows the phase drift associated with a changing period. A constant rate of period change, dΠ/dt, enters as a quadratic term in time:

$$(O-C) \approx \frac{1}{2}\frac{1}{\Pi_{t_o}}\frac{d\Pi}{dt}(t-t_o)^2 \quad [\rm sec] \tag{2.7}$$

where Π_{t_o} is the period at time t_o (see for example Winget et al. 1985, 1991 and Kepler et al. 1995). To measure $d\Pi/dt$ with confidence, the star must of course have stable and fully resolved pulsation periods, with reliable phase measurements from season to season.

Kawaler et al. (1985) and Kawaler & Bradley (1994) present predicted values of $d\Pi/dt$ for models relevant to GW Vir and PNNV stars; the only observed value of $d\Pi/dt$, that for PG 1159 itself, is consistent with these models. However, as Kawaler & Bradley (1994) demonstrated, for a star as hot as PG 1159, $d\Pi/dt$ is strongly affected by mode trapping. They also show that, in general, $d\Pi/dt$ should be positive. This reflects the overall cooling of the model (Winget et al. 1983). Trapped modes, however, are concentrated in the outer layers, within which contraction dominates cooling; therefore trapped modes can show periods which decrease with time. Thus, mode trapping can complicate the interpretation of measured period changes in hot PWDs. As GW Vir stars cool, the surface contraction rate decreases relative to the cooling rate of the interior. So, while mode trapping can still influence the pulsation period distribution, the rates of period change become more similar from mode to mode in cooler GW Vir stars. Kawaler & Bradley (1994) found that the sign of $d\Pi/dt$ could be different for different modes in hot GW Vir models; by the time those models evolve to the cool end of the strip, the period change rates are all positive.

2.5 Summary

We have now compiled a list of questions we can answer by observing PWD pulsations. We can measure individual white dwarf mass and luminosity through identification of the period spacing. Uniform frequency splitting within modes of given ℓ indicate the rate of rotation, and aid in determining the overall pulsation pattern. Abrupt composition gradients show themselves through periodic deviations away from constant period spacing, allowing us to measure envelope layer masses. These are questions of stellar structure, and their answers, derived in Chapter 4, will tell us the precise boundaries of the instability strip, in other words, when the pulsations begin and end in the evolution of PWD stars of various mass. This knowledge, coupled with the timescales of driving and the maximum g-mode period in models

matched to the observations, will provide strict constaints on the allowable form of the driving mechanism. This information is absolutely necessary to any research program designed to discover why PWDs pulsate in the first place. It will also allow us, in Chapter 6, to precisely identify which PWDs should be most dominated by neutrino cooling. We can then show how measurement of their period changes, using the techniques outlined in § 2.4, will test our fundamental knowledge of neutrino interactions in the dense plasma of a stellar interior.

In the next chapter, we will outline the status of our knowledge of PWDs before this investigation was undertaken. Because of their many similarities (and telling differences) to the GW Vir and PNNV pulsations, we also present a summary of previous ZZ Ceti and DBV observations, in the hopes that they will provide hints to help guide our analysis of additional PWD lightcurves in Chapters 4 and 5.

CHAPTER 3 THE PULSATING WHITE DWARF AND PRE-WHITE DWARF STARS

" 'The stars,' she whispers, 'blindly run;
A web is wov'n across the sky;
From out waste places comes a cry,
And murmurs from the dying sun . . . ' "
—Alfred Lord Tennyson, *In Memoriam A. H. H. (1833)*

3.1 Introduction

To put the questions raised in Chapter 2 into context, it is instructive to consider the current status of all classes of pulsating white dwarf stars, including the DBVs and ZZ Cetis. First discovered in 1968, the number of ZZ Ceti pulsators is currently 24. Even though individual ZZ Ceti stars have no clear patterns which underly their observed periods, Clemens (1994) successfully showed that when their periods are considered together, a single pattern emerges. In addition, both the ZZ Ceti and DBV instability strips are precisely defined within narrow ranges of $\log g$ and $T_{\rm eff}$. Each represents a more homogenous group of stellar properties than the PWDs.

There are eight known PNNV stars, and four GW Vir stars (Ciardullo & Bond 1996). Of these, only two have had their pulsations studied in any detail. Therefore, each pulsator must be evaluated alone in terms of its pulsation properties, in order to establish its individual parameters by comparison with the models. If we wish to make specific claims regarding the group properties of either class, we need to explore in detail the pulsations of more of their members. In the Chapter 4 we will move toward this goal.

In the next two sections of this chapter, we present brief summaries of the ZZ Ceti (a.k.a. DAV) and DBV instability strips. Both their similarities to, and differences from, the PWD variables will be instructive when we evaluate the group properties of the latter in Chapter 5. In the final section, we will summarize results from the two successful PWD pulsation studies completed prior to this thesis: those of the GW Vir star PG 1159, and of the PNNV star NGC 1501.

3.2 The ZZ Ceti Stars

The first variable white dwarf was discovered over thirty years ago by Arlo Landolt, who found that the brightness of the DA star HL Tau 76 changed periodically by a few percent every few minutes (Landolt 1968). Further analysis established that the variations were intrinsic, stable, g-mode pulsations (Chanmugam 1972, Warner & Robinson 1972, Osaki & Hansen 1973). Over the next decade, additional variable DA white dwarfs were found, and in 1977, McGraw demonstrated that they represent a well-defined class of pulsators now known as the ZZ Ceti stars. The ZZ Ceti stars occupy the approximate temperature range $11,000\ \mathrm{K} \gtrsim T_{\mathrm{eff}} \gtrsim 13,000\ \mathrm{K}$ (Greenstein 1984; Weidemann & Koester 1984; Bergeron, Wesemael, & Fontaine 1992). Their masses, derived from spectroscopic measurements of $\log g$ (~ 8) and T_{eff}, cluster closely about a mean of $0.56\ M_{\odot}$ (Bergeron, Saffer, & Leibert 1990), and their luminosities are all less than $0.01\ L_{\odot}$. For extensive reviews of ZZ Ceti properties, see Kleinman (1995), Clemens (1994), and Winget (1988).

The pulsation periods of ZZ Ceti stars lie in the range of 100 to 1200 seconds, with a clear trend toward longer periods and larger amplitudes with decreasing T_{eff} (Winget & Fontaine 1982, Clemens 1994). This is generally attributed to the sinking of the driving zone to longer thermal timescales as stars evolve to cooler temperatures through the instability strip. Equation (2.5) then implies longer periods. As the driving zone deepens, the amount of overlying material increases, which increases the heat energy available for conversion to work, explaining the larger amplitudes seen in cooler pulsators as well (Robinson 1979, McGraw 1980, Winget & Fontaine 1982; c.f. Wu 1998).

Despite the large sample of ZZ Cetis available for observation, it is difficult to independently identify the pulsation modes seen in any one star. This is because those with the most stable pulsation patterns generally pulsate with the fewest modes. Conversely, the greater the number of modes observed, the more variable those modes are in amplitude—some disappearing (and sometimes later reappearing) altogether on timescales of days, months, and years (Clemens 1994, Kleinman 1995, Kleinman et al. 1998).

A possible breakthrough in identifying the values of n and l for any of the ZZ Ceti stars was by Clemens (1994). No individual star pulsates in enough stable modes to establish an overall pattern such as the one predicted in Equation (2.2). Clemens reasoned as follows: the narrow range of mass and $T_{\rm eff}$ spanned by members of the class means that their pulsations might all follow the same pattern. He found that if he listed the most "stable" periods from the hotter DAs together—as if they came from a single object—they formed a series of period clumps. These groups conformed to a pattern of equal period spacing consistent with Equation (2.2). This suggested an identity for n and l for every mode in every star in the sample. In particular, he showed that the group with the lowest period should be the $n = 1$, $\ell = 1$ mode, and its observed period implied a large value for the hydrogen layer thickness. Recently, Kleinman (1995, 1998) showed that this same pattern extends to the cooler ZZ Ceti stars as well.

As we mentioned in Chapter 2, the exact source of driving in the ZZ Ceti stars has long been attributed to cyclical ionization of hydrogen at the base of the convection zone (McGaw 1977, and Dolez & Vauclair 1981, Winget 1981). Although models based on this theory reproduce the observed trends just mentioned, they do a poor job reproducing the observed red edge (low $T_{\rm eff}$ limit) of the strip—in other words, they cannot tell us when in the life of a DA white dwarf pulsation will end.

The recent work of Wu (1998), some of which was anticipated by Brickhill (1983), attributes driving to the convection zone itself rather than the partial ionization zone at its base. Wu points to several particular difficulties with the more traditional κ-γ mechanism in ZZ Ceti stars. The thermal timescale in the κ-γ driving zone is actually much smaller than the observed periods. The zone is apparently too thin to overcome radiative damping in the interior. Most

theories of κ-γ driving require that the convective flux be held fixed during pulsation—an assumption shown by Brickhill (1983, 1991a, 1991b) to be incorrect. Wu shows that the base of the convection zone is the likely source of driving, based on Brickhill's assumption that the rest of the convection zone responds *instantaneously* to the changing flux due to driving near its base. One of the most compelling attributes of this theory is its ability to more or less correctly reproduce the observed blue *and red* edges of the ZZ Ceti instability strip.

The theory of convective driving developed by Brickhill and Wu is intriguing, but unfortunately we probably won't be able to use it to help us understand the PWD stars. This is due to the simple fact that models of the PG 1159 stars have weak, if any, convection zones.[1]

3.3 The DBV Stars

After H ionization was identified as the probable cause of pulsation in the ZZ Ceti stars, Winget (1981) developed models which showed that He ionization could drive pulsation in DB white dwarfs as well. Since helium has a higher ionization energy than hydrogen, pulsations at similar periods would require stars with hotter atmospheres, and Winget suggested that variable DB stars should be sought in the 20,000 K to 30,000 K range. This theoretical instability strip would constitute an extension of the classical Cepheid instability strip to lower L and higher $T_{\rm eff}$.

Winget subsequently discovered pulsations in GD 358 (Winget et al. 1982), a DB white dwarf with an effective temperature of about 24,000 K. Seven other DBV stars have since been discovered, all falling in the approximate temperature range $21,500\ {\rm K} \gtrsim T_{\rm eff} \gtrsim 24,000\ {\rm K}$ (Koester et al. 1985; Liebert et al. 1986; Thejll, Vennes, & Shipman 1991). They are more luminous than the ZZ Ceti stars, at ~ 0.1–$0.03\ L_{\odot}$, but their exact g and $T_{\rm eff}$ are more difficult to determine because of their higher temperatures and lack of hydrogen lines. Because of this, and their smaller numbers, it is unclear whether they exhibit any of the trends found in the ZZ Ceti pulsations. GD 358 is an extremely rich pulsator, however, and the analysis of its lightcurve (as well as its discovery) is one of the great success stories of asteroseismology.

[1] They do, however, have partial ionization zones. We have hope, therefore, of determining their driving source without resorting to the invention of even more exotic theories—though of course it could come to that.

In 1990, GD 358 was observed with the WET. Winget et al. (1994) report their analysis of the virtually uninterrupted lightcurve—spanning almost two weeks—that resulted. Over 180 different pulsation periods were identified, conforming to a pattern of equal spacing as in Equation (2.2). Many of these modes were triplets, suggesting they were likely $\ell = 1$ modes.[2] The frequency splitting varied systematically from mode to mode, the larger splittings consistent with a stellar rotation period of 0.88 days, the smaller with 1.6 days. Though initially interpreted as a signal of differential rotation, Kawaler, Sekii & Gough (1998) show that this cannot be so. The $m = 0$ components of the triplets were also slightly off center toward lower frequency. Jones et al. (1989) had already shown that a stellar magnetic field could cause this kind of asymmetry. Here the shift of the $m = 0$ components was consistent with a global magnetic field of 1300 ± 300 G; it is possible that this field could account for the changing mean splitting as well.

Bradley & Winget (1994) determined that the best match to the GD 358 period spectrum was acheived by a model with a mass of $0.61 \pm 0.03\ M_\odot$, a luminosity of $0.050 \pm 0.012\ L_\odot$, and $T_{\rm eff} = 24,000 \pm 1,000$ K. In particular, the luminosity coupled with the measured apparent brightness indicated that GD 358 lies at a distance of 42 ± 3 pc from the Earth. This marked the first use of asteroseismology as a "distance indicator." Finally, periodic deviations from the mean period spacing in the data implied a helium layer $1.2 \times 10^{-6}\ M_\odot$ thick. This last result has implications for a possible evolutionary connection between the DBV and GW Vir stars (Dehner & Kawaler 1995), as we will see when we discuss PG 1159 in the next section.

3.4 The PNNV and GW Virginis Pre-White Dwarf Pulsators

Finally, we arrive at the PNNV and GW Vir stars. At 80,000 K, the cool end (or "red edge") of the instability strip merges with the evolutionary region occupied by the hottest (primarily DO) white dwarfs. The "blue edge" on the other hand is occupied by some of the hottest stars known, some with temperatures in excess of 170,000 K. Of the three post-AGB

[2]Other arguments support this conclusion, including the very low model mass—ruled out by even crude measurement of $\log g$ and $T_{\rm eff}$—required to reproduce the measured value of Π_0 if the triplets were $\ell > 1$ with some components "missing."

instability strips we have discussed, this is the least well defined observationally, for several reasons: the high rate of PWD evolution, which decreases the sample size available for study;[3] the difficulty of determining parameters such as g and $T_{\rm eff}$ for stars above 80,000 K and with $\log g = 6$–8; and the fact that some stars in the strip are probably still approaching maximum $T_{\rm eff}$ while others are already cooling toward white-dwarfdom, making it difficult to establish their precise evolutionary status from the observations (Werner 1995).

Of the two types of PWD pulsators, the GW Vir stars tend to have higher gravities ($\log g \gtrsim 7$), and, by definition, they have no nebula. Thus they appear to be slightly more evolved than the PNNV stars. The PNNV stars in general pulsate at longer periods (around 1000–3000 s) than the GW Vir stars (which all pulsate at periods of less than 1000 s). There is a well-defined trend to shorter period from the most luminous PNNV stars to the coolest, faintest GW Vir stars. This is clearly evident in Figure 3.1, which shows the amplitude spectra of six PNNV and GW Vir stars, ordered with $T_{\rm eff}$ decreasing from top to bottom. Recall that in the ZZ Ceti stars, the opposite trend is seen—cooler stars have longer periods, a fact explained by the sinking of the driving zone to longer thermal timescales. If the periods in GW Vir and PNNV stars are likewise determined by the depth of the driving zone, then variable PWDs of a given mass should follow the same trend, since every opacity feature in PWD model envelopes sinks deeper, toward longer timescales, with decreasing $T_{\rm eff}$ as well. The period trend is a clue that perhaps some mechanism other than the changing depth of a driving zone governs PWD periods.

One possible candidate is the changing value of the maximum g-mode period. If $\Pi_{\rm max}$ is somehow related to the range of periods we see in a particular PWD, then the R dependence might offset the decreasing $T_{\rm eff}$ in Equation (2.6) enough to account for the trend we see, since PWDs are expected to shrink as they evolve through the instability strip. Unfortunately, the precision of spectroscopic measurements of $\log g$ for the stars in Figure 3.1 are insufficient to determine their run of radii.

Asteroseismology gives us the means to determine stellar properties more precisely, in order

[3] Despite their large range of L and $T_{\rm eff}$, PWDs spend less far time in this instability strip than either the DBV or ZZ Ceti stars spend in theirs.

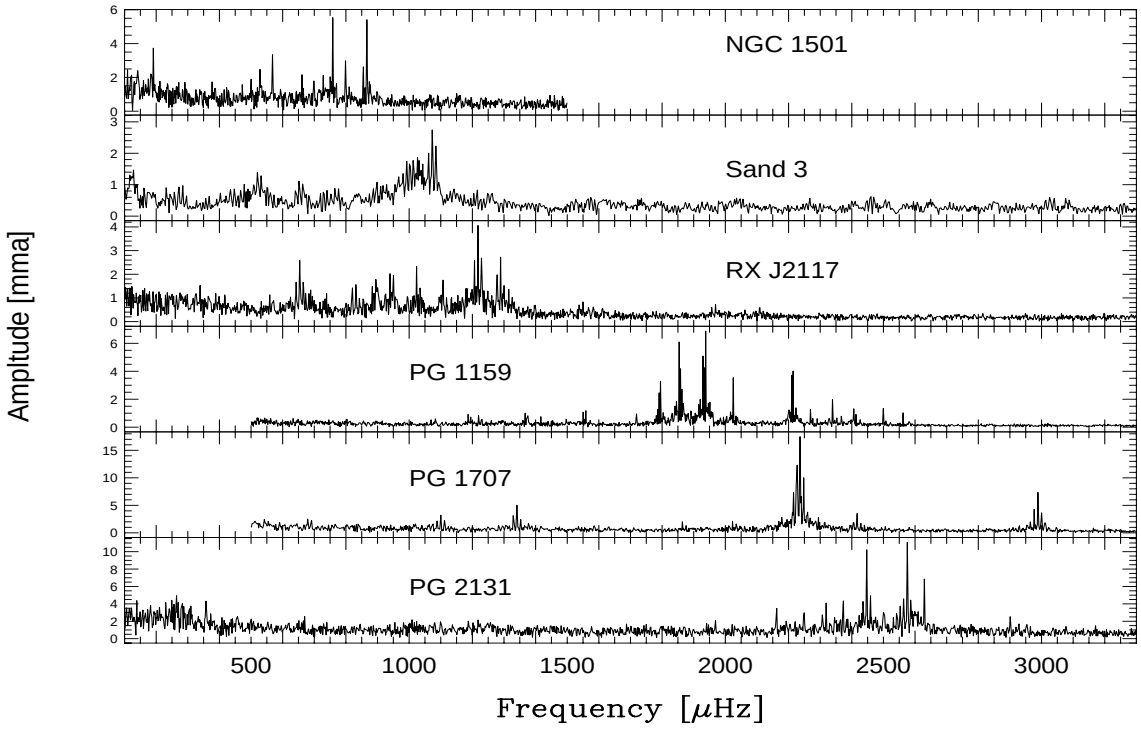

Figure 3.1 Amplitude spectra of six PNNV and GW Vir stars, in order of decreasing $T_{\rm eff}$ from top to bottom (from Kawaler 1996).

to answer the question of whether the trend is caused by this amplitude-limiting factor. One of our goals in analyzing additional PWD period spectra in Chapter 4 is to increase the precision of log g measurements. This will provide us with the data needed to probe the correlation between the period trend pictured in Figure 3.1 and the maximum period implied by Equation (2.6).

We also seek the precise boundaries of the instability strip, in hopes this will illuminate the source of driving by telling us under what conditions PWDs pulsate. Another problem this might help solve is the apparent location of about ten non-pulsatoring PG 1159 stars within the PWD instability region of the H-R diagram. It may be that with more precise knowledge of the instability boundaries, some or all of the non-pulsators can be observationally excluded from the region. Our findings will undoubtedly raise new questions, while allowing us to answer only some of them. For the rest, we will point out directions that might eventually lead us to

anwers. Before we get so far, however, we must first summarize what we already know about specific PWD pulsators.

3.4.1 The GW Virginis Star PG 1159–035

PG 1159–035 (a.k.a GW Vir, hereafter PG 1159) is, as mentioned previously, the prototype of the PG 1159 spectral class, which includes as a subset most of the variable PWDs. It is also the prototype of the GW Virginis pulsators, and it was the first star to which most of the asteroseismological tools from Chapter 2 were successfully applied.

After the discovery of its variability by McGraw et al. (1979) PG 1159 became the target of an increasingly intense observational program that attempted to unravel the many "frequency bands" in the Fourier transform of its lightcurve (Winget et al. 1985). Eventually, it was shown that these bands were separated by multiples of a fundamental period spacing, *if* they were assumed to represent $\ell = 1$ modes (Kawaler 1986, 1987). However, it remained impossible to associate the frequency bands compellingly with specific values of n, since their underlying mode structure could not be resolved with single site data alone.

Winget et al. (1991) report the results of the 1989 WET observations of PG 1159. A portion of the Fourier transform of the WET lightcurve is shown in Figure 3.2. What had been seen formerly as three unresolved bands of power are here resolved into three distinct triplets. The frequency splitting between peaks is nearly the same for each triplet, and the triplets are nearly equally spaced one from another in period. In all, twenty consecutive triplets like these were identified in the PG 1159 transform, with an average period spacing of 21.5 s (Winget et al. 1991). The average frequency splitting within triplets was 4.2 μHz. This was seen as strong evidence that these are $\ell = 1$ modes, with the triplet splitting caused by stellar rotation. Further evidence came from the identification of several quintuplets, each with an internal frequency splitting of 7.0 μHz. The average period spacing between quintuplets was found to be 12.5 s. From Equation (2.1), the expected ratio of $\delta\nu$ for $\ell = 1$ to $\ell = 2$ modes is 0.6, which is nearly the same as the observed ratio between the triplet and quintuplet rotational splittings. Equation (2.2) predicts a ratio of 1.73 between Π_0 for $\ell = 1$ and for $\ell = 2$ modes.

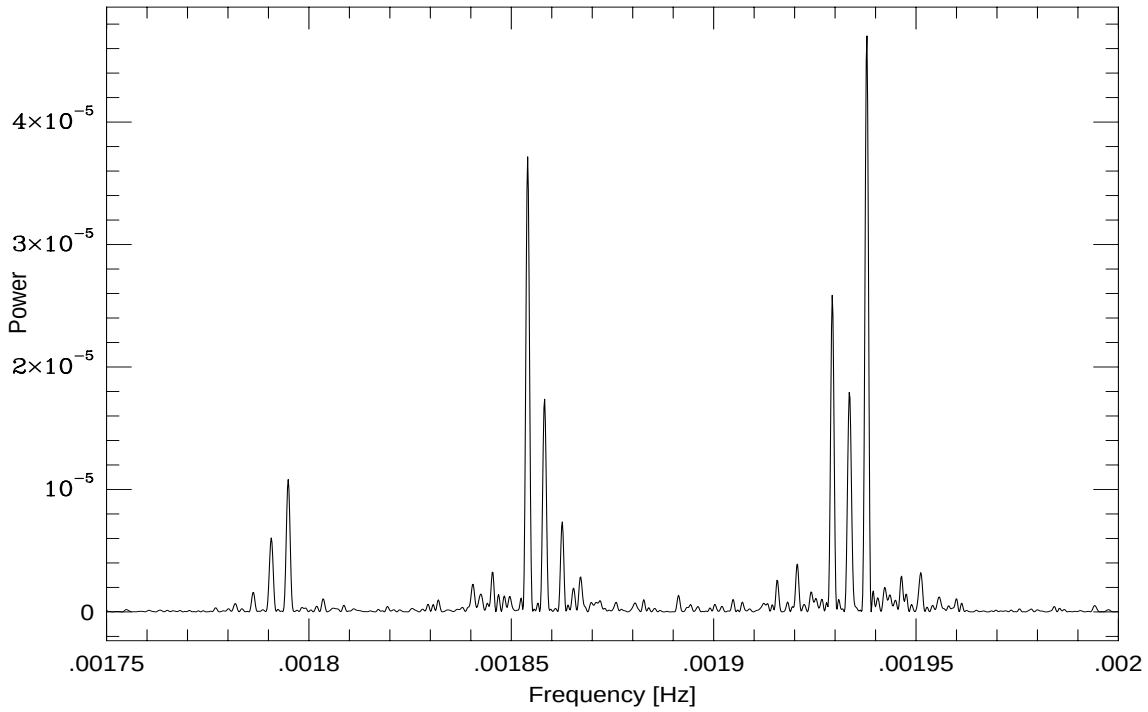

Figure 3.2 Portion of the Fourier transform of PG 1159 data from the 1989 WET run, showing the triplet structure of three modes.

The period spacing for the PG 1159 triplets is 1.72 times that for the quintuplets. This is striking confirmation of the theory of asteroseismology as applied to white dwarf stars. The mass and rotation rate calculated by Winget et al. (1991) from these results is $0.59 \pm 0.01\ M_{\odot}$ and 1.38 days, respectively.

Kawaler & Bradley (1994) compared the PG 1159 periods to those from a grid of static PWD models, and found that the best match occured if PG 1159 has a $\log g$ of 7.38 ± 0.1, $\log L/L_{\odot} = 2.29 \pm 0.05$, and a surface helium abundance of about 30%. Asteroseismology thus established the global properties of PG 1159 much more precisely than (but consistent with) traditional spectroscopic measurements that put its $T_{\rm eff}$ at $140,000 \pm 10,000$ K and its surface gravity at $\log g = 7.0 \pm 0.5$ (Werner, Heber & Hunger 1991).

Periodic deviations from uniform period spacing seen in both the $\ell = 1$ and $\ell = 2$ modes allowed Kawaler & Bradley (1994) to determine the thickness of the helium layer in PG 1159

as $3 \times 10^{-3}\ M_{\odot}$. This result implies a helium layer three orders of magnitude thicker than that measured in the DBV star GD 358. This would seem to preclude the possibility that GD 358 evolved from a PG 1159-like precursor. However, Dehner & Kawaler (1995) showed that the helium near the surface of a PG 1159 model diffuses toward the surface during subsequent evolution, while heavier elements diffuse toward the central regions due to gravitional settling. They show that a PG 1159 star with an initial surface layer composed of 30% helium and a thickness of $10^{-3} M_{\odot}$ can evolve into a DB white dwarf with a surface layer of almost pure helium only $10^{-6} M_{\odot}$ thick. The star has the same amount of helium as before; some of it simply becomes concentrated more toward the surface, with the transition from pure He at the surface to 30% He moving inwards as the star cools. Thus the helium layers seen in PG 1159 and GD 358 are consistent with a common evolutionary origin.

Another asteroseismological "first" achieved in studies of PG 1159 concerns determination of its rate of evolution via measurement of $\dot{\Pi}$ ($\equiv d\Pi/dt$). The expected rate of PWD evolution led to an initial prediction that the e-folding time for period changes in GW Vir stars should be of the order 10^6 years. This translates into $\dot{\Pi} \sim 10^{-11}$s/s for 500 s periods. The periods were expected to increase with time as a result of the overall cooling of the star. Measurement of such small changes requires years of consistent observations, using the $(O - C)$ techniques described in Chapter 2. However, when Winget et al. (1985) finally determined the rate of period change for PG 1159, they found that $\dot{\Pi}$ did indeed have the predicted magnitude but the wrong sign: the period of the 516 s mode was *decreasing* at the rate of $\approx 10^{-11}$ s/s.

Since contraction tends to decrease mode periods, it was initially thought that the cooling rate in PWD models was incorrect, due to a failure of our understanding of neutrino emission, or some other mechanism. If the models cooled more slowly than anticipated, then contraction might be the dominant evolutionary mechanism that determines how the periods change with time. However, Kawaler & Bradley (1994) showed that the 516 s mode is a trapped mode, and that since trapped modes are concentrated toward the surface, their period changes are governed by contraction in the outer layers. The periods of non-trapped modes are still expected to increase with time because of cooling of the core, where their amplitudes are larger than

those of trapped modes.[4]

This complicates the interpretation of $\dot{\Pi}$ measurements in hot GW Vir and PNNV stars where, as Kawaler & Bradley (1994) showed, the contraction of the outer layers can create large differences in $\dot{\Pi}$ from mode to mode. If we wish to test our theory of PWD cooling, we must either make precise mode identifications or measure $\dot{\Pi}$ in modes for which contraction is not a factor. This will be the case for *all* the pulsation modes in GW Vir stars near the low-$T_{\rm eff}$ end of the instability strip, where contraction is almost complete. In Chapter 6 we will explore this issue more fully, when we consider the question of using $\dot{\Pi}$ measurements in cool GW Vir stars to test our theories of neutrino emission in PWD interiors.

PG 1159 showed us what can be accomplished when enough pulsation modes are identified in the period spectrum of a star. However, one star is insufficient to reveal the cause of the pulsations or outline the boundaries of the instability strip for us. While the astroseismological analysis of PG 1159 remained the singular example, we could not answer any detailed questions about the class properties of PWD pulsators. In Chapter 4, we extend asteroseismological analysis to the other GW Vir stars, which cover a wide range of stellar properties. Though none of them show quite so rich a period spectrum as PG 1159 itself, we can still show that PG 1159 is not unique in its pulsation patterns; clues from the other GW Vir stars help us construct a coherent picture of PWD pulsation in Chapter 5.

3.4.2 A Selection of PNNV Stars

The first PNNV star discovered was the nucleus of the planetary nebula K 1-16 (Grauer & Bond 1984). Thereafter, seven more were found, six during the CCD survey of OVI nucleus stars described by Ciardullo & Bond (1996). Also, with the discovery of a faint nebula around the GW Vir star RX J2117.1+3412, it changed classes and became a PNNV star (Appleton, Kawaler, & Eitter 1993). Finally, the variable OVI star Sanduleak 3 is usually counted as a member (despite its lack of a surrounding nebula) because of its long pulsation periods and

[4]Recently, Costa & Kepler (1998) used new data to redetermine the rate of period change in PG 1159, finding a *positive* rate ten times larger than theoretical predictions. Because observations of PG 1159 now span two decades, they were able to confirm this result by comparing the periods over many years to measure the rate of period change directly.

spectral similaries to the PNN stars—including evidence for continuing mass loss from its surface (Bond, Ciardullo, & Meakes 1991).

The potential utility of PNNV asteroseismology is at least as great as that of the GW Vir stars. They are more recently formed, so that studies of their properties provide more direct knowledge of evolution from the AGB. Planetary nebulae fuel a large and active field, with many outstanding questions to which pulsational data might speak. Finally, there are more of them than GW Vir stars, so the potential for unlocking their group properties is inherently greater than for the GW Vir variables.

Unfortunately, the PNNV asteroseismology is plagued by many observational difficulties. Chief among these is the existence of the surrounding nebulosity, which complicates standard aperture photometry. Within even the smallest apertures, parts of the nebula with differing brightness drift in and out in the presence of imperfect telescopic tracking. The resulting signal modulation can easily swamp the pulsation signal from the star itself. CCD photometers are superior for recording PNNV lightcurves, but they tend to be relatively slow (most are designed for long integration times and are ill-suited to high-speed photometry), and they have low sensitivity in the blue—where these hot stars are brightest and their pulsations have the largest amplitude. To date, only two PNNV stars have been observed with multisite CCD campaigns. New, fast, blue-sensitive instruments are under design for use in high-speed photometry that will be applied to observations of PNNV stars.

A second problem is the timescale of PNNV variability. Most have periods of order an hour—close to and below the low-frequency cutoff of WET-style observations used for the shorter period white dwarf and GW Vir stars. Even in stars with low-surface brightness nebulae that have minimal interference with standard aperture photometry, atmospheric extinction variations can swamp the stellar periodicity. Once again, CCD observations will solve this problem.

Because of these difficulties, multisite observations have been undertaken so far for only three PNNV stars. Two—Sanduleak 3 and the central star of NGC 1501—were observed by global networks of CCD cameras. The other, RX J2117.1+3412, has an exceedingly faint

nebula and the shortest periods of any PNNV star. It could be observed effectively, therefore, with the WET network of photoelectric photometers.

One problem with PNNV pulsation studies which neither CCD cameras nor multisite campaigns can overcome is the unstable nature of their pulsation modes. Like many of the ZZ Ceti stars (and unlike the more stable GW Vir pulsators) PNNV stars show amplitude variability on a timescale of days, weeks, and months, with some modes appearing or disappearing completely on short (night-to-night) timescales (Kawaler 1995). Before moving on to additional GW Vir observations in Chapter 4, we will discuss what has been learned from the three PNNV observing campaigns just mentioned.

NGC 1501 After the discovery of 25 minute variability in the lightcurve of this WC4 central star (Bond & Ciardullo 1993), Stanghellini, Kaler, & Shaw (1994) used the HeII Zanstra temperature to determine $T_{\rm eff} = 80,000 \pm 10,000$ K and $L = 2,100 \pm 750\ L_\odot$. In November 1991, a global network of CCD photometers was organized to observe NGC 1501 for 14 consequtive nights. Bond et al. (1996) present the results of this campaign. They identify 10 separate pulsation periods, ranging from 1154 s to 5235 s. Because of the star's highly irregular temporal spectrum, they also rely on archival data to help them identify a mean $\ell = 1$ period spacing of 22.3 s. The rotation rate of NGC 1501 is 1.17 days, based on the observed frequency splitting of 9.9 μHz.

This result explains why single site observations were so difficult to analyze: the daily modulation ubiquitous in single site data is nearly impossible to separate from the modulation of $\ell = 1$ modes caused by NGC 1501's rotation rate of almost exactly one day. Also, for periods near 1500 s the 22.3 s period spacing implies a *frequency* difference of about 10 μHz for modes of consecutive n. This is very close to the rotational frequency splitting of 9.9 μHz, making identification of the overall pattern very difficult. This degeneracy between the frequency splitting due to rotation and that due to the period spacing pattern is expected to plague all PNNV stars with masses and rotation rates similar to NGC 1501.

Based on the identified period spacing, Bond et al. (1996) set the mass of NGC 1501 at $0.55 \pm 0.03\ M_\odot$, consistent with the previous (but less precise) determination of Stanghellini,

Kaler & Shaw (1994).

RX J2117.1+3412 This star was discovered in the ROSAT X-ray telescope all-sky survey, and it was identified as a member of the PG 1159 spectral class by Motch et al. (1992). It was quickly verified as a pulsator with a dominant period near 800 s (Watson 1992, Vauclair et al. 1993). RX J2117.1+3412 (hereafter RX J2117) is one of the hottest known stars, with a $T_{\rm eff}$ around 170,000 K, and it is surrounded by one of the largest and oldest planetary nebulae ever discovered (Appleton, Kawaler, & Eitter 1993). Thus it probably represents an intermediate evolutionary stage between the PNN stars and the naked PWDs. Its dominant period is also intermediate between the longer period PNNV and shorter period GW Vir pulsators.

Based on single site observations of RX J2117, Vauclair et al. (1993) find tentative evidence for two different period spacing patterns, 20.5 s and 12.6 s, with a ratio close to that expected between $\ell = 1$ and $\ell = 2$ modes. If correct, these spacings imply that RX J2117's mass is approximately 0.6 $M_{\odot}$, as expected, but the Vauclair et al. (1993) pattern depends on several insecure mode identifications. Data from a WET run to observe RX J2117 are still in analysis, and it will be interesting to see if the pattern suggested by Vauclair et al. (1993) can be verified.

Sanduleak 3 Another variable PWD with periods intermediate between those of PNNV and GW Vir stars is Sanduleak 3 (hereafter Sand 3). It has an effective temperature around 130,000 K, and it is a very complex pulsator, with typical periods near 900 seconds (Bond, Ciardullo & Kawaler 1993). In 1992, a global CCD network observed Sand 3 intensively for over one week. These data (currently in analysis by Kawaler, Bond, et al.) show that Sand 3 changed its pulsation spectrum significantly in just two years, and indeed changed during the course of the 1992 run. This complicates the analysis significantly compared to simpler pulsators, and the star is still not fully resolved. It is hoped that data from several seasons might provide a large enough sample of modes to decode the underlying spectrum. Toward this end, Sand 3 was made the secondary target for a WET run held in April, 1998, but due to bad weather at many sites, data were only obtained for the primary target (a ZZ Ceti white dwarf).

We have now examined several variable PWDs, but only one, PG 1159, yielded to a relatively complete asteroseismological analysis. Many of its pulsation modes have been conclusively identified, placing strict limits on its mass, luminosity, and helium layer thickness. Among the central stars, an overall pulsation pattern has been identified for NGC 1501, but in general the PNNV variables show highly unstable mode patterns, making detailed asteroseismological analysis difficult. These preliminary studies suggest that the most promising course to extend the success of PG 1159 to other PWDs lies in observations of additional GW Vir stars. In Chapter 4, we describe the observations on which this thesis, and particularly the analysis presented in Chapter 5, are based.

CHAPTER 4 WHOLE EARTH TELESCOPE OBSERVATIONS OF GW VIR STARS

"An analogy founded on a single instance has no logical force."

—Richard A. Proctor, *Other Worlds than Ours (1879)*

4.1 Introduction

The analyses of PWD pulsators outlined in the last chapter are tantalyzing. With PG 1159, we learned that we can apply the tools of asteroseismology to study GW Vir stars. The PNNV stars are more difficult to crack, due to their longer periods, unstable pulsation amplitudes, and the near equality of period and rotational frequency spacings. Since we seek to understand the group properties of PWD variable stars, we must therefore ask: what of the other GW Vir stars?

PG 1159 is the hottest, brightest GW Vir pulsator. There are three others now known, spanning more than two orders of magnitude in luminosity and a large range of $T_{\rm eff}$ as well; the coolest has little more than half the effective temperature of PG 1159. With such a small sample, statistical arguments are of very limited use. Still, given the precise knowledge of their properties that asteroseismology can potentially provide, we can answer important questions. What is the spread in mass and surface gravity corresponding to their enormous ranges in luminosity and $T_{\rm eff}$? We already know they exhibit a trend toward shorter periods with decreasing temperature. Will more precise knowledge of their properties establish other trends that might illuminate this one?

Without detailed observations of additional pulsators, the region of stellar parameter space which must be searched for clues to the pulsation mechanism is enormous. What subset of

models satisfying the weak observational constraints will satisfy them when they are more tightly constrained? Too many different models fit inside the huge error bars of current spectroscopic measurements of $\log g$ and $T_{\rm eff}$ to tell us anything specific about the conditions inside a star that produce pulsation. Any refinement of PWD luminosity and effective temperature refines those required conditions.

In this chapter, we present the results of WET observations of GW Vir variable stars. The next section give an overview of techniques used to observe pulsating PWD stars. We then explore observations of the two stars of intermediate $T_{\rm eff}$ (PG 1707+427 and PG 2131+066). In § 4.4 we present an in-depth analysis PG 0122+200, the star that defines the "red edge" of the PWD instability strip. We do indeed find additional trends, implications of which are briefly outlined in the last section of this chapter. In Chapter 5, we use these trends to help answer some of the questions we have raised.

4.2 Observing Techniques

The observations described in the next two sections were generally undertaken using high-speed photoelectric photometers, which record photon-count rates at equal time intervals (usually around ten seconds or so per integration). Several different photometers were used to obtain the data analyzed for this investigation, the most basic difference among them being the number of simultaneous data channels each records. Single channel instruments require frequent interruptions in the target star's lightcurve to measure the (changing) background sky brightness for calibration purposes. Guiding must be performed with a small CCD camera or other device external to the photometer to avoid further interruptions in the lightcurve and keep the star from drifting out of the aperture during the night. With a second channel, guiding takes place internal to the photometer, though sky calibration still requires that the target channel be interrupted occasionally. Three-channel photometers devote an entire channel to continuous monitoring of a "blank" patch of sky, and the target channel need only be interrupted for one or two brief sky measurements used for cross-channel calibration.

The start time for each nightly data run is set "by eye" to coordinated Universal Time

(UTC), with a precision of about 0.1 s, using the individual observatory's syncronized clock or a WWV radio.[1] Thereafter the length of every integration is controlled by an oscillator built into the photometer electronics, accurate at the 100 μs level (over one hour).

During data reduction, the run start time is transformed to the barycenter of the solar system, to account for the changing light-travel time due to the motion of the Earth in its orbit. Subsequent reduction removes bad data points, subtracts the sky background, and corrects (roughly) for atmospheric extinction. In some cases, a low order polynomial is fit and removed to aid the splicing together of consecutive data runs obtained from different observing sites. The resulting lightcurve is divided by its mean count rate, and unity is subtracted off. We are left with a record of fractional variations away from the average apparent brightness of the star, which has been normalized to zero mean.

The observing and data reduction techniques we have just described treat long term sky brightness and extinction variations only approximately. For periods in excess of an hour or so, this analysis can produce unreliable results. A second, more serious problem arises from the daily gaps that always occur in single site data (since no telescope, except one near one of the Earth's poles, can observe an object continuously for more than a third to half of the time). These gaps create aliases in the Fourier transform of white dwarf and PWD lightcurves which can confound our attempts to decipher them.

The solution to this problem is to observe with a multi-site telescope network such as the Whole Earth Telescope (WET, Nather et al. 1990). The WET can achieve nearly continuous lightcurves for weeks at a time using telescopes at several longitudes to follow a single star. As the object under study sets (or the Sun rises) at one site, the next site in the network takes up the watch, and so on around the globe. The WET has revolutionized the study of short-period variable stars. All of the new analyses of pulsating PWDs presented in this thesis are based on WET observations.

Now that we know something of the theory of pulsating stars, and we understand how they are observed, we can shift our attention to the observations themselves.

[1] In recent years, GPS clocks have come into use, and run start times can be calibrated electronically now at some sites.

4.3 Intermediate GW Vir Stars

4.3.1 PG 2131+066

PG 2131+066 (a.k.a. IR Peg, hereafter PG 2131) was the third GW Vir star to be the target of a WET campaign, after PG 1159 and PG 1707.[2] After the initial discovery of its variability by Bond et al. (1984), it was little observed, partly bcause it is relatively faint ($V = 16.6$, $B - V = -0.34$; Bond et al. 1984). Also, like PG 1707, RX J2117, and PG 0122, it showed very few modes prior to WET analysis. Ground based optical spectra initially indicated it had an effective temperature of $80,000 \pm 10,000$ K and log g of 7.5 ± 0.1 (Werner 1995). More recent UV spectra taken with the HST has led to a revised estimate of $T_{\rm eff} = 95,000 \pm 10,000$ (Dreizler 1998).

One thing that sets PG 2131 apart from other GW Vir stars is a red excess in its optical spectrum that comes from a main sequence companion about 0.3 arcseconds away. At an approximate distance of 470 pc, this separation corresponds to a minimum orbital radius of about 140 AU. Thus, there is little chance for interaction within this binary system. The red companion is detected by the WET's blue-sensitive phototubes only as a slight rise in background counts.

For the September, 1992, WET run, nine different telescopes obtained a total of 70,552 5-second integrations over nine days. The overall duty cycle during that time was 45%. Data reduction followed the procedure outlined in Chapter 2 and discussed in detail by Nather et al. (1990). The reduced data represent the fractional departure of the count rate from the mean, with runs from every site combined into a single light curve. The Fourier transform (FT) of this full data set, depicted in Figure 4.1, shows the "modulation amplitude" (in units of mma = ma/1000, where ma $\equiv \Delta I/I$) of variations in the detected intensity I at a given frequency. Figure 4.2 shows, on the same frequency scale, the window function for this data set. The window represents the FT of a single noise-free sinusoid sampled at the same times that the data were sampled. The central peak in this plot corresponds to the frequency of the

[2]The analysis of the PG 2131 WET run, summarized in this section, was published by Kawaler, O'Brien et al. in the September 1, 1995, issue of *The Astrophysical Journal*.

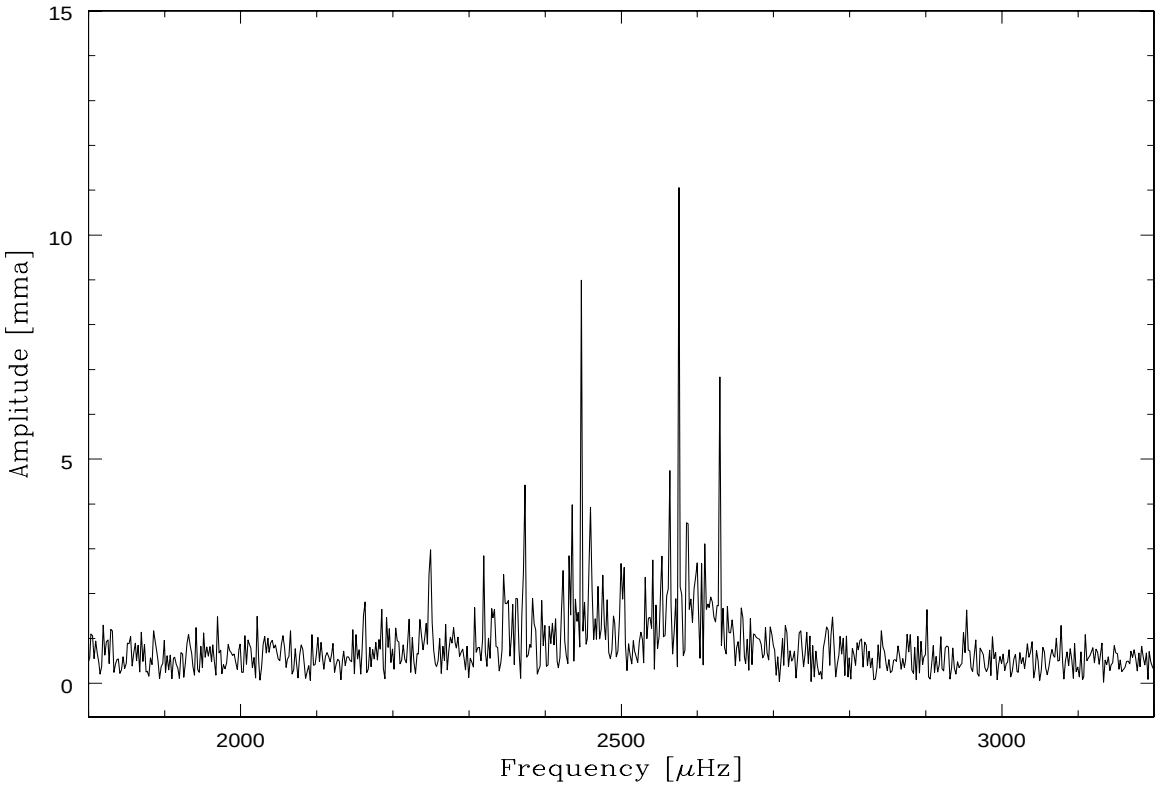

Figure 4.1 Fourier transform of the PG 2131 WET data set.

sinusoid; all other alias peaks on either side are modulations caused by the gaps in the data set. These aliases will affect every true stellar variation found in the FT of the WET data set.

Using a nonlinear least-squares procedure (described in O'Brien et al. 1996), we fitted the time-series data to obtain the frequency, amplitude, and phase of the nine dominant modes seen in the FT. After subtracting sinusoids with these parameters from the light curve, we recomputed the FT to see what was left. This "prewhitening" process was then repeated, with an increased number of peaks included in each successive least-squares fit. In this way, we found 20 independent periodicities. As indicated in Table 4.1, there is one peak that is almost resolved into two (at 2953 μHz); it shows broadened line shapes in the temporal spectra. The 2503 μHz peak has three components in the combined data set; we could resolve two of them, but the lower frequency component was not resolved. Two additional closely spaced pairs are

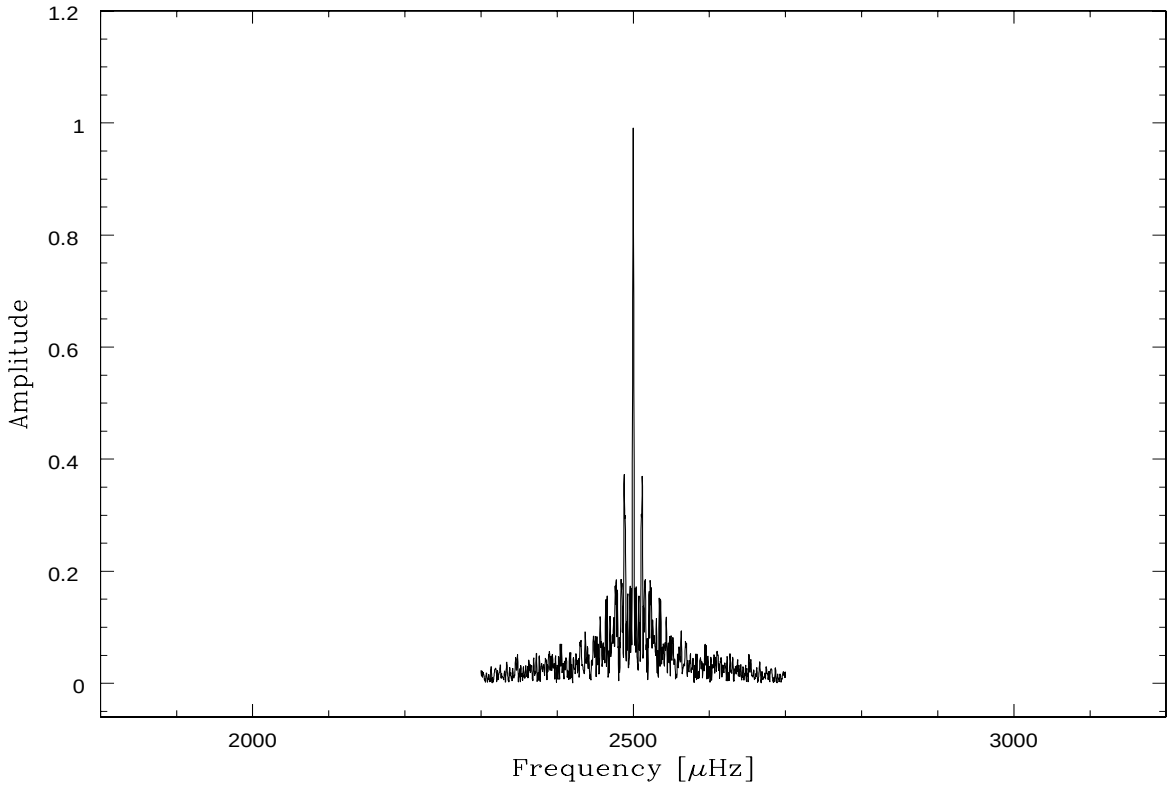

Figure 4.2 Window function for the PG 2131 WET data set.

present in Table 4.1 that were resolved in this analysis.

With the hope and expectation that we would see the signature of rotational splitting, we searched the FT for equal frequency spacing. Five pairs of peaks are split by approximately 54 μHz. Three showed hints of a peak almost exactly in the middle, suggesting they are triplets with spacing of 27 μHz. Upon pre-whitening, all five pairs show significant peaks within 1.5 μHz of the midpoint in frequency. These five triplets show a mean splitting of 27.4 $\pm$ 1.2 μHz. If these triplets are rotationally split $\ell = 1$ modes, then from Equation (2.1) the rotation period of PG 2131 is 5.07 $\pm$ 0.22 hr.

Having identified the central ($m = 0$) frequencies for these five triplets, we see that their period spacings are 42.82, 19.66, 22.43, and 23.92 s. Assuming that there is a mode suppressed between the 341 and 384 s modes, the mean period spacing is 21.76 s. A more rigorous way

Table 4.1 Periodicities of PG 2131+066 from WET Data

Frequency (μHz)	Period (s)	Amplitude (mma)	T^a_{max} (s)	m	comments[a]
2953.25±0.25	338.610±0.029	1.42±0.48	68±37	-1	+1.2 μHz split
2928.66±0.31	341.453±0.036	1.27±0.48	178±41	0	
2900.98±0.17	344.711±0.020	2.23±0.48	264±23	1	LSQ
2629.44±0.06	380.309±0.009	6.34±0.48	228±9	-1	LSQ
2602.34±0.14	384.269±0.021	2.69±0.48	26±22	0:	
2575.55±0.04	388.266±0.006	11.01±0.48	87±5	1	LSQ
2503.50±0.15	399.441±0.024	2.83±0.49	345±22	-1:	
2500.63±0.19	399.899±0.027	2.24±0.49	378±29		
2475.67±0.25	403.930±0.041	1.62±0.49	396±39	0:	
2447.17±0.04	408.635±0.007	9.73±0.48	404±6	1	LSQ
2373.56±0.13	421.307±0.023	3.81±0.50	382±22	-1:	LSQ
2372.18±0.14	421.553±0.024	3.39±0.50	298±25		LSQ
2345.45±0.21	426.358±0.038	1.90±0.48	189±34	0:	
2318.85±0.10	431.248±0.019	4.05±0.48	110±16	1	LSQ
2249.24±0.16	444.595±0.032	2.68±0.48	389±29	-1:	LSQ
2247.56±0.26	444.927±0.051	1.71±0.49	39±46		
2220.86±0.28	450.276±0.057	1.42±0.48	418±48	0	
2192.31±0.18	456.139±0.035	2.21±0.48	392±31	1	
2162.68±0.11	462.390±0.024	3.70±0.48	378±19	-1	LSQ
1968.87±0.19	507.906±0.049	2.02±0.48	386±38	-1:	

[a]Time of first maximum after BJED 2448886.84472

[b]"LSQ" labels the 9 peaks in first least-squares fit to original data

to determine this spacing is to fit the measured values of Π_n to a linear equation of the form

$$\Pi_n = \Delta\Pi \times (n - n_0) + \Pi_{n_0}. \tag{4.1}$$

where $\Delta\Pi$ and Π_{n_0} are related in an obvious way to Π_0 and ϵ from Equation (2.2). A linear least-squares calculation of this type yields a value of $\Delta\Pi = 21.59 \pm 0.37$ s.

Given the two measured quantities $\Delta\Pi$ (from the pulsation data) and $T_{\rm eff}$ (from spectroscopy) stellar models can be used to place limits on the mass and luminosity of a pulsating PWD star. For PWDs with a given mass, the period spacing increases with decreasing effective temperature. In addition, for models with a given effective temperature, period spacing increases with decreasing mass. Thus for PG 2131 to maintain a period spacing almost identical to that of PG 1159—which is far hotter than PG 2131 at 140,000 K—it must be more massive. Based on stellar models, $\Delta\Pi = 21.59$ s implies a mass for PG 2131 of $0.61 \pm 0.02\ M_\odot$. The luminosity corresponding to this mass range is $10 \pm 5\ L_\odot$. [3] Finally, if the triplet modes are really $\ell > 1$ with some components "missing" then the 21.59 s period spacing implies a mass below $0.4\ M_\odot$—below the minimum mass required to make a C/O core white dwarf star. This supports our identification of the triplet modes as $\ell = 1$.

4.3.2 PG 1707+427

PG 1707+427 (hereafter PG 1707) was the target of the sixth WET run, which took place from March 12 to 24, 1991. Because of its declination (+40°), only northern sites were used. Of the five telescopes, three—the McDonald 2.1 m, the 3.6 m CFHT at Mauna Kea, and La Palma's 2.5 m INT—provided the bulk of the data. In support of the run, three additional nights of observation took place using the Mt. Bigelow 1.5 m three months later, in June 1991. Like PG 2131, PG 1707 is relatively faint ($V = 16.7$, $B - V = -0.6$); however, it was the subject of an intense (single site) observational program in the late 1980s that failed to resolve its underlying pulsation pattern (Grauer, Green & Liebert 1992). Following the WET run, Fontaine et al. (1991) published an analysis of its temporal spectrum based on the CFHT

[3] These are not the same values published in Kawaler, et al. (1995). Our numbers are based on the same data interpreted using the new evolution models described in § 5.3).

subset of the run. They claim to find evidence for a pattern based on $\Delta\Pi = 18.3$ s. However, most of the periods they suggest exist in the CFHT data are not evident in the full WET data set.

The FT of the combined data from Texas, Hawaii, and La Palma is shown in Figure 4.3, and the corresponding window function is shown in Figure 4.4. The most striking aspect of the PG 1707 FT is that, with the exception of the largest group of peaks (near 2236 μHz), every significant mode is apparently a singlet. The only obvious multiplet is the 400 s doublet, which shows a frequency splitting of 8.86 μHz. With only a single frequency splitting to go by, it is impossible to claim with certainly the value of ℓ for any of the peaks in Figure 4.3. Normally, the identification of an equal period spacing pattern might be of some help, but the closest spacing between modes is that between the 447 and 414 s (2236 and 2417 μHz) peaks:

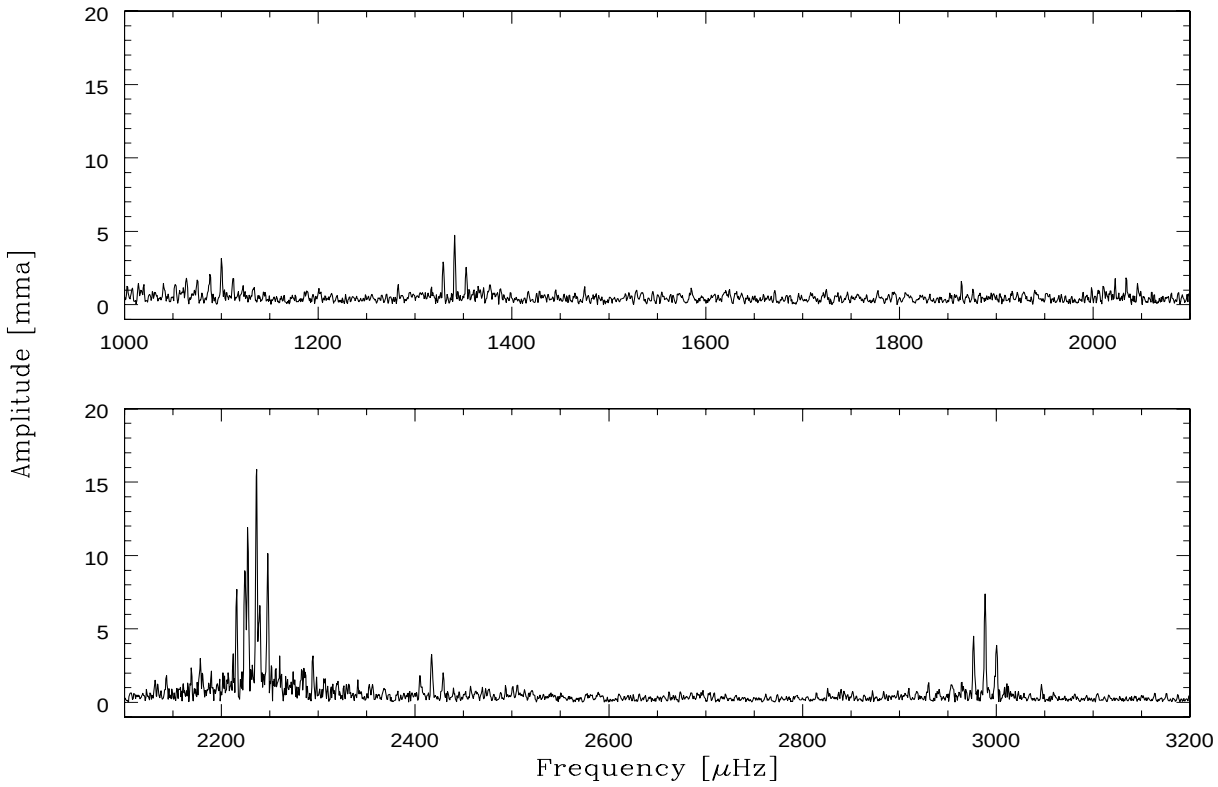

Figure 4.3 Fourier transform of the PG 1707 WET data set.

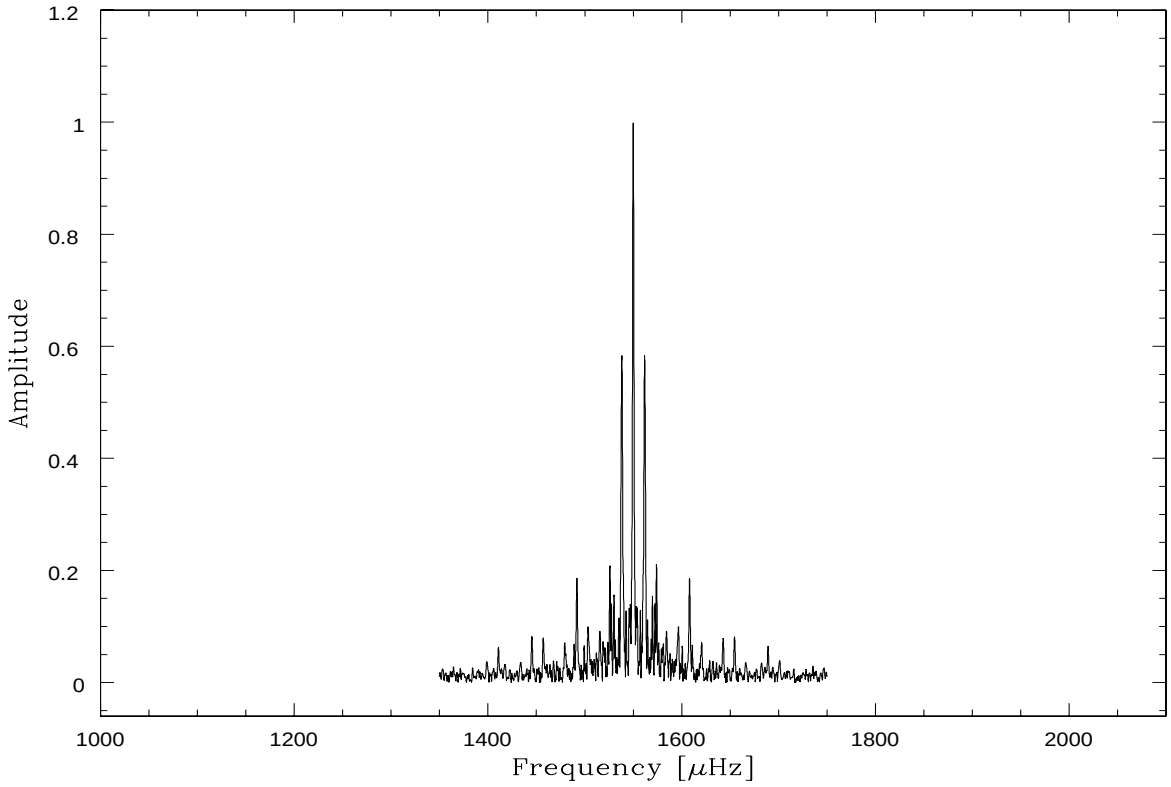

Figure 4.4 Window function for the PG 1707 WET data set.

33 s. For white dwarf masses above about 0.55 $M_{\odot}$, this spacing is too large to represent consecutive n modes of the same ℓ. If there is a mode missing between the two, then the period spacing is about 16.5 s, possible only if the star has a mass of 1 $M_{\odot}$ or greater. The alternative is that these two modes are of different ℓ, but with a frequency splitting only seen in one of them, we cannot tell if this is the case. This problem highlights the usefulness of finding many independent pulsation peaks in the FT of a GW Vir star. With PG 1159, over 100 different modes were found; for PG 2131, we found twenty. Here we have only seven—not much data with which to identify a pattern, unless the peaks are consecutive n, which they certainly are not.

The pulsations of PG 1707 exhibit one additional peculiarity, however, which might contain the seeds of an eventual solution to this problem. The three largest singlet peaks in the transform, at 1341, 2417, and 2988 μHz all show a larger alias on the low-frequency side than

on the high.[4] Two additional (but more marginal) modes at 1100 and 2034 μHz also seem to have inflated low-frequency sidelobes. In sum, every group in the transform shows evidence for a nearby mode split from the largest peak by close to 1/day on the low-frequency side. In all but the large 2236 μHz doublet, this evidence is *individually* very weak, but the ubiquitous nature of the asymmetry makes it worth further study.

We might expect that if every group is made up of two peaks split by almost exactly one cycle per day, then the amplitude of each mode should exhibit a daily modulation, and the phase of this modulation should remain relatively constant over the length of the WET run (assuming that the beat period is significantly longer than the length of the WET run—in this case one week). This will be the case if the splitting is closer than 0.5 μHz to exactly 1/day (11.57 μHz).

Figure 4.5 suggests that this might, indeed, be the case. Since the three WET sites are spaced roughly equally around the globe, they would all see different parts of the beat cycle between the two components of each multiplet. Figure 4.5 shows the section of the FT around the 1341 and and 2417 μHz groups for, from top to bottom: the full WET run, the three individual sites which made up the run, and the Mt. Bigelow data taken three months later. If there was only a single peak present in these two regions, then the largest peak in the FT from each site would be the same as in the WET data. Of course the data are noisy, and this might make alias peaks appear larger than the "real thing." However, a careful look at the middle three sections of Figure 4.5 reveals that the largest amplitude peak rests at the position of a different "alias" peak at each site. This is consistent with the behavior of an 11.57 μHz doublet of uneven amplitude, sampled at different parts of the beat cycle. Note also that the Mt. Bigelow data (close in longitude to Texas) is also switched to a different "alias," consistent with migration in *time* to a different phase in the beat cycle. Noise might be expected to do this for one or more peaks once in a while, but here *all* the groups show evidence of modulation by a nearby peak 1/day lower in frequency than the primary mode.

[4]Though this is not apparent for the the 2417 μHz peak in Figure 4.3, when the lightcurve is prewhitened by the large 2236 μHz mode, the 2417 μHz aliases assume the same amplitude ratio clearly visible in the figure for the 1341 and 2988 μHz modes.

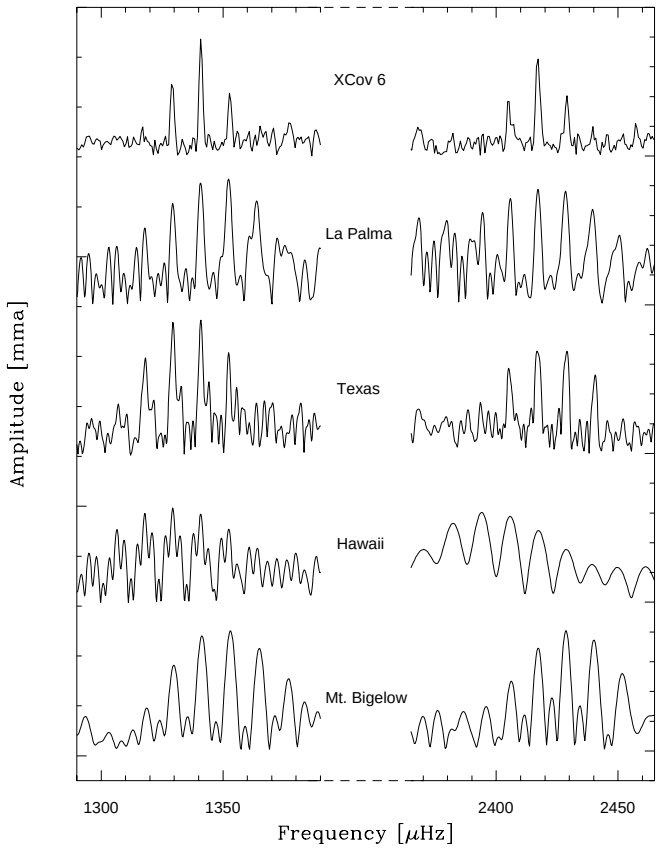

Figure 4.5 Two sections of the Fourier tranform of PG 1707 data from individual sites during the WET run, plus Mt. Bigelow data taken three months later.

The only exception seems to be the largest amplitude mode in the FT, which is split not by 11.57 but rather 8.86 μHz. It is split on the same side, and with a similar amplitude ratio between components, as we are positing for the other modes. If the 11.57 and 8.86 μHz splittings are both real, then there are several possibilities. One is that they represent modes of two different ℓ. The ratio between $\ell = 2$ and $\ell = 1$ rotational splitting is expected to be 0.6; here it is 0.75. Another possibility is that the 2236 μHz doublet is actually made up of one $\ell = 1$ and one $\ell = 2$ component; in other words, it is an accidental degeneracy. Finally, it could be that all the modes we see are $\ell = 1$. In this case, we must invoke some mechanism by which the 2236 μHz doublet is given an atypical splitting.

It turns out that there might indeed be such a mechanism. We have already mentioned the high probability that the 2236 μHz mode is a (maybe severely) trapped mode. According to Kawaler, Sekii & Gough (1998), the quantity $C_{n\ell}$ in Equation (2.1) can be affected by trapping. The effect is proportional to the trapping strength. Highly trapped modes have smaller values of C_{nl} than the asymptotic value of 0.5 (for $\ell = 1$ modes). If the 11.6 μHz splitting represents $\Delta m = 2$, and the splitting of the 2236 μHz mode is $\Delta m = 1$, then this can work. The measured period spacing between this and next closest mode is 33 s or $\sim$ 16.5 s. If, for instance, the average period spacing were 21 s (as in PG 1159 and PG 2131), then the ratio of the trapped to the mean spacing is 0.79 (if the trapped spacing is 16.5 s), while the ratio of the mean to the trapped frequency splitting would be 0.67 (= 5.79/8.86). The similarity of these ratios is consistent with the idea that the 2236 uhz mode is efficiently trapped, causing the large departures from both average period spacing and frequency splitting observed for this mode.

Continuing with our assumption that all the modes are $\ell = 1$ with a 1/day frequency splitting, we can ask: does any reasonable period spacing fit the observed pattern of peaks? If the low-frequency alias and primary peak in each group represent the $m = \pm 1$ components of $\ell = 1$ multiplets, then the inferred position of the $m = 0$, $\ell = 1$ peaks is listed in Table 4.2, along with the predicted periods based on the equal spacing pattern that fits them best—in this case, $\Delta\Pi = 19.87$ s. This fit is good, especially considering the large range in period of the observed modes, and the worst fit mode is of course the 2236 μHz (448 s) doublet. Given a spectroscopically determined temperature of 100,000 K, this period spacing implies that PG 1707 has a mass of something like 0.67 $M_{\odot}$. To put it mildly, this value should be taken as tentative at best.

The game can be played differently than we have played it here. This analysis points out the limitations involved when the frequency splittings get close to one cycle per day—even for multisite observations. Additional observations are needed before we can say anything certain about PG 1707, and it is especially crucial to search the archival data to confirm or rufute, if possible, the nearly exact 1/day modulation. If the 1/day signal is real, then even future WET runs will be of very limited use; it might be better to seek ℓ identification through some other

Table 4.2 Suspected PG1707 $\ell = 1, m = 0$ Periods

	$\Delta\Pi$=19.87 s		
Π_{obs} (s)	Π_{pred} (s)	$n - n_0$	$\Pi_{obs} - \Pi_{pred}$ (s)
335.3	335.3	0	—
414.7	418.8	4	−0.1
448.3	454.5	6	−6.2
493.0	494.3	8	−1.3
538.1	534.0	10	+4.1
749.0	752.6	21	−3.6
913.7	911.5	29	+2.2

means, for instance the methods of time-series spectroscopy recently applied by Robinson et al. (1995) to mode identification in the ZZ Ceti stars. Until then, we can only say that the pulsation pattern of PG 1707 is not clearly inconsistent with those of the other GW Vir stars, though only additional observation and analysis will say how far the similarities go.

4.4 Extending Trends with The Coolest GW Vir Star

The variable star PG 0122+200 (BB Psc, hereafter PG 0122; $m_b = 16.13$) is the coolest variable PWD, with an effective temperature of 80,000 K and a luminosity that is likely two orders of magnitude or so fainter than that of the hottest GW Vir star, PG 1159 (Dreizler 1998). Determining how alike or different these two stars are will shed light on the important question of how variable PWDs change between the blue and red edges of the instability strip.[5]

As discussed earlier, three PWDs have been studied successfully with multisite data: PG 1159 (Winget et al. 1991) and PG 2131 (Kawaler et al. 1995), both observed with the WET, and the central star of the planetary nebula NGC 1501 (Bond et al. 1996), observed with a network of CCD photometers. With the pulsation spectra of three stars in hand, we can now begin to address detailed questions about the variable PWDs as a class of objects. Adding a fourth star—PG 0122—to this list makes the study of its periodicities and structure

[5]The analysis of the PG 0122 WET run, summarized in this section, was published by O'Brien et al. in the March 1, 1998, issue of *The Astrophysical Journal*.

even more exciting.

After discovery of its photometric variations by Bond & Grauer (1987), three separate efforts were made to unravel PG 0122's complex light curve. Hill, Winget & Nather (1987) observed the star on four consecutive nights in late 1986 with the 2.1 m telescope at McDonald Observatory and tentatively identified eight separate pulsation modes between 300 s and 700 s. They proposed a mean period spacing of 16.4 s, which implied a mass of $\sim 0.7\ M_{\odot}$ based on models then available. However, their analysis rested on the technique of averaging together the Fourier transforms of separate nightly data sets, a procedure which, as it turned out, left unresolved the rotational splitting later found in several individual modes of this star. Compelling mode identification was hence impossible for Hill et al. (1987).

A decade later, armed with hindsight created by successes with PG 1159 and PG 2131, O'Brien et al. (1996, hereafter OCKD) reanalyzed the data observed by Hill et al. (1987). OCKD identified 13 individual frequencies, comprising singlets, doublets, and one clear triplet, in the transform of the Hill et al. (1987) data. We identified four probable $\ell = 1$ modes, and one possible $\ell = 2$ mode. The $\ell = 1$ frequency splitting was 3.6 μHz, with a mean period spacing of 21.2 s. These numbers imply a rotation rate of $\sim$ 1.6 d and a mass of 0.64–0.72 $M_{\odot}$ for PG 0122. However, OCKD made significant use of the technique of prewhitening to separate the presumed real peaks from the effects of severe aliasing introduced by daily gaps in the data. Thus these identifications were tentative; other possible "solutions" to this data set could not be ruled out. In particular, the strongest evidence for the 1.6 d rotation period was found in the transform's dominant multiplet at 400 s. A rotation rate of 0.8 d accounted for the peaks in this triplet mode almost equally well if it was assumed that the third largest peak found in the triplet was really an alias of the "true" peak 11.6 μHz away.

In October 1990, a separate group organized a bilongitudinal campaign to observe PG 0122 with the 1.5 m Steward Mt. Lemmon telescope, the 1.5 m Steward Mt. Bigelow telescope, and the 2.5 m Roque de los Muchachos Nordic Optical Telescope. Based on 74.7 hours of data obtained over 11 days, Vauclair et al. (1995, hereafter VPG) suggested a frequency splitting indicative of a $\sim$ 1.8 d rotation rate for PG 0122, consistent (within errors in the frequency

determinations) with the rotation rate deduced by OCKD. Unfortunately, their attempt to fit a pattern of equal spacing to the periods was frustrated by the absence of some low-amplitude modes separately identified by OCKD. Of the thirteen peaks identified by OCKD in the transform of the 1986 data, only seven were identified in the 1990 data described by VPG. VPG's suggestion of a 16 s period spacing was based on two different arguments. The first argument derives from the suggestion of Hill et al. (1987) that, given similar structure, PG 0122 and PG 1159 should have period spacings in the same ratio as their respective dominant periods. However, the resulting estimated period spacing for PG 0122 requires a mass of more than 0.7 $M_{\odot}$, far greater than the 0.58 $M_{\odot}$ of PG 1159, implying that the two stars have significantly different structure. Their second argument assumed that three observed multiplets had $\ell = 1$. They express doubts as to the exact nature of one of these modes, however, suggesting that an $\ell = 2$ identification might also explain the observed peaks. OCKD independently identified the problematic multiplet as a likely $\ell = 2$ mode.

The three attempts at decryption of the PG 0122 light curve discussed above strongly suggested the need for a more comprehensive and concerted observational campaign to resolve the issues of mode identification and hence rotational splitting and period spacing. Indisputable measurement of these quantities would, in conjunction with theoretical stellar models, pinpoint the mass and luminosity of PG 0122 and reveal much about its evolutionary status. In addition, the mass of PG 0122 helps determine the role which neutrino emission plays as a source of cooling (see Chapter 6). If this mass is indeed large—one point on which all three prior analyses concur—then according to stellar models, neutrino luminosity dominates the energy output of PG 0122 more than any other PWD star. This neutrino cooling should produce measurable secular changes in the pulsation periods of PG 0122. We discuss this possibility in Chapter 6.

The revealing but somewhat ambiguous results of single and double site observation of PG 0122 made it an ideal subject for observation with the WET. It was the primary target for the WET campaign held in September, 1996. In the next section, we describe the WET observations and their reduction. Section 4.3.3 outlines our results and their implications for previous mode identification and period spacing arguments. In § 4.3.4, we discuss the physical

properties of PG 0122 in light of the pulsation periods. We summarize and discuss our findings in § 4.3.5, in anticipation of investigating the group properties of the GW Vir stars in Chapter 6.

4.4.1 The WET Data Set

With a battery of a dozen or so observatories from which to watch a single target, the Whole Earth Telescope generally enjoys advantages beyond the obvious ability to follow a star for longer than a few hours at a time. Chief of these is the weather: multiple redundancies at several longitudes give the WET better average weather conditions than can be claimed at all but the best single sites. In the past, this has resulted in relatively uninterrupted data sets for every WET run. It did not in this one; hurricanes in two oceans contributed to the lowest overall duty cycle of any WET run held to date. Over a thirteen day period in September 1996, observers accumulated 13,757 10 s integrations—an overall duty cycle of 14%, far below the 50–90% normally achieved by the WET.

The general quality of the data coverage is exemplified by the spectral window, shown in Figure 4.6. The signature of the large daily gaps is evident in the notorious 1/day aliasing side lobes which surround the central peak. Similar aliasing must affect each peak in the transform of the WET light curve.

Figure 4.7 shows the FTs from the WET run (lower panel) and the 1986 single site run analyzed by OCKD (upper panel). The figure shows that PG 0122 is apparently a very stable pulsator, with almost every group of frequencies seen in 1986 returning faithfully for the 1996 WET run. Excluding frequencies below 100 μHz, there are five obvious groups well above noise, all lying in the region between 1500 and 3000 μHz. Six of the eight frequency groups found by OCKD are apparent in the WET FT (the peaks near 1640 μHz, 2137 μHz, 2220 μHz, 2500 μHz, 2630 μHz, and 2980 μHz), with relative amplitudes similar to those in the 1986 data. One additional peak not present in either 1986 or 1990 is possibly significant near 2800 μHz.

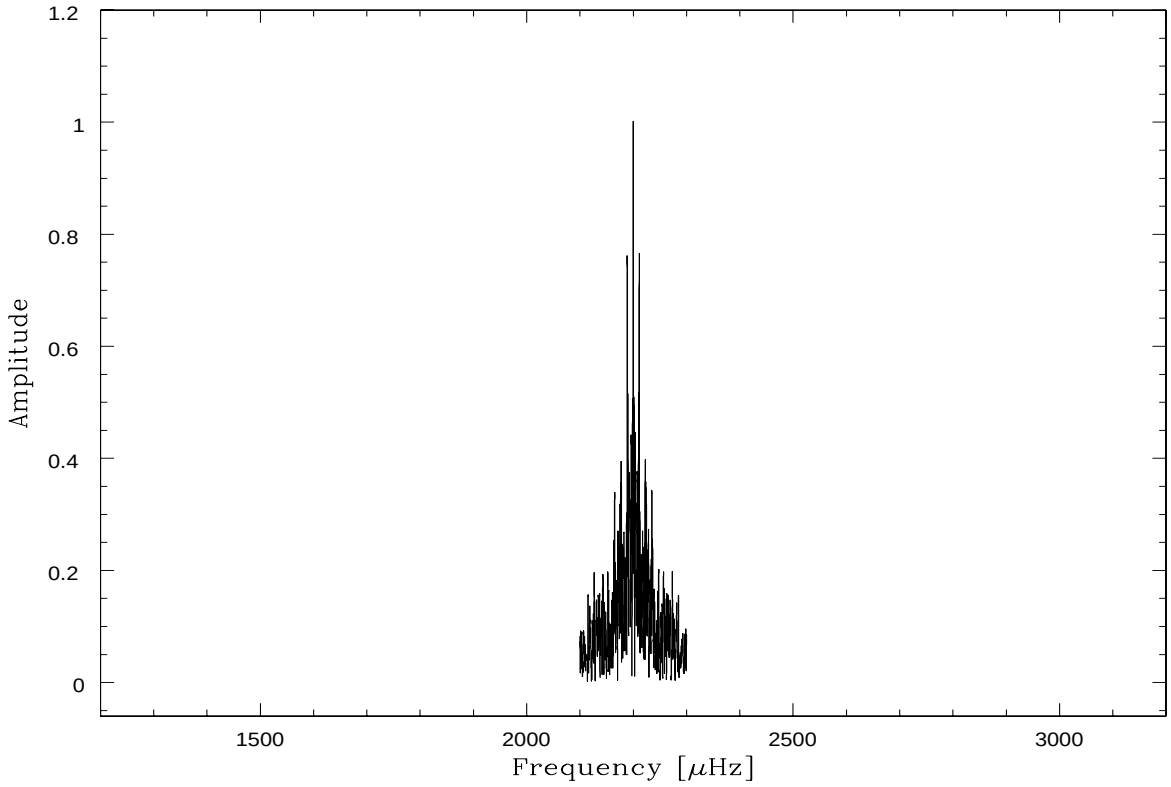

Figure 4.6 Window function for the PG 0122 WET data set.

4.4.2 Frequency Identification

An original hope in assigning PG 0122 as the top-priority WET target during the Fall, 1996 campaign—besides the possibility of finding new modes—was to acquire a data set so complete as to allow unambiguous separation of closely spaced peaks in the Fourier transform. The rotational splitting claimed in previously published data could then be absolutely refuted or confirmed, with the inherent consequences for suggested mode identification and period spacing and hence for the calculated mass and luminosity of the star. Unfortunately, the complexity of our spectral window meant that we again had to resort to prewhitening to discern multiple closely spaced peaks, as was done with previous data.

Using the same prewhitening techniques used for PG 2131, we found one additional peak near the largest mode in the 2220 μHz region, making this group a doublet. We also found two additional peaks near the largest mode in the transform at 2500 μHz. The three peaks

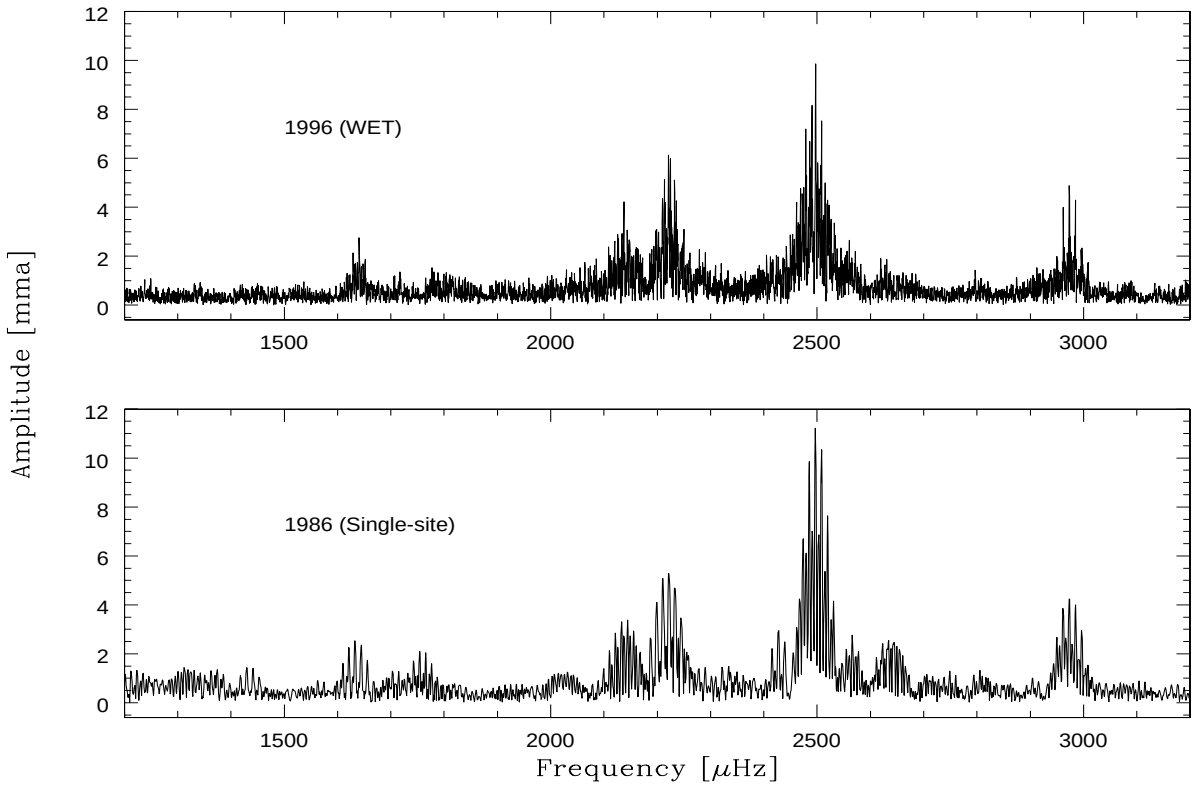

Figure 4.7 Fourier transform of the PG 0122 WET data set (upper panel) and of single site data from 1986 (lower panel).

form a triplet of equal frequency spacing, with $<\delta\nu>$ = 3.581 ± 0.006 μHz. This is an important confirmation of the results of OCKD, who identified these same three frequencies, though less conclusively. The triplet structure suggests an $\ell = 1$ mode; the period spacing (see § 4.3.3) is consistent with this identification, for reasonable white dwarf masses.

In all, we found nine individual periodicities in the WET data, making up four singlets, a doublet, and a triplet. Table 4.3 lists the modes and their identification (values of ℓ and m). In some cases, mode identification was aided by comparison with the peak lists of OCKD and VPG, reproduced here in Tables 4.4 and 4.5, respectively. Thus of the six groups found in the WET data set, five belong to $\ell = 1$ modes, based on the observed frequency splitting. The average consecutive m frequency splitting for all the $\ell = 1$ modes is $<\delta\nu>$= 3.5 ± 0.2 μHz, which from Equation (2.1) implies a rotation rate of 1.6 ± 0.1 d.

Table 4.3 Periodicities of PG 0122 from the WET Data Set

Period (s)	Frequency (μHz)	σ_f (μHz)	Amplitude (ma)	σ_A (ma)	ℓ	m	$\delta\nu$ (μHz)	$\sigma_{\delta\nu}$ (μHz)
609.5729	1640.493	0.004	2.7	0.2	1[a]	-1[a]	7.9[a] (2×3.85)	0.2
467.8656	2137.366	0.003	4.5	0.2	...	...	...	...
450.1753	2221.357	0.002	5.3	0.3	1	$+1$[b]	3.332	0.003
449.5010	2224.689	0.002	5.1	0.3	1	0[b]	...	...
401.5558	2490.314	0.002	8.1	0.3	1	$+1$	3.585	0.004
400.9785	2493.899	0.003	4.2	0.4	1	0	3.577	0.004
400.4042	2497.476	0.002	8.5	0.3	1	-1	...	...
380.1111	2630.810	0.004	2.6	0.2	1[a]	$+1, 0$[a]	3.3[a]	0.3
336.2804	2973.709	0.002	5.4	0.2	1[a,b]	-1[a,b]	3.70[a,b]	0.2

Notes—Numbers in parentheses show the mean consecutive m splitting if the observed doublet is assumed to represent $m = \pm 1, \ell = 1$. A comma separates possible m identifications where constraint to a single value was not possible. Frequency and amplitude errors derive from a formal least squares analysis of the data. The amplitude units are modulation amplitude, ma ($\equiv \Delta I/I$).

[a]Based on the frequency of a nearby peak in data from OCKD.

[b]Based on the frequencies of nearby peaks in the data of VPG.

Table 4.4 Periodicities of PG 0122 from 1986 Single-Site Data

Period (s)	Frequency (μHz)	σ_f (μHz)	Amplitude (ma)	σ_A (ma)	ℓ	m
612.44	1632.8	0.2	2.6	0.3	1[a,b]	+1[a]
570.00	1754.4	0.2	2.5	0.3	?	?
466.37	2144.2	0.2	3.3	0.4	?	?
465.20	2149.6	0.2	2.3	0.4	?	?
450.25	2221.0	0.1	6.3	0.4	1[a,b]	−1[a,b]
401.61	2490.0	0.1	7.3	0.4	1	+1
401.03	2493.6	0.2	3.0	0.4	1	0
400.50	2496.9	0.1	12.3	0.4	1	−1
380.08	2631.0	0.2	1.9	0.4	1	+1, 0
379.61	2634.3	0.2	2.1	0.4	1	0, −1
337.13	2966.2	0.2	3.1	0.4	1	+1
336.29	2973.6	0.1	5.1	0.4	1	−1

Notes—Data are from O'Brien et al. 1996, based on single site observations from 1986. Frequency and amplitude errors derive from a formal least squares analysis of the data. The amplitude units are modulation amplitude, ma ($\equiv \Delta I/I$).

[a]Based on the frequency of a nearby peak in the WET data set.

[b]Based on the frequencies of nearby peaks in the data of VPG.

The final peak, at 2137 μHz, lies at the position of an alias of a peak previously identified by OCKD. This calls into question their identification of this mode, based on frequency splitting arguments, as $\ell = 2$. At present the value of ℓ for this peak remains unconstrained by the data.

Our inability to resolve the identity of the 2137 μHz mode is disappointing, for this region has been a source of particular difficulty. While OCKD tentatively identified it as an $\ell = 2$ mode based on the larger splitting found in what was then a doublet, VPG suggested the possibility of an accidental coincidence of both $\ell = 1$ and $\ell = 2$ modes, though this idea was *not* based on observation of both $\ell = 1$ and $\ell = 2$ splitting within the mode. Identification of

Table 4.5 Periodicities of PG 0122 from 1990 Two-Site Data

Period (s)	Frequency (μHz)	Amplitude (ma)	ℓ	m
450.13	2221.6	1.1	1	+1
449.44	2225.0	1.5	1	0
448.89	2227.7	1.2	1	−1
401.06	2493.4	1.6	?	?
400.90	2494.4	1.8	1	0
400.42	2497.4	4.2	1	−1
336.68	2970.2	0.7	1	0
336.28	2973.7	1.8	1	−1

Notes—Data are from Vauclair et al. 1995, based on double site observations from 1990. The amplitudes, given by VPG in units of mmag, have been converted to modulation amplitude, ma ($\equiv \Delta I/I$).

the value of ℓ for this mode is important because of its close proximity in period to the mode at 2220 μHz. This proximity led VPG to suggest an $\ell = 1$ period spacing of $\sim$ 16 s, while OCKD claim a period spacing of 21.2 s. The possibility of observing several components of the 2137 μHz mode and thereby conclusively deducing its order ℓ was thus an exciting prospect. Unfortunately, after prewhitening of the WET light curve at the single observed frequency there remained only an indistinguishable jumble in the transform: a possible effect of aliasing interference between two or more real periodicities of similar, small amplitude. Until we obtain a more complete record of the light curve of PG 0122, the 2137 μHz mode will remain a puzzle.

4.4.3 Period Spacings

The pulsating PWDs studied with multisite data so far—PG 1159, PG 2131, and NGC 1501—show a pattern of $\ell = 1$ modes spaced at multiples of a fundamental period interval. This interval is determined by the set of modes *available* for pulsation; not all theoretically available modes are excited, leaving gaps of one or more "missing" periods in a chain mostly consecutive

in radial index n. As presented in Chapter 2, the fundamental period spacing is the most important parameter measured in the pulsation spectrum of a white dwarf star, as it is determined almost exclusively by two parameters: the stellar mass and luminosity. The first step in deducing this spacing is identification of the order ℓ of each of the modes in the pulsation spectrum, a process in this case outlined in the previous section. As mentioned above, both VPG and OCKD have already attempted to explain the period spectrum of PG 0122 with different values of the primary spacing. We can now use all of the observed periods to attempt to decide between these two hypotheses.

Table 4.6 compares the observed pattern of $\ell = 1$ modes to periods predicted by strict patterns of 21.10 s and 16.24 s spacing. These values were obtained by taking the likely value of Δn $(= n - n_{\rm o})$ for each mode based only on approximate spacings of 21 s and 16 s and then, for the two resulting sets of Δn (one for each estimate of $\Delta\Pi$) fitting a line to Equation (4.2). $\Delta\Pi = 21.10$ s and 16.24 s represent the two best fits (in a least-squares sense) to the observed periods, given assumed values of Δn listed in Table 4.6.

The smallest observed spacing in the period spectrum between modes confidently identified as $\ell = 1$ is ~ 21 s, between the modes at 401 s and 380 s (2500 μHz and 2630 μHz), and this formed the seed of the original suggestion of 21 s as the average period spacing in the spectrum of PG 0122. The 380 s mode is also one of two (the other being at 570 s) which the proposed 16.2 s pattern misses rather significantly. The 21.1 s pattern, on the other hand, fails at about the same level to explain the mode at 450 s (2225 μHz). All of these "misses" could result from effects of mode trapping, so that both patterns account for the data almost equally well, with $\Delta\Pi = 21.1$ s somewhat preferred. We previously mentioned an additional peak tantalizingly close to 1σ above the local noise band at 2800 μHz (357.1 s). Though by itself not strictly significant, if real this peak would fit the 21.1 s pattern precisely—completing a chain of four consecutive modes—and would in addition allow us to rule out a 16.2 s pattern with high confidence. While this peak is the largest in the transform between the $\ell = 1$ groups near 336 s and 380 s, we cannot claim with certainty that it is a real pulsation mode if considered entirely on its own merits. We will only say that while $\Delta\Pi \sim 21$ s is the most probable solution to the

Table 4.6 Comparison of the PG 0122 Period Spectrum with Patterns of Strict 21.10 s and 16.24 s Spacing between Modes of Consecutive Radial Index n

	$\Delta\Pi$=21.10 s			$\Delta\Pi$=16.24 s		
$\Pi_{\rm obs}$ $(m=0)$ (s)	$\Pi_{\rm pred}$ (s)	$n-n_0$	$\Pi_{\rm obs}-\Pi_{\rm pred}$ (s)	$\Pi_{\rm pred}$ (s)	$n-n_0$	$\Pi_{\rm obs}-\Pi_{\rm pred}$ (s)
611.0*	612.0	+10	−1.0	612.1	+13	−1.1
570.0[a] $(^{+1.2}_{-1.3})$	569.8	+8	$+0.2(^{+1.2}_{-1.3})$	563.4	+10	$+6.6(^{+1.2}_{-1.3})$
449.5	443.2	+2	+6.3	449.7	+3	−0.2
401.0	401.0	0	...	401.0	0	...
379.6,380.1	379.9	−1	−0.3, +0.2	384.8	−1	−5.2, −4.7
336.7	337.7	−3	−1.0	336.0	−4	−0.7

Notes—Period Spectrum at $(\ell=1, m=0)$. An asterisk indicates that the period represents the calculated center of a doublet splitting. Numbers in parentheses show the effects of assuming a value of m other than $m=0$ for the identified peak.

[a]Mode identified by O'Brien et al. 1996. Not observed in the WET data set.

pulsation spectrum of PG 0122, $\Delta\Pi \sim 16$ s cannot, at this point, be ruled out conclusively.

4.4.4 The Mass and Luminosity of PG 0122

For the fourth time, we encounter a PWD with a likely period spacing near 21 seconds. As with PG 2131, to maintain a period spacing so close to that of the far hotter PG 1159, PG 0122 must be more massive. If the period spacing is even shorter (16 s) it must be more massive still. Based on evolutionary models (see § 5.3), the two values of $\Delta\Pi$ discussed above imply a mass for PG 0122 of either $0.68 \pm 0.04\ M_\odot$ (for $\Delta\Pi = 21.1$ s) or $1.00 \pm 0.08\ M_\odot$ (for $\Delta\Pi = 16.2$ s).[6] The luminosities corresponding to these two mass ranges are $5.2 \pm 2.1\ L_\odot$ and $1.5 \pm 0.8\ L_\odot$ respectively. Either solution makes PG 0122 the most massive and least intrinsically luminous GW Vir star known. This result has important consequences for the character of the cooling mechanisms responsible for the star's continuing evolution, as we discuss in Chapter 6.

[6]If these modes are $\ell = 2$, the implied mass is less than $0.4\ M_\odot$. Again, this is below the minimum mass for a C/O white dwarf and supports our identification $\ell = 1$.

Table 4.7 Summary of Variable PWD Parameters

Name	log g	$T_{\rm eff}$	$log(L/L_{\odot})$	$M/M_{\odot}$	$\Delta\Pi$
NGC 1501	~ 6.0	80 ± 10 kK	3.3 ± 0.3	0.55 ± 0.03	$\sim$ 22.3 s
PG 1159	7.22 ± 0.06	14 ± 10 kK	2.3 ± 0.2	0.57 ± 0.01	21.5 ± 0.1 s
PG 2131	7.67 ± 0.12	95 ± 10 kK	1.0 ± 0.2	0.61 ± 0.02	21.6 ± 0.4 s
PG 0122	7.97 ± 0.15	80 ± 10 kK	0.7 ± 0.2	0.68 ± 0.04	21.1 ± 0.4 s

4.5 Implications

We have now discussed four PWDs that yielded to asteroseismological scrutiny, PG 1159, PG 2131, PG 0122, and the central star of the planetary nebula NGC 1501. We summarize the parameters of these four stars in Table 4.7. All show patterns of equal period spacing very close to 21 s. This is a remarkable trend, or more accurately a remarkable lack of a trend! If these stars follow the narrow mass distribution observed in white dwarf stars, then period spacing is expected to increase with decreasing $T_{\rm eff}$ as they evolve from the blue to the red edge of the instability strip. Observationally, this is not the case. In the next chapter, we discuss the deep implications of this curious result.

CHAPTER 5 GROUP PROPERTIES OF THE PULSATING PRE-WHITE DWARF STARS

"Here were a number of strange facts, seemingly too discordant and too perplexing to admit of being interpreted. Yet one discovery only was wanting to bring them all into unison."

—Richard A. Proctor, *Other Worlds than Ours (1879)*

5.1 Introduction

Despite the wealth of pulsational data available to us in studying the variable PWDs, they have so far resisted coherent generalizations of their group properties. Such a classification is required for understanding possible driving mechanisms or explaining the observed period distribution. Until now, the errors bars associated with determination of mass, luminosity, and $T_{\rm eff}$ for a given variable star spanned a significant fraction of the instability strip.

Even given the limited information provided by spectroscopic determinations of $\log g$ and $T_{\rm eff}$, many attempts have been made to form a coherent theory of their pulsations. Spectroscopically, the PG 1159 stars are defined by the appearance of lines of HeII, CIV, and OVI (and sometimes NV) in their spectra. Starrfield et al. (1984) proposed that these stars are driven by cyclical ionization of C and O. However, their proposal suffers from the difficiency that a He mass fraction of only 10% in the driving zone will "poison" C/O driving. Another problem is the existence of non-pulsating stars within the strip with nearly identical spectra to the pulsators (Werner 1995). More precise observations can find subtle differences between the pulsators and non-pulsators. For instance, Dreizler (1998) finds NV in the spectra of all the pulsators but only some of the non-pulsators. It remains to be seen if these differences are important.

Kawaler (1986) showed that pulsation can also theoretically arise in PWDs via the last remnants of nuclear burning that might still take place in their envelopes. This is referred to as the ϵ mechanism. It can only weakly drive the lowest order g-modes, however, and modes with these periods have not been seen.

More recently, Saio (1996) and Gautschy (1997) proposed driving by a "metallicity bump," where the opacity derivative changes sign due to the presence of metals such as iron in the envelope. This is a κ mechanism similar to that currently thought to drive pulsation in the main sequence δ-Scuti variables. Unfortunately, their rather crude models are inconsistent with the evolutionary status of PG 1159 stars. More importantly, their period structures do not match the WET observations described in Chapters 3 and 4.

With so many different pulsational driving mechanisms, stricter constraints on the observable conditions of the pulsators and non-pulsators are badly needed. The most effective way to thin the ranks of competing theories (and perhaps point the way to explanations previously unthought of) is to obtain better knowledge of when the pulsations begin and end for PWD stars of a given mass.

Of course, with so few stars available to study, even complete asteroseismological solutions for all of them might not prove significantly illuminating. Even if their properties follow recognizable patterns, it is difficult to show this compellingly given only a few cases. Up to this point, we have discussed their behavior only in terms of individual objects. With asteroseismological information on the majority of the pulsators now in hand, we can finally investigate their behavior as a class of related objects. As we show below, the variable PG 1159 stars apparently do follow a compelling trend—one spanning their entire range of stellar parameters. Any model of PWD pulsation must conform to this observed pattern.

5.2 Observed Temperature Trends of the PG 1159 Pulsators

5.2.1 Mass Distribution

White dwarfs exhibit a very narrow mass distribution, centered at about 0.56 $M_{\odot}$. If, for a given $T_{\rm eff}$, variable PWD masses conform to the same distribution expected of non-variables,

then we are led to certain expectations concerning the pulsations seen in the former. Based on Equation (2.3), period spacing (proportional to Π_0) should increase monotonically as the luminosity and $T_{\rm eff}$ of a given star decrease. For instance PG 1159, with a $T_{\rm eff}$ of 140,000 K, should see its period spacing increase by about 20%, from 21 s to 26 s, by the time it reaches the effective temperature of PG 0122—80,000 K. In other words, the farther PG 0122's period spacing is from 26 s, the farther is its mass from that of PG 1159. In fact these two objects, representing the high and low $T_{\rm eff}$ extremes of the GW Vir stars, have almost exactly the *same* period spacing despite enormous differences in luminosity and temperature. For PG 0122, its low $T_{\rm eff}$ pushes it toward longer $\Delta\Pi$; this must be offset by a higher mass. With such a significant $T_{\rm eff}$ difference, the mass difference between PG 0122 and PG 1159 must be significant also, and it is: 0.69 $M_{\odot}$ versus 0.58 $M_{\odot}$.

Two stars with a coincident period spacing—despite widely different mass and luminosity—are simply curious. In fact all four PWDs with relatively certain period spacing determinations have the same spacing to within 2 s, or 10%. This includes the central star of NGC 1501, which has a luminosity over three orders of magnitude larger than that of PG 0122 and hence an even lower mass than PG 1159 in comparison. Figure 5.1 shows the mass versus luminosity for the known GW Vir stars plus NGC 1501, based on determinations of $\Delta\Pi$ presented in Chapters 3 and 4. (PG 1707 is included as the open circle, since its period spacing is not firmly established.)

Figure 5.2 shows the implications of the ubiquitous 21-22 s spacing for the instability "strip" in the log g–log $T_{\rm eff}$ plane. The observational region of instability has shrunk significantly. It exhibits such a striking slope in the figure that, unlike most other instability regions in the H-R diagram, it can no longer be refered to accurately as an instability strip (in temperature) at all. Nevertheless, we will continue to refer to the region of instability pictured in Figure 5.2 as the GW Vir "instability strip" with the understanding that the effective temperatures of the red and blue edges are highly dependent on log g (or L).

Why should the PWD instability strip apparently straddle a line of approximately constant period spacing? Normally, theorists search for explanations for the observed boundaries (the

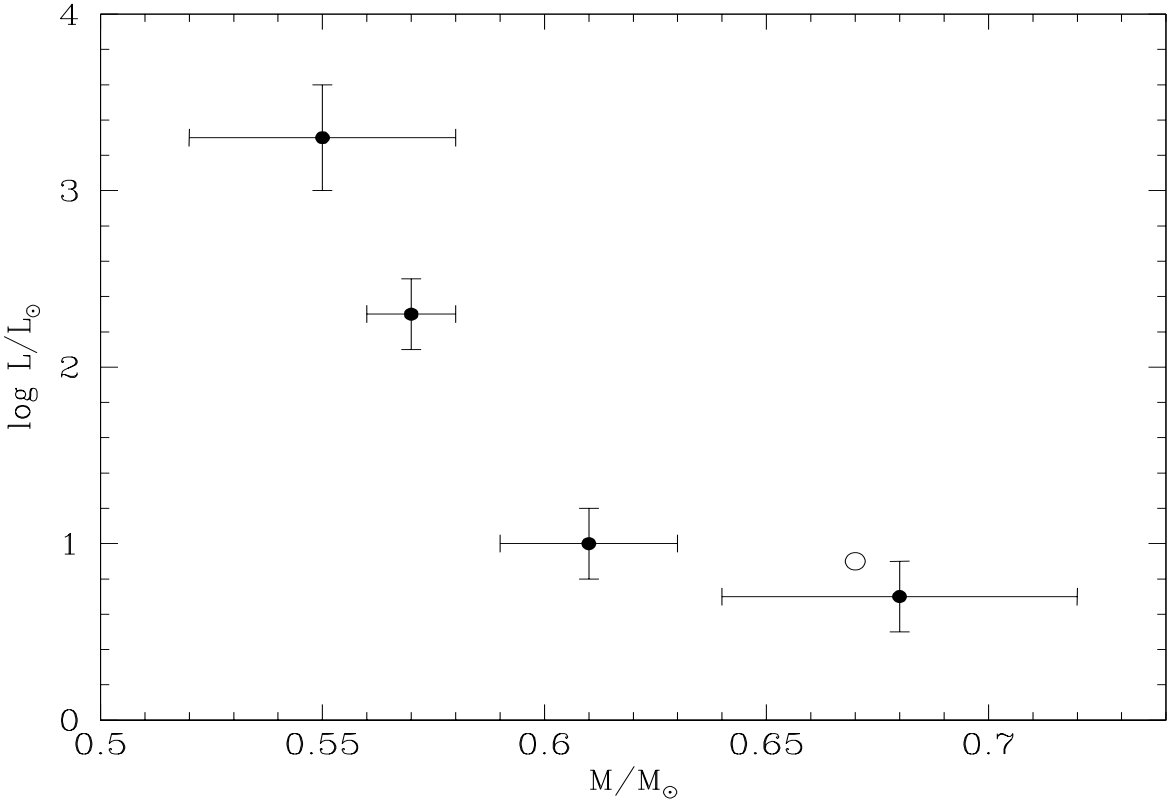

Figure 5.1 Luminosity versus mass determined from pulsation data for the known GW Vir stars plus the PNNV NGC 1501. The open circle represents PG 1707, for which the pulsation structure is uncertain.

red and blue edges) of an instability strip in the behavior of a proposed pulsation mechanism. That behavior is determined by the thermal properties of a PWD star, while its period spacing is determined by its mechanical structure. In degenerate or nearly degenerate stars, the thermal properties are determined by the ions, while the mechanical structure is determined by the degenerate electrons, and normally the two are safely treated as separate, isolated systems. If the 21-22 s period spacing is somehow a *prerequisite* for pulsation, then this implies an intimate connection between the mechanical oscillations and the thermal pulsation mechanism.

The alternative is that the mass-luminosity relationship along the instability strip is caused by some other process—or combination of processes—which approximately coincides with the relationship that governs the period spacing. In this case, some mechanism must shut off observable pulsation in low mass PWDs before they reach low temperature, and delay ob-

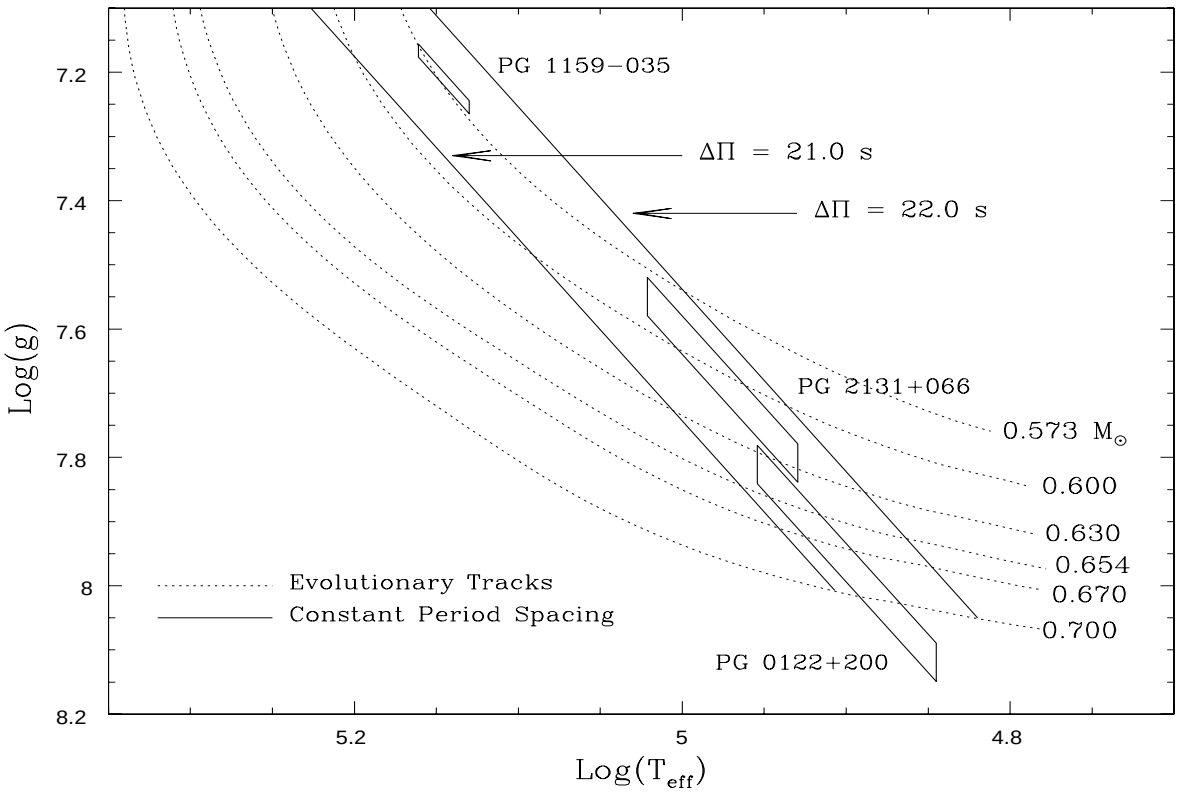

Figure 5.2 Portion of the log g–log $T_{\rm eff}$ plane showing PWD evolutionary tracks based on ISUEVO. The error boxes for each star derive from period spacing combined with spectroscopically determined $T_{\rm eff}$.

servable pulsation in higher mass PWDs until they reach low temperature.[1] We will explore mechanisms which meet these criteria in § 5.4.

5.2.2 Period Distribution

The other clear observational trend exhibited by the PWD pulsators was introduced in § 3.4: their periods decrease with decreasing luminosity (increasing surface gravity). Figure 5.3 shows the luminosity versus dominant period for the same stars from Figure 5.1. The trend apparent in the figure is in marked contrast to the one seen in the ZZ Ceti stars, which show longer periods with lower $T_{\rm eff}$. Recall that the ZZ Ceti period trend is a consequence of the changing thermal timescale in the driving zone, which sinks deeper (to longer timescales) as the star

[1] We use the phrase "observable pulsation" to indicate that possible solutions might reside in some combination of observational selection effects as well the intrinsic behavior of a driving mechanism.

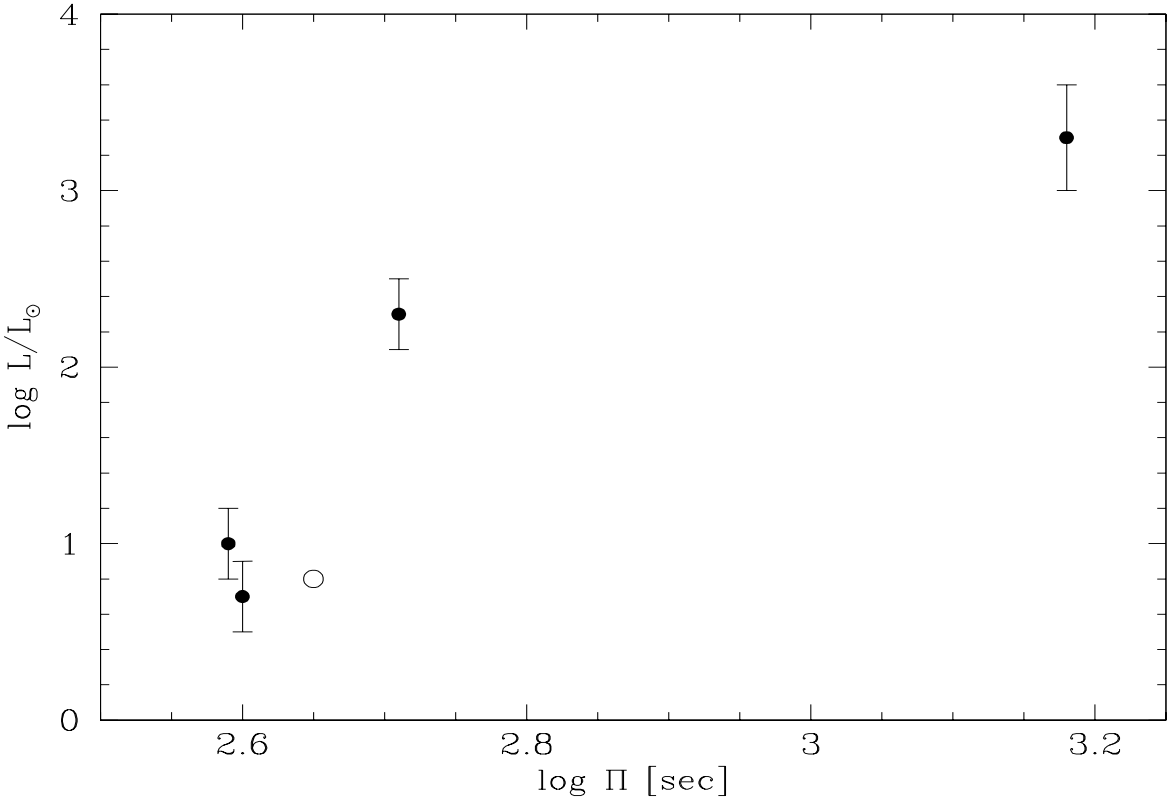

Figure 5.3 Luminosity (determined using the pulsation data) versus dominant period for the known GW Vir stars plus the PNNV NGC 1501. The open circle represents PG 1707, for which the pulsation structure is uncertain.

cools. If the same effect determines the periods in GW Vir and PNNV stars, then Figure 5.3 might indicate that the driving zone becomes more shallow with decreasing $T_{\rm eff}$. We will show that this is not the case in PWD models. We conclude that some other mechanism must be responsible for setting the dominant period in PWD variables.

Are the trends seen in Figures 5.1 through 5.3 related? To explore this question in detail, we developed a new set of PWD evolutionary models, which we summarize in the next section. In the final section of this chapter we analyze the behavior of driving zones in PWD models in light of—and to seek an explanation for—the trends just discussed.

5.3 A New Set of Pre-White Dwarf Evolutionary Models

To understand the various trends uncovered in the hot pulsating PWDs, we appeal to stellar models. Models have been essential for exploiting the seismological observation of individual stars. For this work, though, we needed models over the range of the GW Vir stellar parameters of mass and luminosity. Our principal computational tool is the stellar evolution program ISUEVO, which is described in some detail by Dehner (1996; see also Dehner & Kawaler 1995). ISUEVO is a "standard" stellar evolution code that is optimized for the construction of models of PWDs and white dwarfs.

The seed model for the models used in this section was generated with ISUEVO by evolution of a 3 $M_{\odot}$ model from the Zero Age Main Sequence through the thermally pulsing AGB phase. After reaching a stable thermally pulsing stage (about 15 thermal pulses), mass loss was invoked until the model evolved to high temperatures. This model (representing a PNN) had a final mass of 0.573 $M_{\odot}$, and a helium-rich outer layer.

To obtain self-consistent models within a small range of masses, we used the 0.573 $M_{\odot}$ model, and scaled the mass up or down. For example, to obtain a model at 0.60 $M_{\odot}$, we scaled all parameters by the factor 0.60/0.573 for an initial model. Relaxation to the new conditions was accomplished by taking many very short time steps with ISUEVO. Following this relaxation, the evolution of the new model proceeded as before. In this way, we produced models that were as similar as possible, with mass being the only difference.

Comparison of our evolutionary tracks and trends with the earlier model grids of Dehner (1996) shows very close agreement, given the different evolutionary histories. Dehner's initial models were derived from a single model with a simplified initial composition profile, while our models are rooted in a self-consistent evolutionary sequence. We note that the work by Dehner (1996) included elemental diffusion (principally by gravitational settling), while the models we use here did not include diffusion. Within the temparature range of the GW Vir stars, however, the effects of diffusion have only a small influence on the features of the evolution that we are exploring.

5.4 Selection Effects, Driving, and the Blue and Red Edges

5.4.1 The Observed "Blue" and "Red" Edges

In explaining the observed distribution of pulsating stars with respect to stellar parameters, we must distinguish observational selection effects from causes intrinsic to the objects under study. Usually, understanding selection effects is an important part of decoding the shape of the distribution in terms of physical effects of the latter. In this case, the blue and red edges exhibit a similar slope in the log g–log $T_{\rm eff}$ plane, but we must still separate out selection effects from the shape of one or both of them.

Two of the most common selection effects encountered in stellar astronomy are magnitude and lifetime bias. The more rapid the evolution through a particular region of the H-R diagram, the less likely stars will be found there. Greater luminosity increases the distance of the detection threshold and therefore the relative sample volume. Some combination of these effects will determine the odds of finding stars of a particular mass at a particular point in their evolution. One of the most common ways to depict these combined effects is to construct a luminosity function, which is simply a plot of the expected number density of stars per unit luminosity, based on how bright they are and how fast they are evolving at different times. Figure 5.4 shows schematic luminosity functions for PWD stars of two different masses, based on the models described in the previous section and normalized according to the white dwarf mass distribution (see for instance Wood 1992). One important result of this figure is that higher mass models always achieve a given number density per unit luminosity later (at lower L and $T_{\rm eff}$) than lower mass models. Also, the number density per unit luminosity increases for all models as they evolve to lower $T_{\rm eff}$.

These effects together imply that, *if* PWDs of all mass pulsate all the way down to 80,000 K, then the distribution of known pulsators should be skewed heavily toward those with both low $T_{\rm eff}$ *and* low mass. We don't see such stars; thus the red edge must exclude them from the distribution.

While the observed red edge actually marks the dissappearance of pulsation from PWD

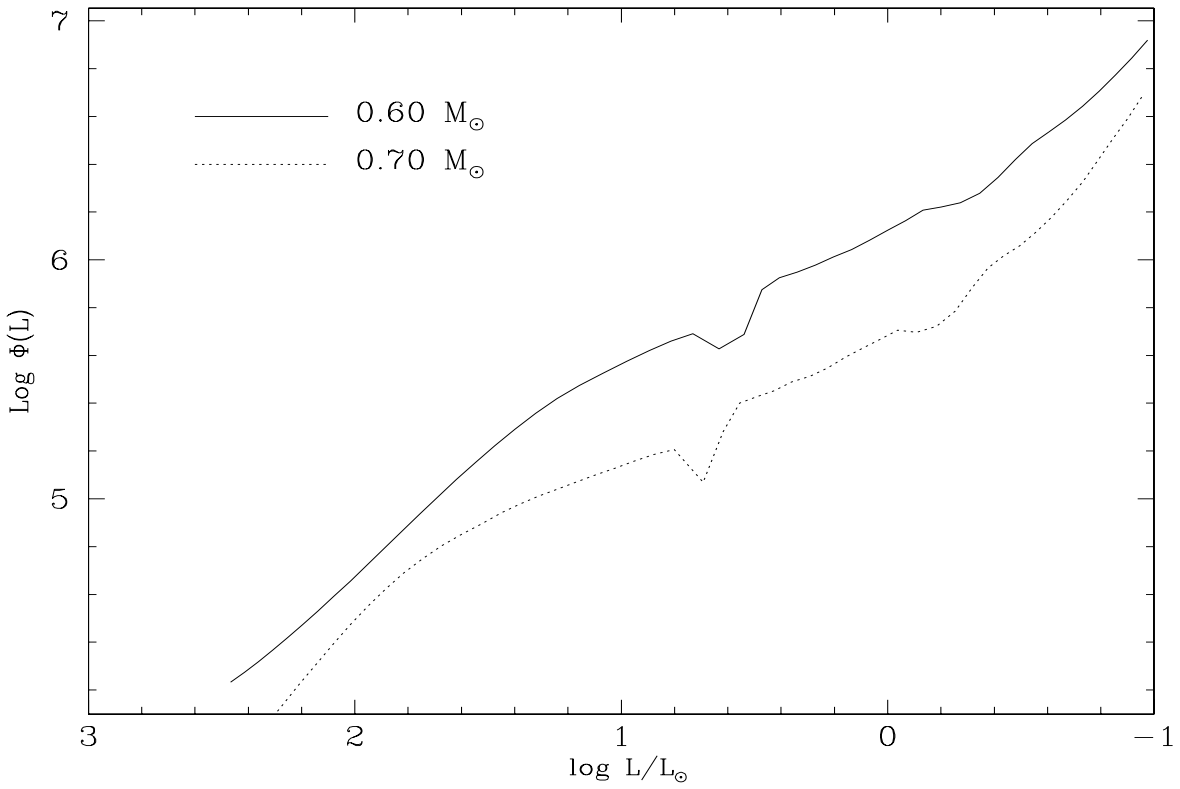

Figure 5.4 Theoretical luminosity functions, log $\Phi(L)$, for two different single-mass populations of PWD stars.

stars, selection effects change our chances of finding high-mass, high-$T_{\rm eff}$ pulsators. In this case, we expect that the likehood of finding stars of a given mass within the instability strip will increase the closer those stars get to the red edge. This would tend to render the theoretical blue edge (as defined by the onset of pulsation in models of a given mass) undetectible in real PWD stars—given the small number of known variables. In other words, stars "bunch up" against the red edge due to their continually slowing rate of evolution, causing the *apparent* blue edge to shadow the slope of the red edge in the log g–log $T_{\rm eff}$ plane. This explains the approximately linear locus of pulsating stars found within that plane implied by their tight distribution of $\Delta\Pi$.

We are left to explain the observed red edge in terms of the intrinsic properties of the stars themselves, which we defer to § 5.4.3. First, however, we will discuss the effects of the observed mass distribution along the strip on the period trend seen in Figure 5.3.

5.4.2 The Π versus $T_{\rm eff}$ Trend

As mentioned previously, the depth of an ionization-based driving zone increases—moves to larger thermal timescales—with decreasing $T_{\rm eff}$ for PWD stars of a given mass. This implies a period trend opposite to that observed in Figure 5.3. What other mechanisms might affect the observed periods? One such mechanism is the changing value of the maximum sustainable g-mode period, $\Pi_{\rm max}$. For the ZZ Ceti stars, $\Pi_{\rm max}$ probably does not influence the period distribution much, since from Equation (2.6) it increases through the ZZ Ceti instability strip. In PWDs, however, the R dependence in Equation (2.6) must be taken into account; we cannot be certain that the trend implied by a lengthening driving timescale won't find itself at odds with a decreasing $\Pi_{\rm max}$.

Figure 5.5 shows the (arbitrarily normalized) run of $\Pi_{\rm max}$ versus $T_{\rm eff}$ for three PWD model sequences of different mass. Clearly, $\Pi_{\rm max}$ decreases significantly as models evolve along all three sequences, with high-mass stars exhibiting a smaller $\Pi_{\rm max}$ than low-mass stars at all $T_{\rm eff}$.[2] These two effects, when combined with the PWD mass distribution, imply that $\Pi_{\rm max}$ should plummet precipitously with increasing $\log g$ in the models in Figure 5.2. For example, the ratio of $\Pi_{\rm max}$ for PG 1159 to that of PG 0122 is expected to be $\sim$ 1.42:1, while the ratio of their observed dominant periods is 540:400 = 1.35:1. The period distribution seen in Figure 5.2 is thus consistent with the idea that the value of $\Pi_{\rm max}$ determines the dominant period in PWD stars. As we will see in the next section, $\Pi_{\rm max}$ probably also plays an important part in determining the more fundamental question of *when* a given PWD star is likely to pulsate.

5.4.3 Driving Zone Depth, $\Pi_{\rm max}$, and the Red Edge

In § 2.3.2, we discussed the relationship between the depth of the driving zone and the period of g-mode oscillations. Equation (2.5) implies that the dominant period should increase in response to the deepening driving zone, as long as other amplitude limiting effects do not intervene. Figure 5.5 shows how one particular effect—the decreasing maximum period—might

[2] If this trend continued all the way to the cooler white dwarf instability strips, then ZZ Ceti stars could only pulsate at very short periods, but $T_{\rm eff}$ begins to dominate below around 60,000 to 70,000 K, pushing $\Pi_{\rm max}$ back to longer and longer periods once the stars approach their minimum radius at the top of the white dwarf cooling track.

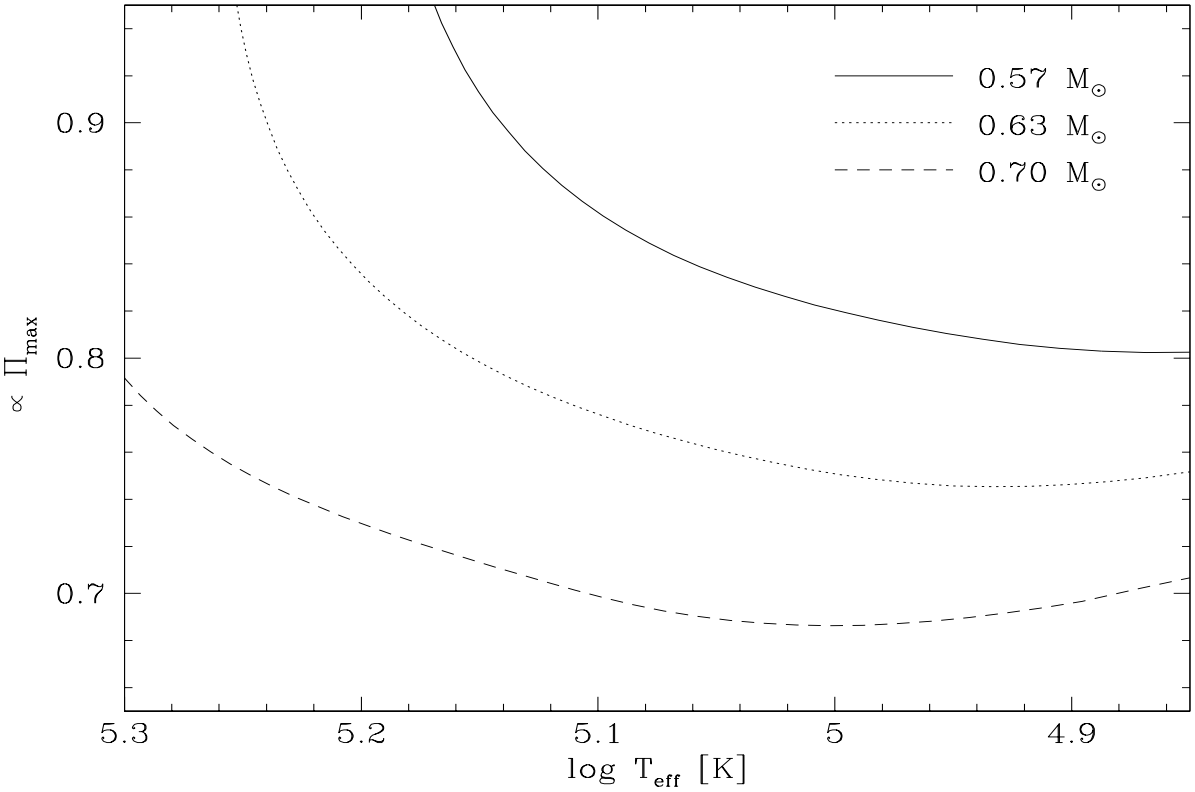

Figure 5.5 Maximum g-mode period, $\Pi_{\mathbf{max}}$, versus $T_{\mathbf{eff}}$ for three PWD evolution sequences of different mass. The absolute normalization of the vertical axis is arbitrary, but the relative position of the curves is not.

reverse the trend connected to driving zone depth, and the observed periods of GW Vir stars supports the suggestion that $\Pi_{\mathbf{max}}$ is the key factor in setting the dominant period. While $\Pi_{\mathbf{max}}$ limits the range of periods that can respond to driving, $\tau_{\mathbf{th}}$ in the driving zone limits the periods that can be driven. However, $\tau_{\mathbf{th}}$ increases steadily for all GW Vir stars, and $\Pi_{\mathbf{max}}$ decreases steadily. Eventually, therefore, every pulsator will reach a state where $\tau_{\mathbf{th}} > \Pi_{\mathbf{max}}$ over the entire extent of the driving zone. In such a state, the star can no longer respond to driving at all, and pulsation will cease. If $\Pi_{\mathbf{max}}$ remains the most important amplitude limiting factor for stars approaching the red edge, then the red edge itself could be caused by the situation just described.

We can test this idea by asking if it leads to the kind of mass-dependent red edge we see. To answer this question, we need to know how the depth of the driving zone (as measured

by $\tau_{\rm th}$) changes with respect to $\Pi_{\rm max}$ for stars of various mass. Figure 5.6 depicts the driving regions for four different model sequences ($M = 0.57, 0.60, 0.63$ and $0.70\ M_{\odot}$) at three different effective temperatures (144,000 K, 100,000 K, and 78,000 K). The driving strength, dk/dr, is determined from Equation (2.4), where k represents the expression inside parentheses. The y-axis has not been normalized and is the same scale in all four panels. The surface of each

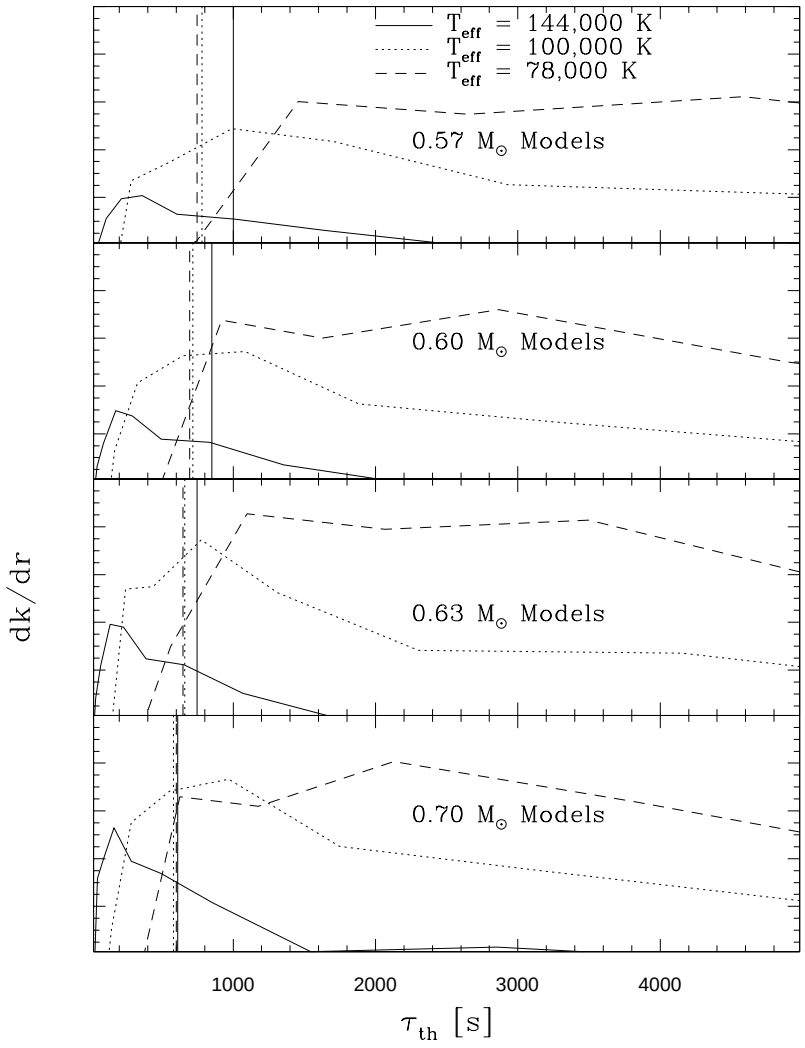

Figure 5.6 Driving strength, $dk/dr > 0$, for four different model sequences at three different effective temperatures. Vertical lines represent the maximum g-mode period, normalized to 1000 s in the $0.57\ M_{\odot}$ model at 144,000 K.

model is on the left, at $\tau_{\rm th} = 0$. The vertical lines in the figure represent $\Pi_{\rm max}$, for each model, normalized to 1000 s in the 0.57 $M_\odot$ model at 144,000 K. We have made no attempt to calculate the actual value of $\Pi_{\rm max}$; the important thing is its changing relationship to the depth of the driving zone with changing mass and $T_{\rm eff}$.

A couple of important trends are clear in the figure. First, the driving zone in models of a given mass sinks to longer $\tau_{\rm th}$, and gets larger and stronger, with decreasing $T_{\rm eff}$. In the absence of other effects, this trend would lead to ever increasing periods of larger and larger amplitude as $T_{\rm eff}$ decreases. Meanwhile, $\Pi_{\rm max}$ changes more moderately, moving toward slightly shorter timescales with decreasing $T_{\rm eff}$ and increasing mass. If we make the somewhat crude assumption that the effective driving zone consists only of those parts of the full driving zone with $\tau_{\rm th} < \Pi_{\rm max}$, then a picture of the red edge emerges. At $T_{\rm eff}$ =144,000 K, the driving zone is relatively unaffected in all three model sequences. As $T_{\rm eff}$ decreases, and the driving zone sinks to longer $\tau_{\rm th}$, the $\Pi_{\rm max}$-imposed limit encroaches on the driving zone more and more for every mass. Thus the longer periods, while driven, are eliminated, moving the locus of power to shorter periods than would be seen if $\Pi_{\rm max}$ was not a factor. Eventually, *all* the driven periods are longer than the maximum period at which a star can respond, and pulsation ceases altogether. This is the red edge.

Pulsations will not shut down at the same $T_{\rm eff}$in stars of every mass. High mass models retain more of their effective driving zones than low mass models at a given $T_{\rm eff}$. This occurs because at a given $T_{\rm eff}$, the top of the driving zone moves toward the surface (to smaller $\tau_{\rm th}$) with increasing mass. This effect of decreasing $\tau_{\rm th}$ at the top of the driving zone outstrips the trend to lower $\Pi_{\rm max}$ with increasing mass. The result is that, at 78,000 K, the driving zone in the 0.57 $M_\odot$ model (upper panel of Figure 5.6) has moved to timescales entirely above the $\Pi_{\rm max}$ limit, while the 0.63 $M_\odot$ and 0.70 $M_\odot$ models (appropriate for PG 0122; two lower panels in Figure 5.6) still produce significant driving at thermal timescales below $\Pi_{\rm max}$.

Recall from Table 4.7 and Figure 5.2 that GW Vir stars of lower $T_{\rm eff}$ have higher mass. Why? We can now give an answer: at low $T_{\rm eff}$, the low mass stars have stopped pulsating because they only drive periods longer than those at which they can respond to pulsation!

Higher mass stars have shallower ionization zones (at a given $T_{\rm eff}$) that still drive periods shorter than the maximum allowed g-mode period, even at low $T_{\rm eff}$. This causes the red edge to move to higher mass with decreasing luminosity and $T_{\rm eff}$, *the same trend followed by lines of constant period spacing.* The interplay between driving zone depth and $\Pi_{\rm max}$ enforces the strikingly small range of period spacings ($\Delta\Pi \sim 21.5$ s) seen in Table 4.7 and Figure 5.2.

These calculations are not an attempt to predict the exact location of the red edge at a given mass. We are only interested at this point in demonstrating how the position of the red edge is expected to vary with mass, given an ionization-based driving zone with an upper limit placed on it by $\Pi_{\rm max}$. In the particular models shown in Figure 5.6, the top of the driving zone corresponds to the ionization temperature of OVI, but the behavior of the red edge should be the same no matter what species causes the driving. Its absolute location, though, would probably be different given driving by different species. In order to use the location of the red edge for stars of different mass to identify the exact species that accomplishes driving, we would need to calculate $\Pi_{\rm max}$ precisely for all the models in Figure 5.6 and better understand exactly how the value of $\Pi_{\rm max}$ affects the amplitudes of modes nearby in period. Such a calculation is beyond the scope of this thesis, and we leave it to future investigators to attempt one.

Alternatively, the discovery of more GW Vir stars would help us better understand these processes by defining the red edge with greater observational precision. The simplest test of our theories would be to find low-$T_{\rm eff}$ GW Vir pulsators of low mass. If they exist, then $\Pi_{\rm max}$ is probably not a factor in determining their periods, and variation should be sought in their lightcurves at longer periods than in the GW Vir stars found so far; Figure 5.6 suggests their dominant periods should be in the thousands of seconds. It is possible that these stars could be quite numerous (and *should* be quite numerous if they exist at all, given their slower rate of evolution) and still escape detection, since standard time-series aperture photometry is not generally effective at these timescales. Most current CCD photometers are quite capable of searching for such variability, however. Based on these results, we encourage future studies to determine whether or not low-mass, low-$T_{\rm eff}$ GW Vir pulsators do indeed exist.

In summary, the observed trend toward shorter dominant periods with decreasing $T_{\rm eff}$ pro-

vides evidence that the maximum g-mode period, $\Pi_{\rm max}$, is an important factor in determining the range of periods observed in GW Vir stars. Eventually, models suggest the driving zone in all PWD pulsators will sink to thermal timescales longer than $\Pi_{\rm max}$, and pulsation will cease. Since this takes place at lower $T_{\rm eff}$ for stars of higher mass, this process is consistent with the observed red edge, which shows a significant shift to lower temperature with increasing mass. The blue edge is not constrained by this mechanism, but for GW Vir stars the intrinsic blue edge is undetected because of selection effects due to rapid evolution. Discovery of additional GW Vir stars might eventually allow us to place statistical limits on the location of the "intrinsic" blue edge: i.e., we should look for higher mass (smaller $\Delta\Pi$) *hot* pulsators.

CHAPTER 6 LOOKING FOR THE NEUTRINO SIGNATURE

"Had science merely measured this minute variation, the work would have given striking evidence of the exact spirit in which men of our day deal with natural phenomena. But science was to do much more. The variations of this minute variation were to be inquired into; their period was to be searched for; the laws by which they were regulated, and by which their period might perhaps itself be rendered variable, were to be examined; and finally their relation to other natural laws was to be sought after."

—Richard A. Proctor, *Other Worlds than Ours (1879)*

6.1 Introduction

In general, stars are too remote—and observables too few—to make them practical experimental physics test-beds: our data are spent in simply describing the dimensions of the objects under study. In many cases we must extrapolate experimental data over many orders of magnitude, or resort to untested calculations from first principles, to reach the regions of phase space that apply to stellar interiors.

If we hope to overcome these problems and pursue "experimental" astrophysics, we can either attempt to increase the number of observables or find simpler stars. As first realized by Mestel (1952), the evolution of white dwarfs and PWDs is primarily a simple cooling problem. In general, our growing understanding of white dwarf interiors and evolution has paralleled advances in the theory of dense plasmas, with the recognition of important influences like electron degeneracy (Chandrasekar 1939), Coulomb interactions (Salpeter 1961), crystallization (Kirzhnitz 1960; Abrikosov 1960; Salpeter 1961; Stevenson 1980) and neutrino cooling effects (Chin, Chiu, & Stothers 1966; Winget, Hansen, & Van Horn 1983; Kawaler, Hansen, & Winget

1985). Iben & Tutukov (1984) summarize the various mechanisms which dominate white dwarf evolution from the planetary nebula nucleus (PNN) stage to the coolest white dwarfs.

The cooling of a GW Vir interior tends to increase the periods of each given pulsation mode. Their high luminosity ($\log L \sim 0 - 3$) means they cool much more rapidly than either ZZ Ceti or DBV variables. GW Vir period changes are therefore expected to be more rapid also. Winget, Hansen & Van Horn (1983) show that the e-folding time for period changes in GW Vir stars should be about 10^6 years; such rapid changes are measurable in $1 - 3$ years. This is an exciting prospect: to measure directly, on human timescales, the rate of evolution of a star, and specifically to place strict constraints on the mechanisms which regulate the evolution of a stellar interior. Over 30 years ago, Chin, Chiu, and Stothers (1966) showed that at some point in PWD evolution neutrino losses should dominate all other cooling processes. Asteroseismological analysis can tell us which stars these are, and then measurement of period changes can tell us if our neutrino physics is right.

Such a test has implications far beyond the study of PWD evolution. For instance, in Chapter 1 we mentioned that one of the most fundamental questions of stellar astrophysics is the length of time stars spend on the main sequence. Answering this question requires precise knowledge of the p-p and CNO nuclear reaction rates. Currently, the best laboratory for measuring these rates is our own Sun, since terrestrial labs cannot in general reproduce the conditions of the stellar interior. However, models which successfully reproduce the known structure of the Sun predict a neutrino flux two to three times that measured by earthly detectors (Bahcall & Pinsonneault 1996, and references therein). For a long time, it was thought the problem might reside in our incomplete knowledge of conditions in the solar interior. Recently, helioseismology projects such as the Global Oscillation Network Group (GONG) have resulted in the measurement of millions of solar pulsation frequencies (Harvey et al. 1996). With so many parameters to constrain model properties, the possibility that the solar neutrino problem can be solved through variations in the thermodynamics or mechanics seems to be excluded (Bahcall & Pinsonneault 1996). The problem, then, almost certainly lies with the way we handle the nuclear physics.

Under the most intense scrutiny is the standard theory of lepton interactions. Our calculations of neutrino emission from PWDs are based on this same theory. In PWDs, however, the energy loss rate due to neutrinos is thousands of times greater than in the Sun. Measurement of the effects of neutrino interactions in PWDs would afford a critical independent test not only of the standard lepton theory but also of non-standard theories brought forward to solve the solar neutrino problem.

To explore this possibility, we calculated PWD evolutionary tracks using different neutrino production rates. In the next section we describe the calculation of those rates and summarize the basic interactions that lead to neutrino emission in PWD interiors. Section 6.3 describes PWD sequences with varied neutrino production rates and examines effects on measurable quantities such as $T_{\rm eff}$, surface gravity, and rate of period change. Finally, in § 6.4 we discuss prospects for placing observational constraints on neutrino physics, and we identify appropriate targets for future observation.

6.2 Neutrino Cooling in Pre-White Dwarf Interiors

Unlike the solar neutrino flux, neutrino emission in PWDs is not a by-product of nuclear fusion. Instead, the density and temperature in their cores are high enough ($\log \rho_{\rm c} \sim 6$–7, $\log T_{\rm c} \sim 7$–8) to produce neutrinos directly through several different scattering processes. The two most important processes are *neutrino bremmstrahlung* and *plasmon* scattering. Neutrino bremmstrahlung is much like the normal bremmstrahlung process familiar to astrophysicists, in which high-energy electrons scatter off nuclei, emitting X-rays. At the high density and temperature of PWD interiors, however, neutrinos can be produced instead. The second mechanism of neutrino emission derives from the dispersion relation of a photon in an electron gas, given by

$$(\hbar\omega)^2 = (\hbar\omega_0)^2 + (\hbar kc)^2 \tag{6.1}$$

where ω is the photon angular frequency, k is the wave number of the photon, and ω_0 is the so-called plasma frequency. The plasma frequency depends on the electron temperature and density, and vanishes in free space. A photon obeying Equation (6.1) behaves like a particle

with an effective mass of $\hbar\omega_0/c^2$, and is therefore called a *plasmon*. Their effective mass means that (unlike photons in free space) plasmons can decay directly into electron-positron pairs which then annihilate into electron neutrinos and antineutrinos.

The possible relevance of the plasma process to stellar astrophysics was first pointed out by Adams, Ruderman, & Woo (1963), who subsequently calculated rates based on the theory of Feynman & Gell-Mann (1958). Beaudet, Petrosian & Salpeter (1967) were the first to incorporate them into stellar evolution calculations. Later, Dicus (1972) recalculated the rates of various neutrino processes in the unified electro-weak theory of Weinberg and Salam (Weinberg 1967, Salam 1968). The rates used in the stellar evolution code described in § 5.3 derive from updated calculations by Itoh et al. (1996), and include the plasmon, bremmstrahlung, and several less important neutrino production processes.

To study the direct effects of neutrino losses on PWD evolution, we introduced artificially altered rates well before the evolving models reached the PWD track. If we simply changed the rates beginning at the hot end of the PWD sequence, the thermal structure of each model would take several thermal timescales to relax to a new equilibrium configuration based on the new rates. Unfortunately, this relaxation time is of the same order as the PWD cooling time, and so only the cool end of the sequence would see the full effects of the new rates on their evolutionary timescales. Therefore, the enhanced and diminished rates described in the next section were introduced into evolutionary calculations beginning at the base of the AGB. The resulting thermal structure of the initial PWD "seed" models was then already consistent with the neutrino rates used during the prior evolution that produced them.

6.3 Pre-White Dwarf Sequences with Different Neutrino Rates

Starting with the PWD seed models above, we evolved the models from high L and $T_{\rm eff}$ down toward the white dwarf cooling track. Three sequences were calculated. The base sequence used the normal neutrino production rates. Another sequence used rates diminished by a factor of three (at any given ρ and T in the stellar interior) over the normal rates, while the third sequence used rates enhanced by a factor of three. This trio spans nearly one order

of magnitude in neutrino production.

The resulting 0.6 $M_\odot$ evolutionary sequences are shown in Figure 6.1, from $T_{\rm eff} \sim 170,000\,K$—equivalent to the hottest PWDs known—down to about $35,000\,K$. Luminosity decreases by almost four orders of magnitude in approximately five million years. The GW Vir instability strip occupies the left half of the figure, above $T_{\rm eff} \sim 80,000\,K$ ($\log T_{\rm eff} = 4.9$), a temperature reached by the PWD models in only 500,000 years.

The most striking aspect of Figure 6.1 is the similarity of the tracks: changing the neutrino rates seems to have little effect on the luminosity at a given $T_{\rm eff}$ at *any* point in PWD evolution, despite the importance of neutrino losses as a cooling mechanism over much of this range. In Figure 6.2, we find that, for all three sequences, neutrino losses are the *primary* cooling mech-

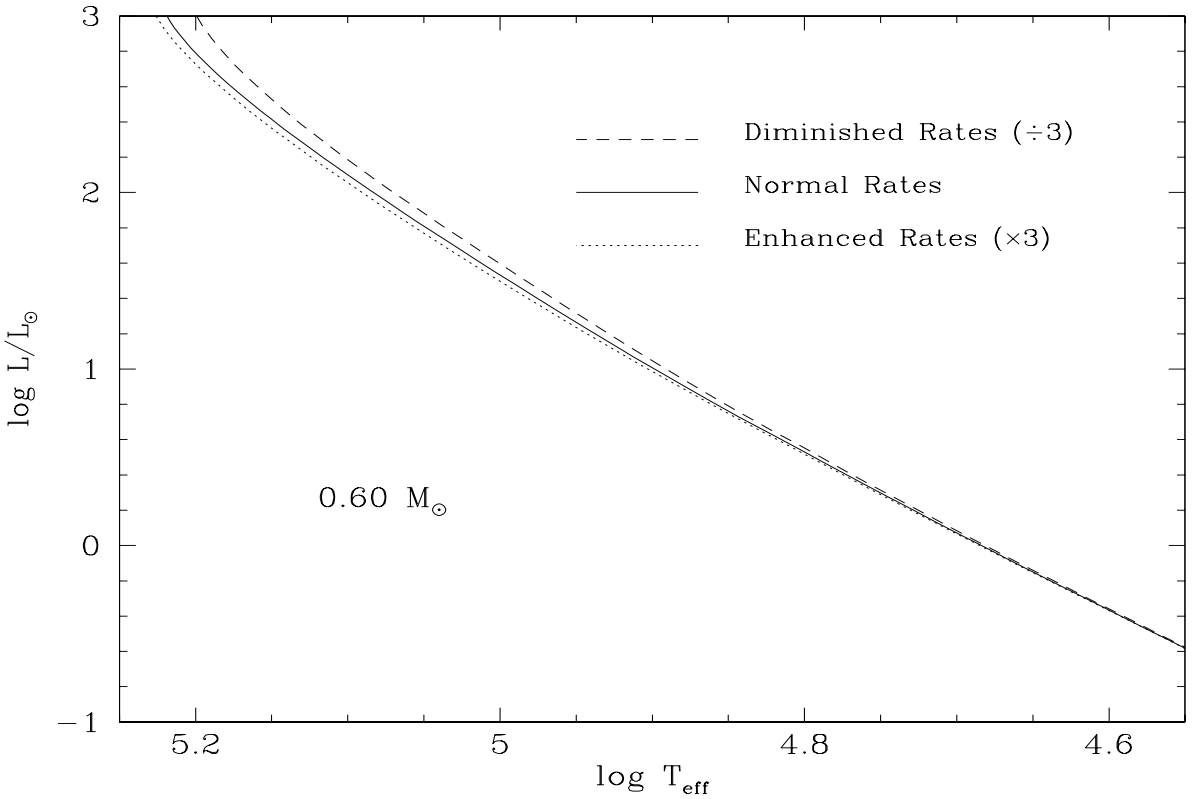

Figure 6.1 Evolutionary tracks for three 0.6 $M_\odot$ model sequences with different input neutrino production rates. The upper and lower tracks were calculated with rates one-third and three times the normal rates (middle track), respectively.

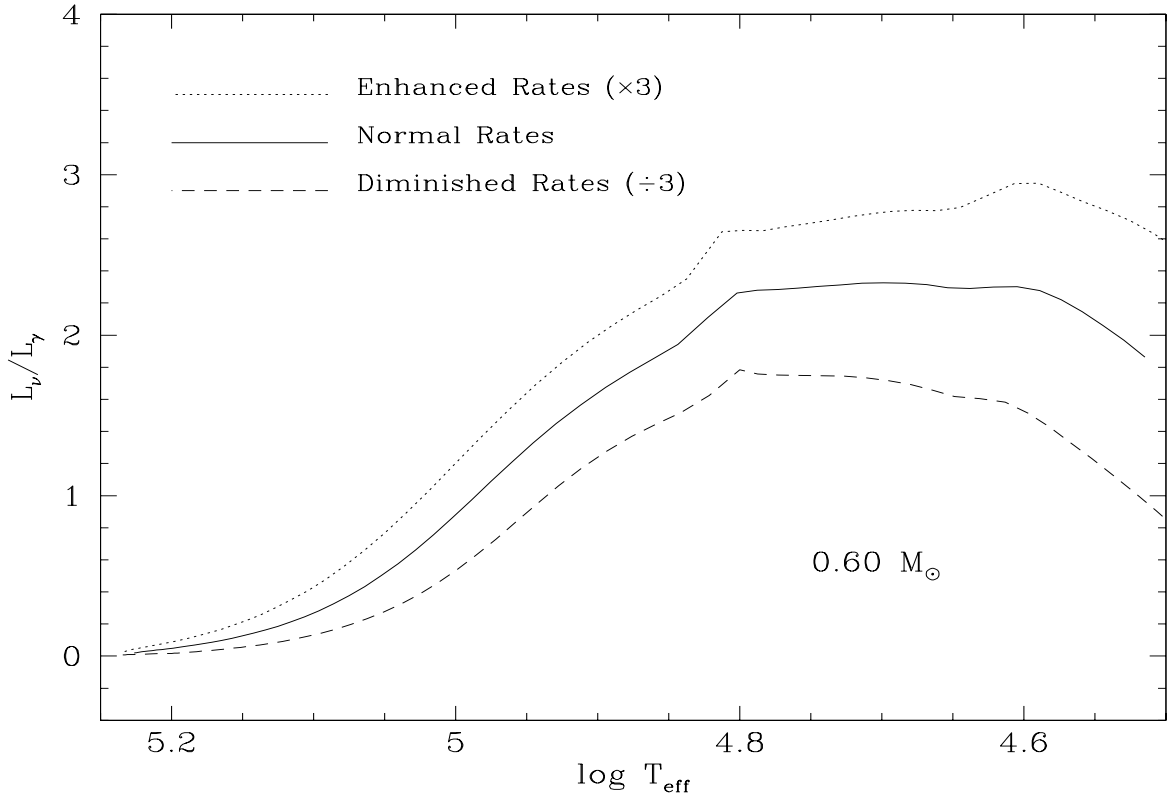

Figure 6.2 Ratio of the neutrino luminosity to the photon luminosity as a function of $T_{\rm eff}$, for three 0.6 $M_\odot$ model sequences with different input neutrino production rates.

anism over the approximate range $100,000\,K < T_{\rm eff} < 30,000\,K$. Plasmon reactions dominate over the bremmstrahlung process for 0.6 $M_\odot$ models at all stages of PWD evolution, as shown in Figure 6.3.

The ratio L_ν/L_γ also increases with stellar mass. In the $T_{\rm eff}$ range 80,000–100,000 K, L_ν/L_γ for a 0.66 $M_\odot$ model sequence is nearly 30% higher than for a 0.60 $M_\odot$ sequence.

Figures 6.1 and 6.2 show that the differences in L and $T_{\rm eff}$ are smallest when the neutrinos are important. This is because the primary *structural* effect of changing the neutrino rates is on the radius of the models (Figure 6.4), causing the tracks to assume a position in the L–$T_{\rm eff}$ plane normally occupied by models of slightly higher mass (for enhanced rates) or lower mass (for diminished rates). However, at lower temperatures electron degeneracy becomes increas-

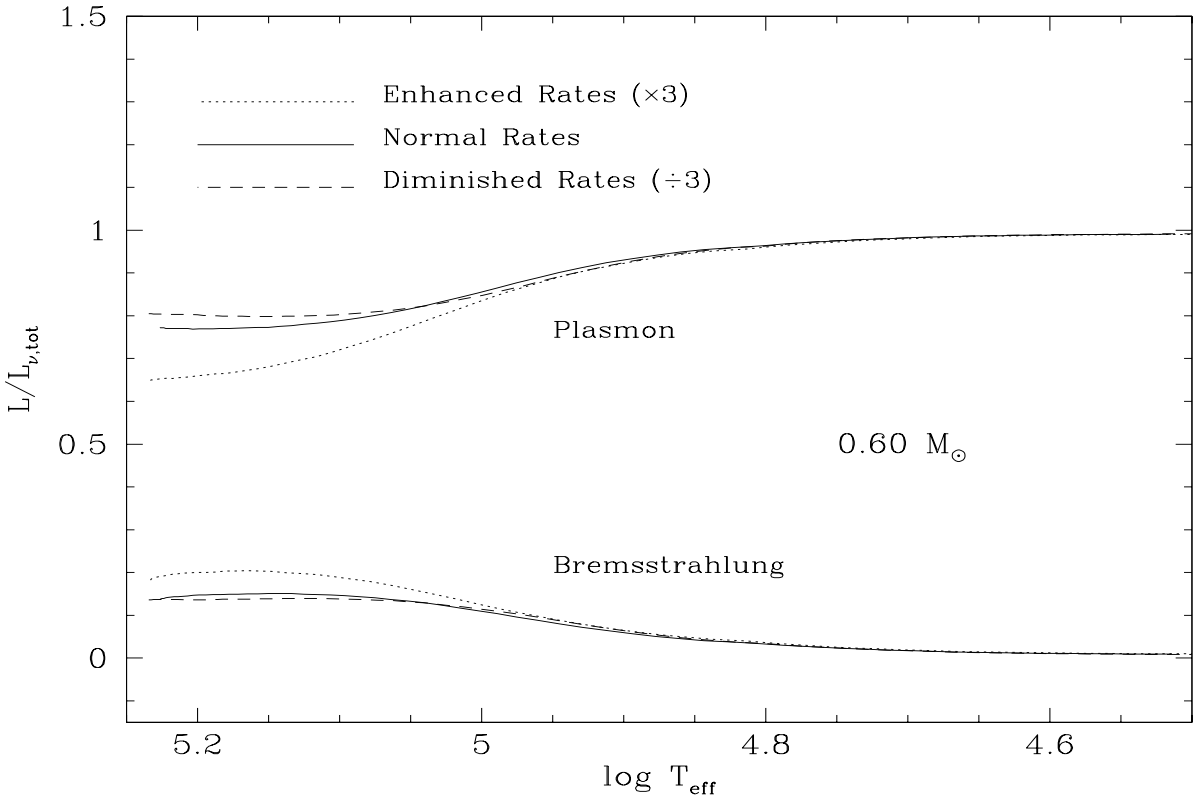

Figure 6.3 Fraction of total neutrino luminosity contributed by the plasmon and bremsstrahlung processes, as a function of $T_{\rm eff}$, for three 0.6 $M_\odot$ model sequences with different neutrino production rates.

ingly important as a mechanical support against gravity (and thus in determining the final stellar radius); neutrino cooling only affects the thermal processes participating in the mechanical structure. Even at high luminosity, however, different neutrino rates result in only small changes in measurable quantities such as surface gravity. Current observational techniques could not hope to resolve such small differences.

Figure 6.5 shows a more tangible effect of changing the rates. Even though models with different rates look much the same at a given $T_{\rm eff}$, they get there at widely differing times, since the rate of evolution along a track is directly dependent on the importance of neutrino emission as a source of cooling. For example, the model with enhanced neutrino rates cools from 100,000 K down to 65,000 K in 600,000 years, while the model with diminished neutrino

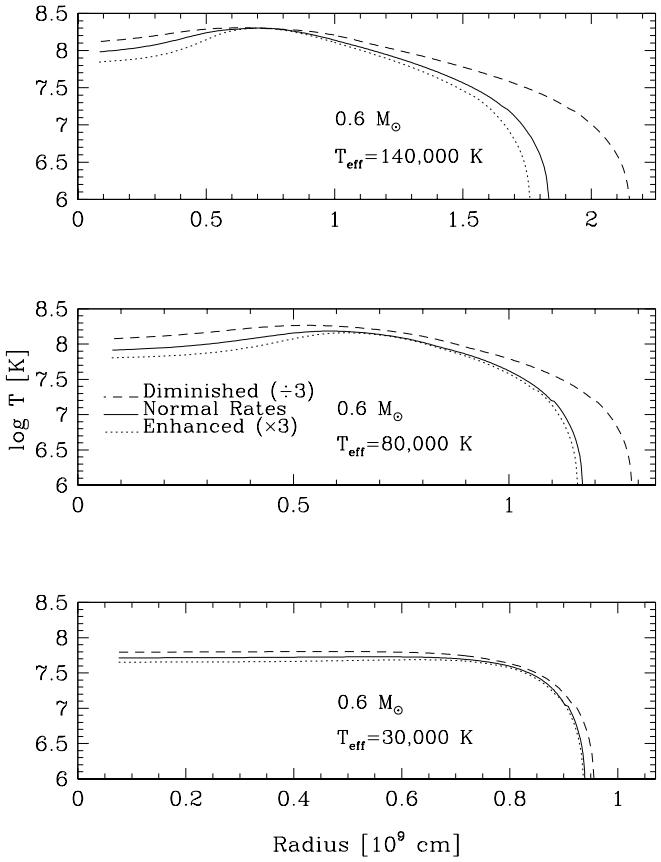

Figure 6.4 Thermal structure at three different evolutionary stages, $T_{\rm eff} = 140,000$ K (upper panel), 80,000 K (middle panel), and 30,000 K (lower panel), for 0.6 $M_{\odot}$ models with different neutrino production rates.

rates takes 1.3 million years, more than twice as long, to cool by the same amount. The maximum difference in the slope of the different curves in Figure 6.5 occurs at $T_{\rm eff} \sim 80,000$ K. Thus the epoch where the rate of evolution is most sensitive to the assumed neutrino physics corresponds to the position in the H-R diagram occupied by the coolest pulsators in the PWD instability strip. On the other hand, for stars in the strip hotter than 100,000 K Figure 6.5 shows that evolutionary rates do not depend on neutrino rates.

Our expectations are borne out in Figure 6.6, which shows the rate of change in period, $\dot{\Pi}/\Pi$ ($\equiv d(\ln \Pi)/dt$), as a function of period, Π, for PWD models at 140,000 K (lower panel)

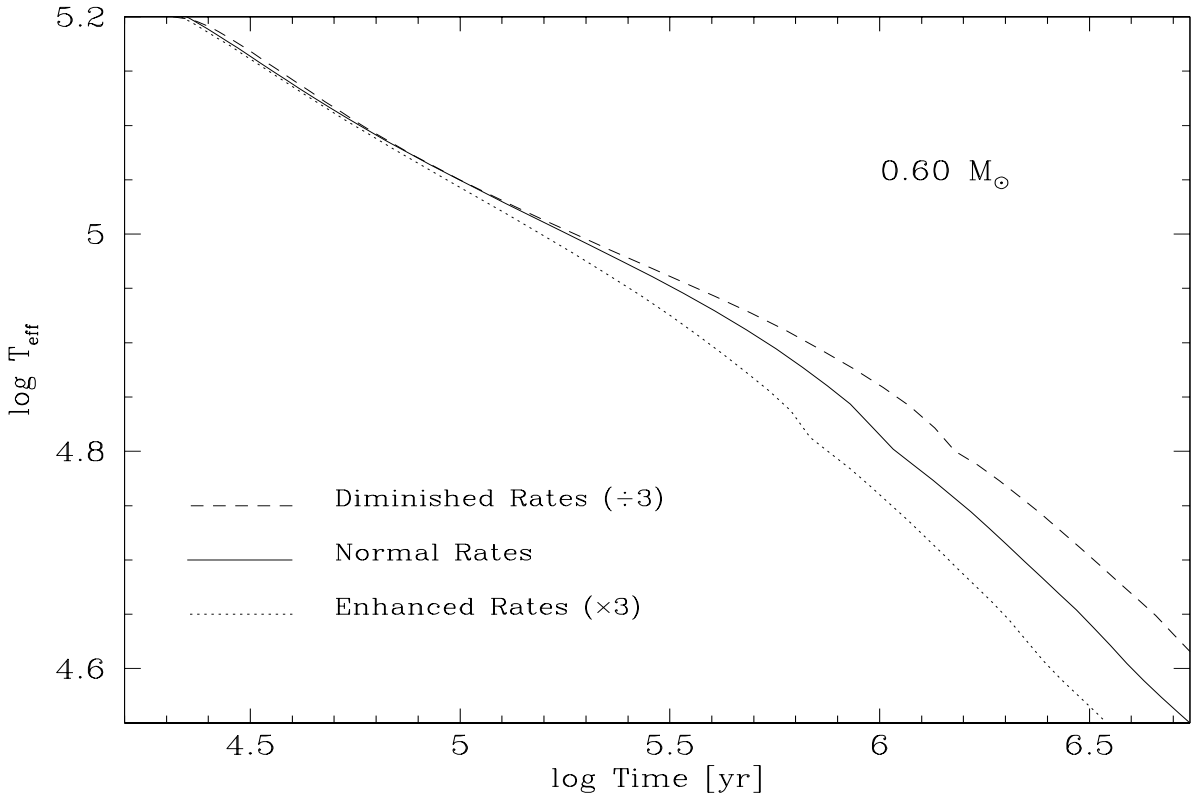

Figure 6.5 Evolution of $T_{\rm eff}$ with time for three $0.6\,M_\odot$ model sequences with different input neutrino production rates.

and 80,000 K (upper panel), given normal, enhanced, and diminished neutrino production rates. The rate of period change $\dot{\Pi}/\Pi$ in the cooler models changes by a factor of four between the enhanced and diminished rates. Changing the neutrino rates has little effect on $\dot{\Pi}/\Pi$ in the hotter model, consistent with the results from Figure 6.5. We now turn to the exciting implications of these results, and explore the possibility and practicality of measuring $\dot{\Pi}/\Pi$ in cool pulsating PWD stars. We can then identify likely targets for future observational campaigns.

6.4 Prospects for Measuring Neutrino Cooling Effects

Measurements of secular period change, $\dot{\Pi}/\Pi$, in white dwarfs have been attempted by a number of investigations, with either measurements made or tight upper limits set for the

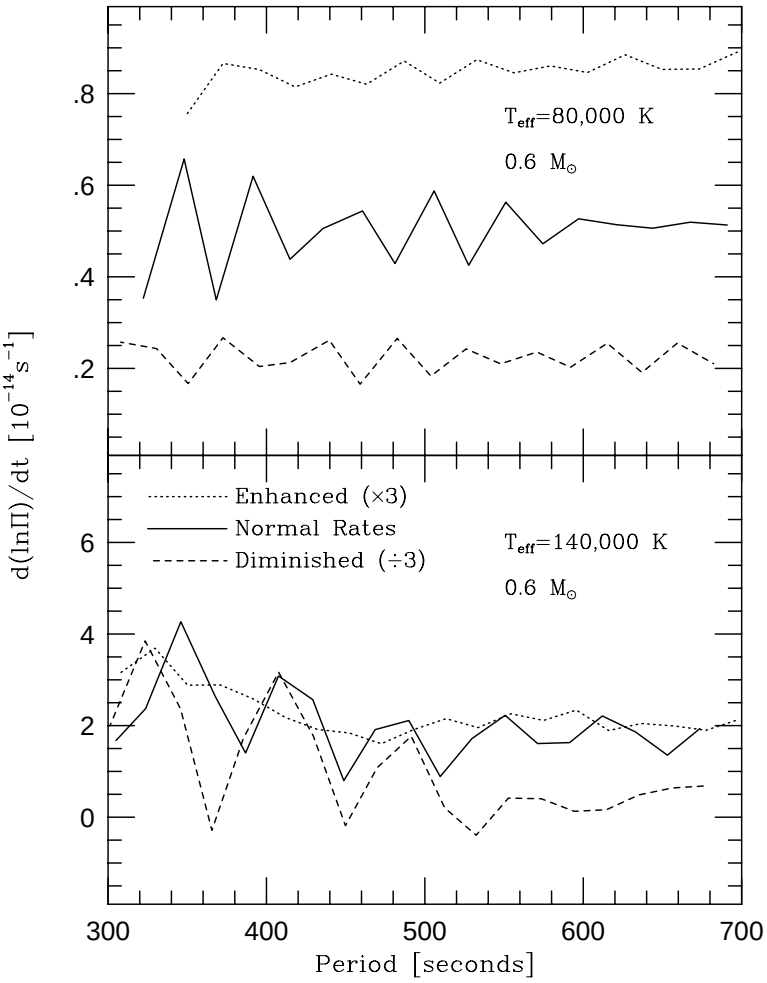

Figure 6.6 Rate of period change for 0.6 $M_\odot$ models with different neutrino rates.

GW Vir star PG 1159 (Winget et al. 1985, 1991, Costa & Kepler 1998) and G117-B15A (Kepler et al. 1995). Unfortunately, neutrino cooling is not expected to be an important effect for any of these stars. On the other hand PG 0122, with a $T_{\rm eff}$ of 80,000 K, occupies the stage in GW Vir evolution most highly dominated by neutrino emission. In Chapter 4, we found that PG 0122 is in addition the most massive GW Vir star, which should enhance neutrino effects as well.

In order to measure $\dot{\Pi}/\Pi$ with confidence, a star must have a stable and fully resolved pulsation, with stable phase measurements from season to season. PG 0122 is a very stable

pulsator: over the past decade, it has shown a consistent pulsation spectrum (see Figure 4.7), with the large-amplitude modes present at the same frequencies during each of the three intensive observing seasons in 1986, 1990, and 1996. The amplitudes of each of the dominant modes remained approximately constant as well.[1] Therefore, PG 0122 is an excellent candidate for measurement of the rate of secular period change caused by the evolutionary cooling of its interior.

In addition to the physics governing neutrino production, PG 0122 is an ideal target for measuring neutrino emission rates because of the minimal influence of any mode trapping on interpretation of its $\dot{\Pi}/\Pi$. As we show in Chapter 2, the surface contraction rate decreases with decreasing $T_{\rm eff}$ relative to the cooling rate of GW Vir stars. For stars below 100,000 K, trapping no longer significantly affects $\dot{\Pi}/\Pi$ from mode to mode.

From Figure 6.6, we estimate the value of $\dot{\Pi}/\Pi$ for the 400 s mode in PG 0122 to be about 6×10^{-15} sec $^{-1}$. With this rate of period change, the period should increase by about 0.001 s in 10 years; this is smaller than the period uncertainty for a run length of several months (assuming a frequency precision of $\frac{1}{10 \times \text{run length}}$). However, the accumulated phase advance over a ten year period should be *nearly two full cycles*.

Using the periods alone from the 1986, 1990, and 1996 data, we can attempt to calculate $\dot{\Pi}/\Pi$ directly. From the best periods from 1996 and 1986, we calculate a period change of -0.10 ± 0.2 s, implying $\dot{\Pi}/\Pi = (-7 \pm 15) \times 10^{-13}$ sec $^{-1}$. Thus in practice the data currently available only allow an upper limit to be set on the absolute magnitude of $\dot{\Pi}/\Pi$ for PG 0122 of 1.5×10^{-12} sec $^{-1}$. In view of the importance of measuring $\dot{\Pi}/\Pi$ for this star—as well as for the other cool GW Vir stars—we must continue analysis of archival data and mount observing campaigns in the near future to monitor all the known GW Vir stars with $T_{\rm eff} < 100,000$ K. With frequent observation, an accumulated phase advance of half a cycle, combined with the techniques described in § 2.4, could be used to determine $\dot{\Pi}/\Pi$ for PG 0122, PG 2131, and PG 1707 in two to three years. The data presented in Chapter 4 provide a key anchor for this

[1] The amplitudes in 1990, as reported by Vauclair et al. (1995; see Table 4.5), average 3.6 times smaller than found in both 1986 (Table 4.4) and 1996 (Table 4.3). However, examination of the original data from 1990, kindly provided by Al Grauer (1997 private communication) shows the amplitudes in 1990 were essentially the same as in 1986 and 1996. The amplitudes reported by Vauclair et al. (1995) appear to be in error.

investigation.

We have shown that the predicted rates of period change in GW Vir stars near the cool end of the instability strip are sensitive to the neutrino production rates used in stellar models. The persistence of the solar neutrino problem has made the standard model of neutrino interactions one of the most intensely scrutinized theories in all of physics. Determination of $\dot{\Pi}$ in the GW Vir stars PG 0122 and PG 2131 will provide an important test of the standard model and of any new theories put forward to replace it.

CHAPTER 7 SUMMARY AND IMPLICATIONS

"As a matter of fact, the theory we have chosen may be pretty lousy. It may contain contradictions, it may conflict with well-known facts, it may be cumbersome, unclear, ad hoc in decisive places, and so on. But it may still be better than any other theory that is available at the time. It may in fact be the best lousy theory there is ..."

—Paul Feyerabend, *How to Defend Society Against Science (1975)*

We come for now to the end of our investigations. This chapter summarizes our results, reflects on their meaning, evaluates our progress in pursuing the purposes laid out in Chapter 1, and finally, asks what is left to be done.

7.1 Summary

Our purpose is to understand how and why PWD stars pulsate, so that astronomers can confidently apply knowledge of PWD structure—gained via asteroseismology—to study how white dwarfs form and evolve and better understand the physics that governs these processes. We have pursued PWD structure via the pulsation periods and the additional constraints they provide for our models. Before the beginning of this work, the pulsation spectrum of only a single GW Vir star was understood in detail. We used Whole Earth Telescope observations to study the pulsations of the three other known GW Vir variables; with the tools of asteroseismology, we succesfully determined the mass and luminosity of two of these (PG 0122 and PG 2131), and made a fair beginning toward unraveling the pulsation spectrum of the third (PG 1707).

A surprising similarity emerged among the pulsating PWDs: their patterns of equal period spacing span a very small range from 21–23 s. Including the PNNV star NGC 1501, this

uniformity extends over three orders of magnitude in PWD luminosity. Since period spacing increases with decreasing luminosity—and decreases with increasing mass—this result implies a trend toward significantly higher mass with decreasing luminosity through the instability strip. This trend has several important implications for our understanding of PWD pulsations. The instability is severely sloped toward lower $T_{\rm eff}$ with mass increasing down the instability strip.

To understand this sloped instability strip, we needed information inherent in the other fundamental observed trend: the dominant period in PWD pulsators decreases with decreasing luminosity. We found that the dominant period is correlated with the maximum g-mode period, $\Pi_{\rm max}$. If $\Pi_{\rm max}$ is a factor in determining the range of periods observed in pulsating PWD stars, then it should play a role determining when pulsation ceases, because the driving zone tends to drive longer and longer periods in models of given mass, as those models evolve to lower $T_{\rm eff}$. At low enough temperature, the driving zone is only capable of driving periods longer than $\Pi_{\rm max}$, and pulsations should then cease. Since the top of the driving zone moves to shorter timescales with increasing mass, and does so faster than $\Pi_{\rm max}$ *decreases* with increasing mass, higher mass models should pulsate at lower $T_{\rm eff}$ than lower mass models. This behavior is compatible with the observed slope of the red edge in the log g–log $T_{\rm eff}$ plane.

This mechanism does not account for the lack of observed high-mass pulsators at high $T_{\rm eff}$, however. Theoretical luminosity functions for the PWD stars indicate the observed blue edge is probably significantly affected by selection effects due rapid evolution at high $T_{\rm eff}$. Since higher mass models evolve more quickly, and are less luminous, at a given $T_{\rm eff}$ than models of lower mass, we are more likely to detect low-mass than high-mass PWDs at a given temperature. This will cause stars to "bunch up" against the red edge in the observed instability strip, and the apparent blue edge will thus "artificially" resemble the shape of the red edge—no matter what that shape might be. This selection mechanism, in isolation, would imply that low-mass, low $T_{\rm eff}$ GW Vir pulsators should be most numerous of all. That we in fact find *none* strengthens our confidence that the mass-dependence of the red edge is a real effect—that we find no low-mass, low-$T_{\rm eff}$ GW Vir stars because they don't exist.

Finally, we explored the exciting possibility of constraining the input lepton physics in our

stellar models by exploring the effects of neutrino-cooling in low-$T_{\rm eff}$GW Vir models. We found that neutrino luminosity in PWDs increases significantly as a fraction of total energy output as PWD models evolve to lower temperatures. This effect is enhanced in models of higher mass, so the PWDs most dominated by neutrino cooling are high-mass, low-$T_{\rm eff}$ stars like PG 0122. We predict a ratio of neutrino to photon luminosity in PG 0122 of nearly 3:1. This prediction can be tested by observing the rate of period change, $\dot{\Pi}$, in PG 0122 or in other cool GW Vir stars like PG 2131 and PG 1707. To check the feasibility of such a test, we evolved models with different neutrino emission rates and found that $\dot{\Pi}$ is a sensitive indicator of neutrino cooling effects. A concerted observing campaign could determine $\dot{\Pi}$ in PG 0122 and other cool GW Vir stars in two to three years.

7.2 Some Applications

7.2.1 Non-Pulsators within the Instability Strip?

The boundaries of the PWD instability strip derived from our pulsation studies are far smaller than those based on spectroscopic measurements alone. Though the actual range of log g and $T_{\rm eff}$ spanned by the known pulsators is no smaller than before, the newly discovered mass-luminosity relationship implies that the width of the strip in $T_{\rm eff}$ *at a given log* g is quite small, and vice versa. We can therefore no longer say for certain that *any* non-pulsators occupy this newly diminished instability strip, since the uncertainties in log g and $T_{\rm eff}$ as determined from spectroscopy are larger now than the observed width of the strip itself at a given log g or $T_{\rm eff}$.

This highlights the importance of finding additional pulsators with which to further refine our knowledge of the instability strip boundaries. In particular, we still have no observations with which to constrain theories of the blue edge, since it is unlikely that the *instrinsic* blue edge lies near the current *observed* blue edge at any effective temperature.

If the trend we have discovered continues to effective temperatures below the coolest known pulsating PWDs, then high-mass ($\sim 1\ M_{\odot}$ or greater) white dwarfs should pulsate at temperatures perhaps as low as 50,000–60,000 K (and log $g \sim 8$). Their dominant periods (again,

assuming they follow the trends outlined in Chapter 5) would be shorter than any known PWDs, perhaps as low as 200-300 s. Such stars would not be PWDs at all but rather white dwarfs proper. Their discovery would complete a "chain" of variable stars from PNN stars to "naked" PWDs to hot white dwarfs, and as such they would represnent a incalculable boon to astronomers who study the late stages of stellar evolution.

7.2.2 The Driving Mechanism Revisited

The results of Chapter 5 should apply equally well to any driving mechanism based on ionization, independent of species. The driving region in our models arises from the ionization of OVI, but we cannot conclude therefore that OVI is the source of the observed instability. In particular, these models do not include a significant fraction of either nitrogen or neon, even though nitrogen is observed only in the PWD pulsators (Dreizler 1998), and neon should exist in PWD stars at a mass fraction of about 1%. The driving zone will occur at different depths in models of a given mass and $T_{\rm eff}$, depending on the ionization temperature of the species responsible for driving. Therefore the observed position of the red edge, along with its slope in the log g–log $T_{\rm eff}$ plane, contains information on the (one or more) species responsible for pulsation.

If the red edge is caused by incompatible timescales between driving and $\Pi_{\rm max}$, then we need to understand how the amplitudes of modes are affected by their proximity in period to $\Pi_{\rm max}$. In Chapter 5 we restricted our analysis to the proportionality of $\Pi_{\rm max}$ to mass and $T_{\rm eff}$. A detailed calculation of $\Pi_{\rm max}$ has never been performed for a PWD model, but if we could determine how the changing depth of the driving zone shuts off pulsation in response to $\Pi_{\rm max}$, then we could use the observed red edge to calibrate $\Pi_{\rm max}$ in our models, assuming driving via ionization of various different species. This might narrow the range of possible driving mechanisms. Alternatively, if we could somehow calibrate $\Pi_{\rm max}$ seperately, then we could use the observed red edge to identify the species responsible for driving.

7.2.3 The Formation and Evolution of White Dwarf Stars

An important problem to which we might apply PWD studies is the mechanism by which white dwarfs are formed. This requires that we link together the different kinds of observed white dwarfs with their various precursors. Since the PG 1159 stars show no visible hydrogen, it seems unlikely that they can form DA white dwarfs. Dehner & Kawaler (1995) and Dehner (1996) established an evolutionary link between PWDs like PG 1159 and DBV stars like GD 358. This link currently depends on observations of a single GW Vir star and a single DBV. Unfortunately, none of the cooler GW Vir stars studied in this thesis showed enough consecutive modes to determine a trapping cycle and therefore to make a diffinitive measurement of a helium layer thickness, as was done for PG 1159.[1] However, now that we understand the basic mode structure (i.e., the period spacing) for the other GW Vir stars, we can predict approximately where in period additional modes—presumably too small in amplitude to be detected in previous observations—should be.

The best place to look for additional modes is in very high signal-to-noise light curves obtained at large (4.0 m class or larger) telescopes. Multi-site data are not necessary for these observations, because we already know the basic pulsation pattern from the WET observations presented in Chapter 4. Finding a single additional period at the approximate position predicted by the previously determined pattern is now enough to make a relatively firm mode-identification. The *precise* position of such modes can then fill in the the holes in the pattern, allow us to identify a trapping cycle, and lead to measurement of the helium layer thickness.

The helium layer thickness of GW Vir stars also determines the cooling rate of their descendents. Wood (1992) and Winget & Van Horn (1987) showed that the helium layer mass affects the apparent ages of white dwarfs. The white dwarf luminosity function is one of the most precise ways to determine when the galactic disk was formed, and therefore measurement of additional GW Vir helium layer thicknesses is an important means to calibrate the age of the galaxy.

[1] Kawaler, O'Brien, et al. (1995) suggest evidence that the helium layer in PG 2131 is comparable in mass to that found in PG 1159, but this result is based on only three modes that don't span even one complete trapping cycle.

Finally, if GW Vir stars evolve to eventually become DB stars, the problem remains of explaining the DB gap between 30,000 and 45,000 K. In Chapter 1, we mentioned that mass loss has been identified as a likely means to mask hydrogen in the atmospheres of PWDs. In this case, it is important to set observational limits on mass-loss rates from GW Vir stars, to further test the evolutionary link between PG 1159 stars and DBVs.

Recently, a star with a spectrum very similar to the PG 1159 stars, except showing signs of hydrogen, was discovered (Dreizler et al. 1996). This star, HS 2324+3944, is also a pulsator (Silvotti 1996) and so should be classified as a new (hydrogen-rich) GW Vir star. The possibility thus arises of determining its evolutionary state via pulsation studies. Perhaps mass-loss has ceased in HS 2324, causing the hydrogen to quickly diffuse to visibility. The H and He layer thicknesses for this star also place limits on both its evolutionary past *and* future, by telling us at which stage during a thermal pulse cycle it left the AGB, and how fast it will cool as a white dwarf. Finally, with precise measurement, via pulsation, of log g and log $T_{\rm eff}$ for HS 2324, we can test our ideas of the blue and red edges of the GW Vir instability strip laid out in Chapter 5.

7.3 The Future in Observation and Theory

More PWD targets are needed to refine our knowledge of the instability strip. In particular, we need to solve more known PNNVs and GW Vir stars, to test our theory of the red edge and to place statistical limits on the location of the blue edge. For instance, we predict that, if $\Pi_{\rm max}$ determines the range of observed periods as well as when pulsation ceases in a particular star, then there should be no low-mass pulsators with $T_{\rm eff}$ similar to the coolest GW Vir stars. If, on the other hand, such variables are found, they will likely have much longer periods than the other GW Vir stars. In this case $\Pi_{\rm max}$ is *not* important in determining their periods, which instead likely follow the lengthening thermal timescale of the driving zone. It is possible such stars do indeed exist, since most searches for PWD pulsation concentrate on shorter periods that we predict low-mass, low-$T_{\rm eff}$ PWDs should have: 5000–1000 s. A comprehensive obseravational program is called for to determine if such stars exist. Either outcome for such

a study would severly constrain the possible mechanisms responsible for pulsation in PWD stars.

A concerted effort should also be made to measure the rate of period change in the three cool GW Vir stars PG 0122, PG 2131, and PG 1707. Any measurement of $\dot{\Pi}$ for these stars will constrain our theories of neutrino emission in PWD interiors and provide a unique test of the standard lepton theory in dense plasma. Several alternatives to this theory have been forwarded in an attempt to solve the solar neutrino problem. Calculations of the plasmon and bremmestrahlung neutrino emission rates in PWDs based on these theories should be made, to see if they can be excluded by PWD $\dot{\Pi}$ measurements.

On the stellar evolution side, we need to understand how PWD stars react to driving near the maximum g-mode period. Studies should be undertaken to determine the actual maxium period in PWD models. PWD evolution sequences should be constructed that contain all the elements thought to exist in PWD stars. We have observational information to test all these calculations, and with the observational program proposed above, we will gain more. There is much to do.

7.4 Conclusion

The observation and theoretical modeling of PWD variability will be rich and rewarding fields for some time to come. Many problems remain to be solved, and the observations and analysis presented in this thesis provide initial constraints to test future ideas. As our knowledge of PWD pulsations increases, so does the confidence and scope with which we can apply the results of pulsation studies to those problems which ultimately interest us most: white dwarf formation, stellar evolution in general, and the physics of stellar interiors. Greater understanding of these extrinsic problems will then feed back into greater understanding of intrinsic questions of PWD structure and evolution, and so on. Perhaps we will find that Eddington was right, when he claimed back in 1926 that

> *"...it is reasonable to hope that in the not too distant future we shall be competent to understand so simple a thing as a star."*

APPENDIX THE MAXIMUM PERIOD

A variable pre-white dwarf star is a resonant cavity for non-radial g-mode oscillations. This spherically symmetric cavity is bounded by the stellar center (or the outer edge of the degenerate core in ZZ Ceti and DBV white dwarfs) and surface. At sufficiently long periods, however, the surface layers no longer reflect internal waves. The pulsation energy then leaks out through the surface, damping the pulsation. This idea was first applied to white dwarf pulsations by Hansen, Winget & Kawaler (1985), who attempted to calculate the approximate critical frequencies to explain both the red edge and maximum observed periods in ZZ Ceti stars. Assuming an Eddington gray atmosphere, they derive the following expression for the dimensionless critical g-mode frequency:

$$\omega_g^2 \approx \frac{\ell(\ell+1)}{V_g} \tag{A.1}$$

where

$$V_g = \frac{3g\mu R}{5N_a k T_{\rm eff}}. \tag{A.2}$$

Here g and R represent the photospheric surface gravity and radius, and N_a, k, and μ have their usual meaning.

The dimensionless frequency, ω, is related to the pulsation frequency, σ, according to

$$\omega^2 = \frac{\sigma^2 R}{g}. \tag{A.3}$$

The pulsation period is $\Pi = 2\pi/\sigma$, so combining Equations (A.1) through (A.3) we arrive at the maximum g-mode period:

$$\Pi_{\rm max} \approx 940s \left(\frac{\mu}{\ell(\ell+1)}\right)^{0.5} \left(\frac{R}{0.02R_\odot}\right) \left(\frac{T_{\rm eff}}{10^5{\rm K}}\right)^{-0.5}, \tag{A.4}$$

or, using the relation $R^2 = L/4\pi\sigma T_{\rm eff}^4$,

$$\Pi_{\rm max} \approx 940s \left(\frac{\mu}{\ell(\ell+1)}\right)^{0.5} \left(\frac{L}{35L_\odot}\right)^{0.5} \left(\frac{T_{\rm eff}}{10^5{\rm K}}\right)^{-2.5}. \qquad \text{(A.5)}$$

For PG 1159, with $L = 200\ L_\odot$ and $T_{\rm eff} = 140,000$ K, Equation (A.5) predicts $\Pi_{\rm max} = 780$ s for $\ell = 1$ modes and 450 s for $\ell = 2$ modes.[2] PG 0122, with $L = 5.6\ L_\odot$ and $T_{\rm eff} = 80,000$ K, would have $\Pi_{\rm max} = 530$ s for $\ell = 1$ and 310 s for $\ell = 2$. Because of the simplicity of the gray atmosphere assumption, these numbers are more useful in comparison to each other than as quantitative diagnostics of the maximum period. For instance, Hansen, Winget & Kawaler (1985) find that the values of $\Pi_{\rm max}$ derived from this analysis are "within a factor of 2" of those based on more rigorous calculations. We are more interested here in the run of $\Pi_{\rm max}$ with respect to global stellar quantities such as L and $T_{\rm eff}$.

If $\Pi_{\rm max}$ determines the long-period cutoff in GW Vir pulsators, then the the longest period $\ell = 1$ modes should be (approximately) a factor of 1.73 times longer than the longest period $\ell = 2$ modes. PG 1159 is the only GW Vir star with positively identified $\ell = 2$ modes. In the period list of Winget et al. (1991), the longest period (positively identified) $\ell = 2$ mode has a period of 425 s, while the longest period $\ell = 1$ mode has a period of 840 s. The ratio of these two periods is 1.98, close to the predicted ratio. The periods themselves are also surprisingly close to the calculated values.

The predicted ratios between the longest period modes also hold for intercomparison of different stars. The longest period mode so far identified for PG 0122 is 611 s, 1.37 times smaller than the longest period in PG 1159, again very close to the predicted ratio of 1.43 from Equations (A.4) and (A.5). The agreement between $\Pi_{\rm max}$ from our rough calculations and the observed maximum periods in GW Vir stars is impressive enough to warrant further study. In particular, more rigorous theoretical calculations of $\Pi_{\rm max}$ should be undertaken to corroborate or refute these results.

[2] Assuming a mix of C:O:He = 0.4:0.3:0.3 by mass, implying $\mu = 1.33$.

BIBLIOGRAPHY

Abrikosov, A. 1960, *SvPhJETP*, *39*, 1797

Adams, J.B., Ruderman, M.A. & Woo, C.H. 1963, *Phys. Rev.*, *129*, 1383

Appleton, P.N., Kawaler, S.D. & Eitter, J.J. 1993, *AJ*, *106*, 1973

Bahcall, J.N. & Pinsonneault, M.H. 1996 *BAAS*, *189*, 56.01

Beaudet, G., Petrosian, V. & Salpeter, E.E. 1967, *ApJ*, *150*, 979

Bergeron, P., Wesemael, F. &Fontaine, G. 1992, *ApJ*, *387*, 288

Bergeron, P., Saffer, R. & Liebert, J. 1992, *ApJ*, *394*, 228

Bond, H.E., Ciardullo, R. & Meakes, M.G. 1991, in *Objective-Prism and Other Surveys, in Memory of Nicholas Sanduleak*, ed. A.G.D. Philip & A.R. Upgren, (Schnenectady: Davis), p91

Bond, H.E. & Ciardullo, R. 1993, in *White Dwarfs: Advances in Observations and Theory*, ed. M.A. Barstow, (Dordrecht: Kluwer), p491

Bond, H.E., Ciardullo, R. & Kawaler, S.D. 1993, *Acta Ast.*, *43*, 425

Bond, H.E., Grauer, A.D., Green, R.F. & Liebert, J. 1994, *ApJ*, *279*, 751

Bond, H.E. et al. 1996, *AJ*, *112*, 2699

Bowen, G.H. & Willson, L.A. 1991, *ApJ*, *375*, L53

Bradley, P.A. 1994, *PhD thesis*, Univ. Texas at Austin

Bradley, P.A. & Winget, D.E. 1994, *ApJ*, *430*, 850

Brassard, P., Fontaine, G., Wesemael, F., Kawaler, S.D. & Tassoul, M. 1991, *ApJ*, *367*, 601

Brickhill, A.J. 1975, *MNRAS*, *170*, 405

Brickhill, A.J. 1983, *MNRAS*, *204*, 537

Brickhill, A.J. 1991a, *MNRAS*, *251*, 673

Brickhill, A.J. 1991b, *MNRAS*, *252*, 334

Chandrasekhar, S. 1939, *An Introduction to Stellar Structure*, (Chicago: Univ. Chicago Press)

Chin, C.W., Chiu, H.Y. & Stothers, R. 1966, *AnPhy*, *39*, 280

Ciardullo, R. & Bond, H.E. 1996, *AJ*, *111*, 2332

Clemens, J.C. 1994, *PhD thesis*, Univ. Texas at Austin

Costa, J.E.S. & Kepler, S.O. 1998 *Balt. Ast.*, *7*, 83

Cox, J.P. 1980, *Theory of Stellar Pulsation*, (Princeton: Princeton Univ. Press)

Dehner, B.T. 1996, *PhD thesis*, Iowa State Univ.

Dehner, B.T. & Kawaler, S.D. 1995, *ApJ*, *445*, L141

Dicus, D.A. 1972, *Phys. Rev.*, *D6*, 941

Dicus, D.A., Kolb, E.W., Schramm, D.N. & Tubbs, D.L. 1972, *ApJ*, *210*, 481

Dolez, N. & Vauclair, G. 1981, *A&A*, *102*, 375

Dorman, B., Rood, R. & O'Connell, R. 1993 *ApJ*, *419*, 596

Dreizler, S. 1998, *Balt. Ast.*, *7*, 71

Dreizler, S., Werner, K., Heber, U. & Engels, D. 1996, *A&A*, *309*, 820

Dreizler, S. & Heber, U. 1998, *A&A*, *334*, 618

Dziembowski, W. 1977 *Acta. Ast.*, *27*, 1

Fontaine, G., McGraw, J.T., Dearborn, D.S.P., Gustafson, J. & Lacombe, P. 1982, *ApJ*, *258*, 651

Fontaine, G. et al. 1991, *ApJ*, *378*, L49

Fontaine, G. & Wesemael 1987, in *The Second Conference on Faint Blue Stars*, IAU Colloq. 95 eds. A.G.D. Philip, D.S. Hayes & J. Liebert, (Schenectady: Davis) p319

Feynman, R.P. & Gell-Mann, M. 1958, *Phys. Rev.*, *109*, 193

Gautschy, A. 1997, *A&A*, *320*, 811

Goldreich, P.& Wu, Y. 1998, *ApJ*, in press

Grauer, A.D. & Bond, H.E. 1984, *ApJ*, *277*, 211

Grauer, A.D., Green, R.F. & Liebert, J. 1992, *ApJ*, *399*, 686

Greenstein, J.L. 1982, *ApJ*, *258*, 661

Greenstein, J.L. 1984, *PASP*, *96*, 62

Greenstein, J.L. 1986, *ApJ*, *304*, 334

Hansen, C.J. & Kawaler, S.D. 1994, *Stellar Interiors: Physical Principles, Structure, and Evolution*, (New York: Springer-Verlag)

Hill, J.A., Winget, D.E. & Nather, R.E. 1987, in *Second Conference on Faint Blue Stars*, eds. A.G.D. Philip, D.S. Hayes & J. Liebert, (Schenectady: Davis) p627

Harvey, J.W. et al. 1996 *Science*, *272*, 1284

Hansen, C.J., Winget, D.E. & Kawaler, S.D. 1985, *ApJ*, *297*, 544

Iben, I. Jr. 1984, *ApJ*, *277*, 333

Iben, I. Jr. 1991, *ApJSupp*, *76*, 55

Iben, I. Jr. & Renzini, A. 1983, *ARAA*, *21*, 271

Iben, I. Jr. & Tutukov, A.V. 1984, *ApJ*, *282*, 615

Itoh, N., Hayashi, H., Nishikawa, A. & Kohyama, 1996 *ApJSupp*, *102*, 411

Jones, P.W., Pesnell, W.D., Hansen, C.J. & Kawaler, S.D. 1989, *ApJ*, *336*, 403

Kawaler, S.D. 1986, *PhD thesis*, Univ. Texas at Austin

Kawaler, S.D. 1987, in *The Second Conference on Faint Blue Stars*, IAU Colloq. 95, eds. A.G.D. Philip, D.S. Hayes & J. Liebert, (Schenectady: Davis) p297

Kawaler, S.D. & Weiss, P. 1990, in *Progress of Seismology of the Sun and Stars*, eds. Y. Osaki & H. Shibahashi, Lecture Notes in Phys. 367, p431

Kawaler, S.D. 1995, *Balt. Ast.*, *4*, 329

Kawaler, S.D. 1996, in *Stellar Remnants*, SAAS-Fee Course 25, (New York: Springer-Verlag)

Kawaler, S.D., Hansen, C.J. & Winget, D.E. 1985, *ApJ*, *295*, 547

Kawaler, S.D. & Bradley, P.A. 1994, *ApJ*, *427*, 415

Kawaler, S.D., Bond, H.E., Sherbert, L.E. & Watson, T.K. 1994, *AJ*, *107*, 298

Kawaler, S.D., O'Brien, M.S. et al. 1995, *ApJ*, *427*, 415

Kawaler, S.D., Sekii, T. & Gough, D. 1998, *ApJ*, submitted

Kleinman, S.J. 1995, *PhD thesis*, Univ. Texas at Austin

Kleinman, S.J. et al. 1998, *ApJ*, submitted

Koester, D. et al. 1985, *A&A*, *149*, 423

Kirzhnitz, D.A. 1960, *SvPhJETP*, *38*, 503

Kukarkin, B.V. et al. 1969, *General Catalogue of Variable Stars*, 3rd ed. (Moscow: Nauka)

Liebert, J. et al. 1986, *ApJ*, *309*, 241

Loup, C., Forveille, T., Omont, A. & Paul, J.F. 1993, *A&ASupp*, *99*, 291

O'Brien, M.S., Clemens, J.C., Kawaler, S.D. & Dehner, B.T. 1996 (OCKD) *ApJ*, *467*, 397

O'Brien, M.S. et al. 1998 *ApJ*, *495*, 458

Mestel, L. 1952 *MNRAS*, *112*, 583

McGraw, J.T. 1977, *PhD thesis*, Univ. Texas at Austin

McGraw, J.T. 1980, *Sp. Sci. Rev.*, *27*, 601

Motch, C., Werner, K. & Pakull, M.W. 1993, *A&A*, *268*, 561

Nather, R.E., Winget, D.E., Clemens, J.C., Hansen, C.J. & Hine, B.P. 1990, *ApJ*, *361*, 309

Nikolov, N. & Tsvetko, T. 1972, *Ast. Sp. Sci.*, *99*, 291

Paczynski, B. 1970, *Acta Ast.*, *20*, 47

Robinson, E.L. 1979, in *White Dwarfs*, IAU Colloq. 53, p343

Robinson, E.L., Kepler, S.O. & Nather, R.E. 1982, *ApJ*, *259*, 219

Robinson, E.L. et al. 1995 *ApJ*, *438*, 908

Saio, H. 1996, in *Hydrogen Deficient Stars*, eds. C.S. Jeffrey & U. Heber, ASP Series 96, p361

Saio, H., Winget, D.E. & Robinson, E.L. 1983, *ApJ*, *265*, 982

Salam, A. 1968, in *Elementary Particle Physics*, ed. N. Svartholm, (Stockholm: Almquist & Wiksells), p367

Salpeter, E. 1961, *ApJ*, *134*, 669

Savedoff, M.P., Van Horn, H.M. & Vila, S.C. 1969, *ApJ*, *155*, 221

Schönberner, D. 1981, in *Physical Processes in Red Giants*, eds. I. Iben, Jr. & A. Renzini, (Reidel: Dordrecht), p463

Schönberner, D. 1986, *A&A*, *169*, 189

Silvotti, R. 1996, *A&A*, *309*, L23

Sion, E.M. 1984, *ApJ*, *282*, 612

Stanghellini, L., Cox, A.N. & Starrfield, S.G. 1990, in *Confrontation between Stellar Pulsation and Evolution*, eds. C. Cacciari & G. Clementini, ASP Conf. Ser. Vol. 11, p524

Stanghellini, L., Kaler, J.B. & Shaw, R.A. 1994, *A&A*, *291*, 604

Starrfield, S.G., Cox, A.N., Hodson, S.W. & Pesnell, W.D. 1983, *ApJ*, *268*, L27

Starrfield, S.G., Cox, A.N., Kidman, R.B. & Pesnell, W.D. 1984, *ApJ*, *281*, 800

Stevenson, D.J. 1980, *JPhys*, *41*, C2

Tassoul, M. 1980, *ApJSupp*, *43*, 469

Thejll, P., Vennes, S. & Shipman, H.L. 1991, *ApJ*, *370*, 355

Vauclair, G. et al. 1993, *A&A*, *215*, L17

Vauclair, G. et al. 1995, *A&A*, *299*, 707 (VPG)

Watson, K. 1992, *IAU Circ.*, # 5603

Werner, K. 1995, *Balt. Ast.*, *4*, 340

Werner, K., Heber, U. & Hunger, K. 1991, *A&A*, *244*, 437

Werner, K. & Rauch, T. 1994, *A&A*, *284*, L284

Weidemann, V. & Koester, D. 1984, *A&A*, *132*, 195

Weinberg, S. 1967, *Phys. Rev. Letters*, *19*, 1264

Winget, D.E. 1981, *PhD thesis*, Univ. Rochester

Winget, D.E. 1988, in *Advances in Helio- and Astero-seismology*, IAU Symp. 123, eds. J. Christensen-Dalsgaard & S. Frandsen, (Reidel: Dordrecht), p305

Winget, D.E. & Fontaine, G. 1982, in *Pulsations in Classical and Cataclysmic Variable Stars*, eds. J.P. Cox & C.J. Hansen, (Boulder: Univ. Colorado), p46

Winget, D.E., Robinson, E.L., Nather, R.N. & Fontaine, G. 1982, *ApJ*, *262*, L11

Winget, D.E., Hansen, C.J. & Van Horn, H.M. 1983, *Nature*, *303*, 781

Winget, D.E., Kepler, S.O., Robinson, E.L., Nather, R.E. & O'Donoghue, D. 1985, *ApJ*, *292*, 606

Winget, D.E. & Van Horn, H.M. 1987, *The Second Conference on Faint Blue Stars*, IAU Colloq. 95 eds. A.G.D. Philip, D.S. Hayes & J. Liebert, (Schenectady: Davis) p363

Winget, D.E. et al. 1987, *ApJ*, *315*, L77

Winget, D.E. et al. 1991, *ApJ*, *378*, 326

Winget, D.E. et al. 1994, *ApJ*, *430*, 839

Wood, M.A. 1992, *ApJ*, *386*, 539

Wu, Y. 1998, *PhD thesis*, Caltech